Models of Vascular Pattern Formation in Leaves.

François G. Feugier

Doctorate thesis from the University of Paris 6

Biology

Defended by

François G. Feugier

For the degree of
Philosophy Doctor from the University of Paris 6

Models of Vascular Pattern Formation in Leaves.

Thesis Co Directors :
Jacob Koella
Yoh Iwasa

Defended on the 14th of December, 2006

Jury members :
Yves Couder (President)
Stéphane Douady (Referee)
Christophe Godin (Referee)
Jacob Koella (Inspector, Co Director)

Preface

I chose to make my thesis on models of leaf pattern formation for several reasons. Firstly, the last paper published on leaf pattern models is from the 80s, and until 2003 there was not much publications on modeling of this phenomenon. However, during these 23 years progress has been done in molecular biology, and vascular formation in plants has been studied comprehensively in *A. thaliana* at the gene level. New data were available to improve our understanding. Therefore it was time to restart working on that topic. Secondly, I am interested in self-organization processes. Plants are a nice example of self-assembled structures. Just adding some phytohormone to plant cells in culture starts to create order and roots and shoots come out from the anarchic callus. Thirdly, I simply love plants…

This thesis is made out from two papers published in JTB :

- Feugier, F.G., Mochizuki, A. and Iwasa, Y.,2005. Self-organization of the vascular system in plant leaves: Inter-dependent dynamics of auxin flux and carrier proteins. Journal of Theoretical Biology, Volume 236, Issue 4, 21 October 2005, Pages 366-375.

- Feugier, F.G. and Iwasa, Y., 2006. How canalization can make loops: A new model of reticulated leaf vascular pattern formation. Journal of Theoretical Biology, 243, 235-244.

I also added some non-published material taking in account recent publications.

General Introduction

For all organisms, resources are the essential condition for subsistence. Once resources are extracted from the environment they have to be distributed throughout all the parts of the organism to supply each cell. The best way Nature found to do so is to fill the body with a network of tubes: a vascular system. The more complex the organism, the more sophisticated the network.

1. Plant physiology

1.1 Utility of a vascular system.

Plants are autotrophic: they do not need to eat any other living creature to survive; they need only three basics which are the carbon dioxide, water and light, to create their own organic matter. Plants assemble carbon dioxide molecules to create plant bricks: cellulose. Water is the second ingredient the previous reaction but also plays a mechanical role to erect the plant by the creation of a turgor pressure. Finally, light is the energy required for the reaction creating cellulose from the two previous ingredients. This reaction is called the photosynthesis, and only plants can do that. This is the reason why plants are the lower level of the food chain.

Leaves of the plant are the cellulose factories where photosynthesis takes place. Ingredients of the cellulose must meet there for the photosynthesis to occur. But the plant faces a problem. The three basics required by the plant to build its cellulose, and therefore grow, are segregated in the environment: water is underground, and carbon dioxide and light are above the ground. Thus, to solve this problem and bring water in leaves for the photosynthesis to take place, the plant uses an upward network of pipes called xylem. Water is absorbed by the roots and goes through the xylem toward the leaves. On the other hand, carbon dioxide enters directly the leave through holes in the leaf epidermis, called the stomata. Finally, light is captured directly by the leaves to give the energy required for the reaction. Once all the basics are gathered, bricks of cellulose are produced by photosynthesis for the plant growth.

Plants grow via the shoot apical meristems but also the roots. Therefore bricks are needed in the underground part of the plant to allow roots to elongate and explore new areas of the ground to take more water and avoid competition with other plants roots. Thus, to convey bricks of cellulose in the roots, plants use a downward network, this time, called the phloem. It happens that xylem and phloem are on the same tracks in the vascular system but anti parallel.

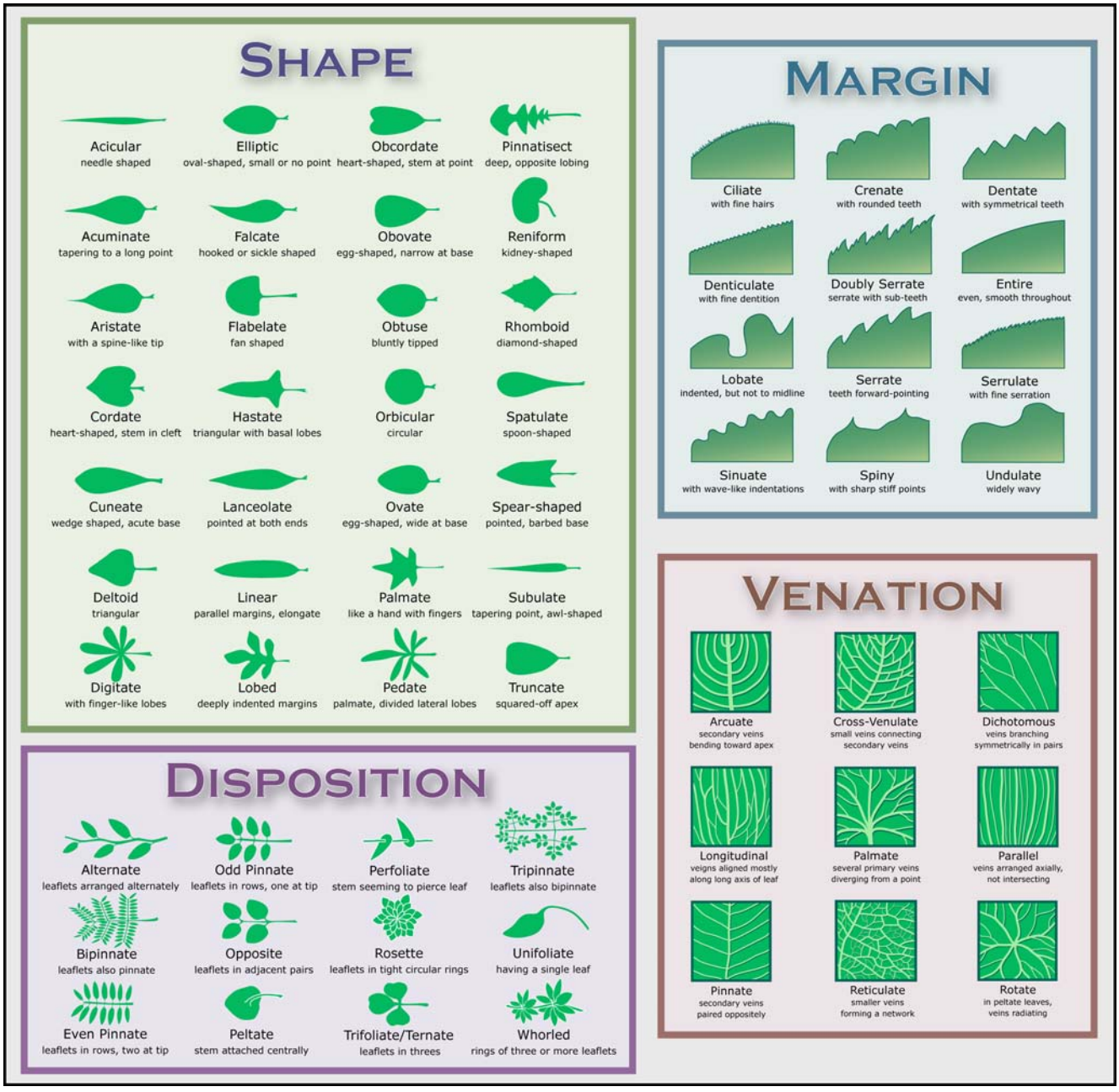

Figure 1 : Leaf shape, margin, disposition and venation. (From http://en.wikipedia.org/wiki/Leaf)

The vascular system is particularly ramified in the leaves. There, it is not only a conveyor but it plays the role of an exchange platform for gases and light. Each cell doing photosynthesis must be close to a vein to be supplied, therefore the vascular network fills the flat surface of the leaf as efficiently as possible. Leaves and their network can take very divers shapes depending on the plant species, although its purposes are always the same (Figure 1).

1.2 How does plant vascular network form?

Plant vascular network and animal vascular network are formed in very different fashions due to different constraints.

In animals it is formed by special cells that migrate and arrange together in a cylindrical cell layer surrounding a lumen, in order to create a tubular structure where fluids circulate. On the other hand, given that plant cells cannot migrate and rearrange due to the cellulose wall surrounding them, the network must be assembled in a different way.

During vascular formation files of cells - the pre-procambial cells - are selected among surrounding equivalent cells to draw the place of the future vascular system. Once they are selected they eventually differentiate into cambium cells and divide longitudinally to give on one side the xylem and on the other side the phloem. Especially cells on the xylem side become empty and lose the wall separating them, creating as a result tubes going throughout the plant from the roots to the shoots where fluids circulate. Contrarily to the case of animal vascular system where fluids circulate within a cylindrical layer of leaving cells, in plants fluids circulate inside dead cells.

But how does a plant manage to draw this network connecting the very end of the roots to the shoots?

The way these files of pre-procambial cells are selected among many equivalent cells has been studied for several decades. Some molecules having a strong effect on the vascular formation have been discovered. One of the most important morphogen is a phytohormone called auxin. The major macroscopic effect of auxin is the promotion of growth, and its most remarkable microscopic property is a polar movement through cells, making auxin the only phytohormone transported polarly from the shoots of the plant to the roots.

This transportation is performed by another important molecule in plant morphogenesis: the auxin efflux carrier proteins of the PIN family. Auxin can enter passively into a cell but needs PIN carrier proteins to leave it. Other carrier proteins have been discovered, such as the AUX family proteins that facilitate the entrance of auxin inside the cell. But recently all the attention has been focused on PIN proteins.

Since auxin is produced in the shoots and travels to join the roots during the whole life of the plant, a constant flow of auxin is maintained. The only cells likely to contribute actively to the auxin transport during the plant life are the cambial cells, the ones which were selected in first place to give birth to the vascular system. This perpetual transport may play several roles in the plant such as for cell division axis and elongation and healing of wounds. It is known that auxin can also travel through the phloem but not polarly.

Auxin and PIN proteins are also involved in phyllotaxis – the positioning of the leaves around the stem. The way these molecules interact to recruit the cells that form the vascular system and also elaborate phyllotaxis is an issue for theoretical studies for more than thirty years. Several principles have been proposed – reaction diffusion, canalization, and mechanical constraints – to explain this phenomenon based on empirical studies.

2. Earlier and recent theoretical works.

Here, I review chronologically different theoretical approaches for the modeling of leaf venation pattern and works on phyllotaxis. Because the same actors operate in both phenomena, results from each are informative. This short review deals with works published until 2006.

1.3 Models of leaf vascular formation.

In 1976, before any evidence of auxin transport by carrier proteins, Meinhardt proposed a model of leaf vascular formation based on Turing system (1952). In his model a substrate *s*, auxin for instance, is produced in the whole leaf. An activator *a* is produced from the substrate and produces in turn an inhibitor *h* and a molecule for differentiation into vascular cells *y*. The inhibitor *s* prevents *a* to diffuse and create a massive differentiation. Activator is at first supplied from the petiole. When a peak of *a* is formed, it creates enough *y* so that *y* can be produced independently

from *a* by self catalysis. Now *y* is high it consumes *s*, decreasing in turn the production of *a*. But other non-differentiated surrounding cells contain a large amount of *s*. Since *a* and *s* diffuse into these cells, a news peak of activator can take place in the non-differentiated cells, and so on. The result is a moving peak of activator, surrounded by a faster diffusing inhibitor, and followed by a trail of differentiated cells rich in *y*. The peak can divide into two peaks going apart to form a tip bifurcation, or a peak can emerge along the formed trail to create a lateral branching. The pattern stops when the surface is evenly covered by a branching pattern consuming the substrate.

Although there is no directional substrate movement, the growth is clearly oriented toward sites of high substrate concentration. As a result, two peaks will avoid colliding because substrate concentration decreases as a peak comes close to another one, and because of inhibitor diffusion around each peak. Therefore the model produces no connection.

Mitchison (1980, 1981) was the first to propose a model based on the canalization hypothesis made by Sachs (1969). In his earliest model he assumes that permeability of the interface between cells can change according to the squared value of the net flux through that interface. In a lattice of cells this facilitated diffusion principle can amplify a small perturbation in an initially uniform laminar flow of auxin through the lattice, creating eventually stable preferential paths where auxin flows toward a sink. Mitchison could obtain loops where auxin flows in two opposite directions, by moving punctual sources of auxin. In a second model he introduces an asymmetric diffusion between cells, creating a polar transport of auxin. Contrary to facilitated diffusion, where auxin movement is improved between two cells whatever the direction of the movement, in this second case auxin movement is improved in one direction. This change creates also preferential paths.

Independently, Honda and Yoshizato (1997) were working on the formation the branching pattern of blood vessels in the wall of avian yolk sac. They start their model with many islands of cells between which blood is flowing from a source to a sink, which is actually the heart of the embryo. They use the Kirchhoff law to calculate blood flux in each vessel. Resistance of a vessel increases when the blood flow in it decreases, and vice versa. The results show that some paths between islands vanish, whereas other spaces increase to form preferential blood paths. Since this model is mode only with loops (closed network) it shows many flux bifurcations, contrary to the canalization model proposed by Mitchison.

By means of a completely different approach Markus et al. (1999) used cellular automata (CA) for the creation of leaf venation pattern. This CA, based on Turing system, has four variables: activator, inhibitor, genetic switch and substrate; and twelve rules to make possible autocatalysis, tip death, dichotomous branching, lateral branching, chemotaxis and anastosmosis (vein connections). In the model the role of the vein is to deplete from the field the auxin produced. They overcome the problem of vein connection, which is the same problem for almost all models of leaf venation, by assuming that older veins leak auxin, so as to attract younger surrounding veins. They obtain nice resulting patterns comparable to what is observed in real leaves.

A more physical approach is proposed by Couder et al. (2002) who suggest that the strain that cells experience in a growing leaf can be the trigger of vascular differentiation. This assumption is based on the observation of cracks in silicon gels. Surprisingly, cracks have the same constitutive property as veins in a leaf: angle formed between three joined cracks are comparable to the angles made by the meeting of three veins, and the width of the cracks, which is physically related to the angles, are of same order as the veins thickness (Bohn et al., 2002). Furthermore, Bohn et al. (2002) showed that this vein property is the same for any plant.

Feugier et al. (2005) started from Mitchison's model (1981). In their model a lattice of cell can exchange auxin through their sides by using auxin carriers. Carrier concentration on each side can change according to the net flux through them. They introduce carrier conservation in the cell, which improves the stability of the model and creates auxin preferential paths richer in auxin than the surrounding cells, contrarily the existing models. Instead of using the upper row of the lattice as auxin source and the lower row as auxin sink they use a global auxin production hypothesis and one cell as a sink. They study nine functional shapes of the self enhancement by the flux of the auxin transport, and conclude that only accelerating functions can create preferential paths. In their results the paths can branch to fill the whole lattice. On the other hand they observe no vein connection.

Runions et al. (2005) introduced an algorithm to generate realistic venation patterns. In their method, veins grow toward the auxin sources in the leaf closest to their tip; a source is removed once a vein is close enough to it; finally, leaf grows following an anisotropic scaling and new auxin source are placed in new spaces out of veins' range. To obtain loops they assume that veins connect by their tip on an auxin source. To insure that two or more veins, reach the source, they maintain the source until all the veins are arrived. Then, anastomose occurs. The resulting

patterns are very realistic, ranging from mono or dicotyledonous venation patterns to gingko pattern.

Rolland-Lagan and Prusinkiewicz (2005) started from Mitchison's models of auxin facilitated diffusion and polar transport, and added to both passive auxin diffusions. They deduced from their results that passive diffusion may play an important role in controlling veins that connect auxin sources to sinks, since they observe only one channel of auxin rather than several when passive diffusion is high. By setting a movement schedule to several sinks and sources during simulations they obtain loops as seen in the Arabidopsis young cotyledon. Finally, by using two auxin sources of different concentration they obtain a transient discontinuous venation.

To mix reaction diffusion models and canalization, Fujita and Mochizuki (2006) made a model based on the diffusion of an activator of auxin transport. This activator is produced by the sum of the auxin fluxes in cells and diffuses amongst them. If a cell experiences a low flux, by receiving the activator from nearby active cells, it will increase its carrier allocation. Orientation of carrier allocation is done by calculating the direction vector of the mean flux vector of the cell. Carriers are allocated preferably on sides in the direction of the mean flux, and to keep the total amount of carrier constant, carrier level on each side is normalized with the total amount of carriers in the cell. In their model all cells produce auxin. Results show branching pattern wherein auxin flows toward an auxin sink. To obtain a netlike structure Fujita and Mochizuki start from a lattice with random noise in auxin concentrations. Noise provides some cells with a higher auxin concentration than their neighbors. Therefore, due to flux enhancement, cells start to flush away auxin around them. These circular waves propagate to the neighborhood until the moment all waves front meet to form a network pattern covering the lattice, in a way circles grow to meet and form a Voronoi segmentation.

To test an alternative of flux sensing by the cells, Dimitrov et al. (2006) propose a model based on the sensing of auxin gradient rather than auxin flux, and where auxin transport is done by improved diffusion (Mitchison, 1980). In their model they start from an already formed leaf areole. Cells in the center are undifferentiated and produce auxin and cells around, forming the areole, are vascular and drain auxin. In undifferentiated cells auxin diffuses passively. The authors set a threshold so that at some auxin gradient value between two cells, they increase to a higher constant value the diffusion coefficient between them. As initial condition for the growth of the veins they use an areole in which auxin has reached diffusion equilibrium. In their results, areas near the

border of the areole have the largest auxin gradient with the lowest concentration, and the gradient goes to zero as going toward the point with highest auxin concentration in the center of the areole. Cells in the areas with an auxin gradient larger than the threshold, near the areole boundary, start increasing their diffusion coefficient toward the neighboring cell with which the threshold is exceeded. This behavior repeats from near to near climbing the gradient toward the center of the areole, to create a path where auxin flows in direction if the areole boundary. Their model can predict precisely where veins should emerge from the areole and where they should converge to finally connect.

1.4 Models of Phyllotaxis

Phyllotaxis has for a long time intrigued, and numerous hypotheses for its formation have been proposed. A first idea is that mechanical forces due to growth in the shoot apical meristem (SAM) can decide the place of emergence of primordia.

Douady and Couder (1996) made a very elegant experiment to check whether placement of primordia results from a processus of energy minimization in the meristem. At the center of a Teflon plate under a vertical magnetic field, they drop periodically droplets of ferrofluid representing the primordia. The periodicity at witch they are dropped represents the growth speed of the SAM. In these conditions, droplets are slowly attracted outward due the magnetic field. Droplets behave such as a dipole and repulse each other. Hence, at some dropping speed the density of droplets on the plate increases, and the spatial configuration demanding the lowest energy should emerge. The result shows nice spirals of phyllotaxis as observed in real plants. The divergence angle between droplets converges to the golden angle and the parastichies (phyllotactic spirals) number changes following consecutive Fibonacci series numbers as the period between two droplets decreases.

This shows that new primordia try to emerge the furthest from already existing primordia, due to energy minimization (here magnetic field). Other phenomena can give identical results to the previous experiment if the underlying physical principle is the same, e.g. energy minimization. This is observed in buckling and Turing reaction-diffusion systems.

Meinhardt (1998) also proposed a reaction-diffusion model for phyllotaxis by running a typical activator-inhibitor model on a cylinder elongating at one end. Starting from uniform initial

conditions and according to parameters, peaks of activator emerge following a distichous, decussate or phyllotactic spiral pattern during elongation of the cylinder. Peaks of activator emerge in the areas of lowest inhibitor concentration, which is the furthest from other activator peaks (since peaks of activator are surrounded by high inhibitor concentration). This principle is the same as the one proposed by Douady and Couder in their experiment.

Shipman et al. (2005) proposed a model based on the buckling pattern that minimizes elastic energy. Constraints in the growing SAM could generate a buckling that can induce special behavior on cells such as growth and differentiation.

Since the observation of a particular layout of PIN1 proteins in the tunica that presages the emergence of primordia of leaves (Reinhardt[b] et al., 2003), new modeling based on auxin transport by PIN1 has been applied to phyllotaxis.

Accumulation of auxin in the tunica is thought to give birth to leaf primordia. To check this hypothesis Barbier de Reuille et al. (2006) verified whether the observed layout of PIN1 in the tunica leads really to the accumulation of auxin presaging leaf primordia. To do so, they analyzed a real SAM by computer and constructed a map of connections of each cell with its neighbors and PIN concentration in each connection. Using this map they ran dynamics of passive auxin diffusion and auxin transport with PIN1 until steady state is reached. Results show, indeed, auxin accumulation in area of future primordia. Furthermore they confirm the experimental fact (Reinhardt[a] et al., 2003) that the summit of the SAM has no influence on the pattern of auxin accumulation.

Jönsson et al. (2006) propose a model of phyllotaxis based on dynamics of active auxin transport and passive diffusion. In this model each cell contains a pool of free PIN1 carrier proteins. Allocation of carriers on one side of the cell depends in a monotonically increasing fashion on the concentration of auxin in the neighboring cell on that side. Thus, if two cells have a slightly different auxin concentration, the one with a lower level will send more auxin toward the second with a higher level. As a result, auxin converges toward areas of high concentration to form peaks of auxin. To estimate the parameters of their model they make a template of an observed SAM by computer, with the connection map of the cells, and use an optimization algorithm. After estimation of the parameters they run their model on a 3D shape representing the SAM, on which all cells can divide and produce auxin. Results show, while elongation of the shape, repeated

emergence of auxin concentration peaks following a spiral or a whorled configuration according to parameters.

Smith et al. (2006) also proposed a model where auxin is pumped preferably toward cells with high auxin concentration. They run their 2D model by mapping it on a 3D growing shape representing a SAM where cells divide. They use different rates of auxin production according to the area (central zone, peripheral and proximal) of the SAM. Their results show very realistic patterns of all the different types of phyllotaxis.

3. Terminology

In the following I deal often with the words “bifurcation” and “junction”. To avoid any confusion I clarify their use here.

Usually a bifurcation is about a branch or a road which splits into two new branches or roads such as a “Y” shape. If one walks upward on the “Y”, one meets a bifurcation. But if one walks downward on one branch of the “Y”, one meets a junction. There is a crucial notion of direction. In the following, when I use one of these words about some phenomenon (auxin movement, vein growth), I always take into account the direction of this phenomenon.

For example, if I look at salmons traveling from the sea to the source of a river, I would say the salmons will meet many bifurcations on their way, whereas streams of water meet only junctions. It is just a matter of direction.

If this looks simple to you (I hope!), then you are ready for the following!

4. Principle of canalization

To explain the formation of preferential paths of auxin Sachs proposed the canalization hypothesis (Sachs, 1969) inspired by the formation of rivers.

Let us start with a readily observable example of this process. On the beach at low tide it is often possible to observe on the flat sand some branching patterns formed by the sea water flowing back slowly to the sea (Figure 2). When a thin layer of water flows gently and evenly on a sand slope, if there is a small gutter in the sand, water will rush into it due to gravity. As a result the flow increases in that gutter and sand is carried away, increasing in turn the gutter size. Since a larger

and deeper gutter receives more water, the flow in the gutter increases and removes more sand, and so on, creating a preferential path for water. The increase in gutter size due to the water flow makes this process a self enhancement process which is the foundation of the canalization hypothesis.

Figure 2 : branching pattern on the sand at low tide.

A typical river (with erosion and sediment transport) is a branching network without any closed loops. A closed loop can be done by a bifurcating stream with the two branches connected somewhere else downstream. But this configuration is unstable and therefore transient. Indeed, at the bifurcation point the stream of water will eventually flow into either one branch, opening one side of the loop.

One can extend this canalization principle to plants vascular formation now. In the case of plants, the role of water is played by auxin, and the variation in the gutter size is mimicked by PIN1 carrier proteins concentration.

The majority of plants have a reticulate network exhibiting many closed loops. Since several empirical results support the hypothesis of auxin canalization for the vascular system formation, their must be an additional process to canalization, absent from river formation, to create stable closed loops of veins.

1.5 Principle of canalization.

To introduce canalization let us take an image with the simplest possible enhancement model. In first place, consider a box in which one supplies water with a constant rate *r*, the water level being *A*, and with two valves plugged at the bottom of the box with constant openings P_1 and P_2 as shown in Figure 3a. The dynamics of the water level follow

$$\frac{dA}{dt} = r - AP_1 - AP_2$$

where AP_i is the flux of water through valve i ($i=\{1,2\}$) resulting from the mass action law between the height of water in the box and the valve opening value.

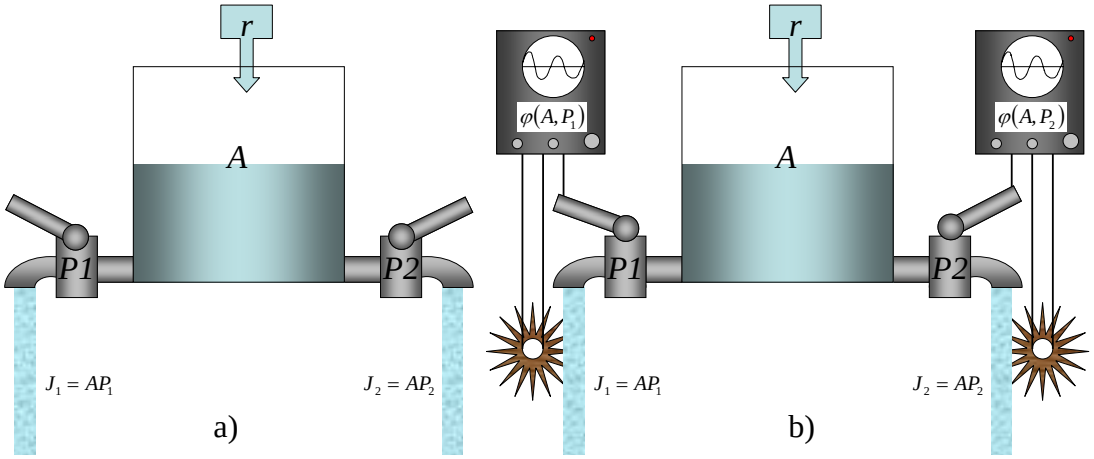

Figure 3 : Canalization example with a box and two valves. Water is added in the box at a constant rate *r*. a) The openings P_1 and P_2 are constant. b) A machine measures the flux through the valves with a water while and controls their openings with the response function $\varphi(A, P_i)$.

If one sets an opening for each valve P_1 and P_2, as supplying water with a constant rate, box fills and the water level reaches an equilibrium height which is the ratio of supply rate over the sum of the valve openings:

$$A^* = \frac{r}{P_1 + P_2}$$

Now let us allow valve opening to change by introducing their dynamics. Simplest opening self enhancement for one valve would be the activation of its opening according to the flux of water AP_i going through it. The opening will respond to the flux going through it following a certain behavior which one will call the response function $\varphi(A, P_i)$. But in order to be a self enhancement process as compared with a river broadening, the response function needs to be a monotonically increasing function of the flux. The simplest one would be a linear response. Therefore a basic canalization model would be

$$\frac{dP_1}{dt} = \varphi(A, P_1)$$
$$\frac{dP_2}{dt} = \varphi(A, P_2)$$

where the simplest activation would be a response function proportional to the flux as $\varphi(A, P_i) = \alpha A P_i$ with a α constant which one fixes to 1 for the following. These equations are the essence of self enhancement with the flux. But in these conditions the box will fill for ever if the valves are initially closed, or the valves will remain opened even after water supply has stopped and the box is empty. Thus, for a slightly more robust model one needs to guaranty that valves never close completely neither stay wide opened for ever. To do so, let us introduce a ground value q for the openings so the valves never close completely, and a decay of the openings so the valves never stay opened when the flux is null. The system becomes

$$\frac{dP_1}{dt} = \varphi(A, P_1) + q - P_1$$
$$\frac{dP_2}{dt} = \varphi(A, P_2) + q - P_2$$

This system is the one proposed by Mitchison in 1981. One can increase complexity by adding other variables in the response function term, as well as changing the rest of the dynamics,

but this simple self enhancement model offers a simple and intuitive approach to start studying vein pattern formation with canalization.

1.6 How does a preferential path of auxin form?

To explain how flux self enhancement creates a preferential let us use the box introduced earlier.

The system reaches a steady state with

$$A^* = \frac{r}{2q + r}$$

$$P_1^* = P_2^* = q + \frac{r}{2}$$

One remarks that what ever the value of *r* and the initial openings of each valve, the both valves converge to the same opening at steady state.

Now let us try an accelerating response function: valves will change there opening according to the squared flux of water going through them. In that case dynamics of water level is unchanged but the response function becomes $\varphi(A, P_i) = (AP_i)^2$.

In this situation the steady state offers a more surprising particularity explained in more mathematical details in Appendix B. Now, valves openings value at the steady state depend on water supply rate and noise in the openings.

- If *r* is below some threshold, both valves will end up stably with the same opening.
- If *r* is above some threshold, the valve having initially a larger opening than the other one will end up full opened, whilst the other one will end up to the minimal opening (cf. Appendix B).

Finally, a decelerating response function such as $\varphi(A, P_i) = \sqrt{AP_i}$ gives always a steady state with both valve openings equal.

The three types of response function give completely different steady states. With the linear response function both valves end up with the same opening whatever the initial conditions and the water supply value. With the quadratic response function valves behave similar to the linear

response when the supply of water is small, but with a larger supply value the equality of the openings becomes an unstable situation and one of the valves “wins”. And finally the square root response gives also equality of the two valves at steady state.

Let us explain these results more intuitively. The valve opening is clearly self-enhanced since a wider valve creates a larger flux, and a larger flux creates a larger response to open the valves. One also understands intuitively that the lower the level of water in the box, the more stable the system. Therefore, to have a low level of water one needs the total outward flux (the sum of both fluxes) to be the largest. Thus, because the sum of he openings is proportional to the total response φ_{tot}, the total flux $J_{tot} = J_1 + J_2$ is proportional to φ_{tot}, e.g. $J_{tot} \propto \varphi_{tot}$. As a result, to get the lower level of water one needs J_{tot} to be the largest, hence φ_{tot} has to be maximum. Let us try to find the value of he fluxes for which φ_{tot} is maximal with a fixed J_{tot}, in the case of the linear response, an accelerating (squared) response and decelerating (square-rooted) response.

Let $J_i = AP_i$ be the flux through valve *i*, and $J_{tot} = J_1 + J_2$ be the total outward flux, so $J_2 = J_{tot} - J_1$. In the case of the linear response, φ_{tot} is equal to the sum of the fluxes: $\varphi_{tot} = J_1 + J_2 = J_{tot}$. One can notice that whatever the value of J_1 (and implicitly J_2) φ_{tot} is equal to J_{tot} which is constant. Therefore the total response φ_{tot} cannot be maximized.

In the quadratic response case, φ_{tot} is equal to the sum of the squared fluxes: $\varphi_{tot} = J_1^2 + J_2^2 = J_1^2 + \left(J_{tot} - J_1\right)^2$. One can see that φ_{tot} is maximal when $J_1 = J_{tot}$ or when $J_2 = J_{tot} - J_1 = J_{tot} - 0 = J_{tot}$. Therefore the total response is the largest, and consequently the total opening, when only one of the two valves is opened and takes the total outward flux. When the system ends up with one valve wide opened and the other one nearly closed, the configuration is stable. Indeed, if the larger opening starts to decrease, water level will increase in the box and the flux through both valves will also increase. But due to the non linearity of the response the larger opening will open back faster than the smaller one, taking more flux and staying the larger. Then the level of water will come back to the previous level.

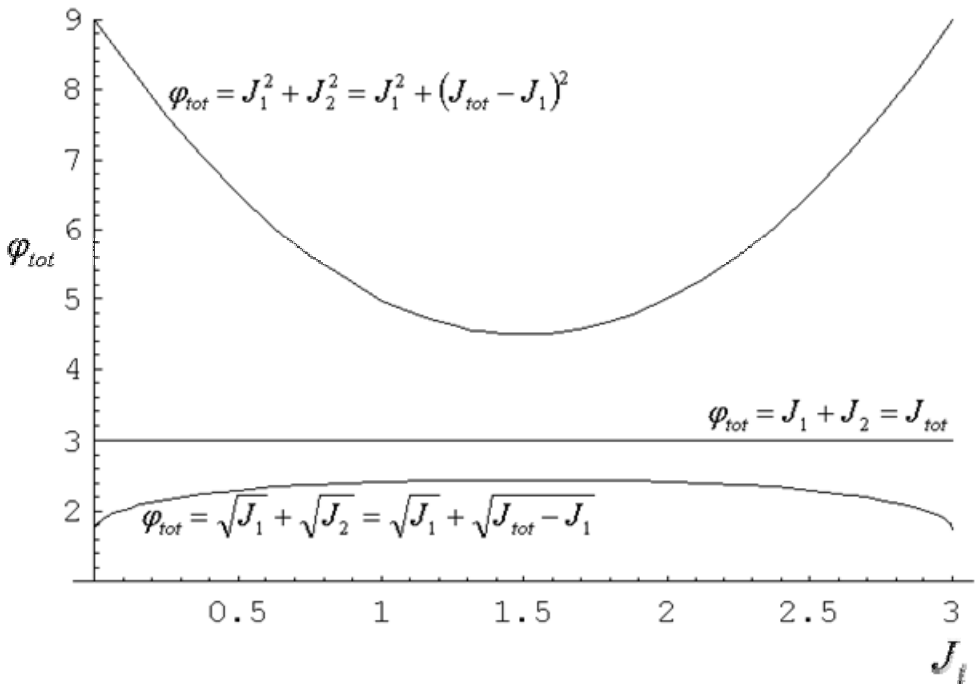

Figure 4 : Profile of the total response depending on either the linear, square or square root response functions. $J_{tot} = 3$.

Finally, when looking at the square root response function, φ_{tot} will look like $\varphi_{tot} = \sqrt{J_1} + \sqrt{J_2} = \sqrt{J_1} + \sqrt{J_{tot} - J_1}$. In this case φ_{tot} is maximized when $J_1 = J_2 = \frac{J_{tot}}{2}$. This gives the reverse result to the squared response function. The Figure 4 illustrates all the cases.

To summarize, when the activation is quadratic, one valve opens more than the sum of two valves openings. Therefore the lowest water level is reached only when one of the both valves is fully opened and the other one is closed. In the linear response case the openings tend to have the same value but actually any opening values that sum up to J_{tot} are equivalent, as seen in Figure 4, and give the lowest water level. Finally, with the square root response both openings have to be equal for the lowest water level. By the way, in the current model valve never close completely but settle down to the minimum opening *q*.

The same situation occurs for a box with *n* valves. When the water supply is large, with a square root response all the valves tend to open equivalently, whereas with the linear response all the valves end up to any opening as long as their sum equals the total out flux, and at last with a

quadratic response only one valve becomes fully opened and all the others *n-1* pipes converge to the smallest opening possible in the model, which is *q*.

In the system with quadratic response of the valve opening in regard to the flux the threshold of water supply, and therefore the flux through each valve, is critical: below this threshold the flux is low, the system behaves similarly to the linear regulation and noise in the openings has no effect, whereas above this threshold flux through valve is large, the system becomes unstable and sensitive to noise, so as soon has the symmetry is broken it moves in the situation where only one valve wins against all the others.

So far we were speaking about a system unable to produce any spatial pattern because deprived of dimension. Now instead of using only one box let us use several square boxes arranged together like a chess board (Figure 5a). For reasons which become clear later let us forget the valves and use pumps between the boxes. Each box has an outward pump toward each of its neighboring boxes. The net flux between two boxes *i* and *j* is defined as

$$J_{ij}^{net} = J_i - J_j = A_i P_{ij} - A_j P_{ji},$$

where P_{ij} is the strength of the pumping from box *i* to box *j*. If the net flux is negative one sets the response function to null so the pump strength decreases toward a minimum *q*.

Furthermore, water is supplied in every box with the same constant rate, and only one of them, on the border of the chess board, the box 0 has a hole in it preventing it to fill with water (Figure 5a). The question is, given that we know the behavior of one box emerging from the type of the response function, what is going to happen in this situation where each box interacts with its neighbors?

Let us see what happens when one uses the linear response function in such a system. As soon as water is supplied boxes fill up, except for the box 0 having a hole in it (Figure 5a). Since box 0 is leaking its level of water is always below the one of its neighboring boxes. As a result boxes 1_1, 1_2 and 1_3 will start to flow in box 0 (Figure 5b). Due to this flux through the pumps, each one will strengthen proportionally to the positive net flux between each box 1_i and the sink. Now that the 1_i boxes lose water into the box 0 their level is lower than boxes 2_i. The same process continues from near to near to the whole chess board. The emerging flow pattern shows no preferential paths and each box mean flux vector is oriented toward the box 0. The mean flux

vector of a box is a vector centered on the middle of a box, and taking the sum of the positive net fluxes value on each opposite side as coordinates.

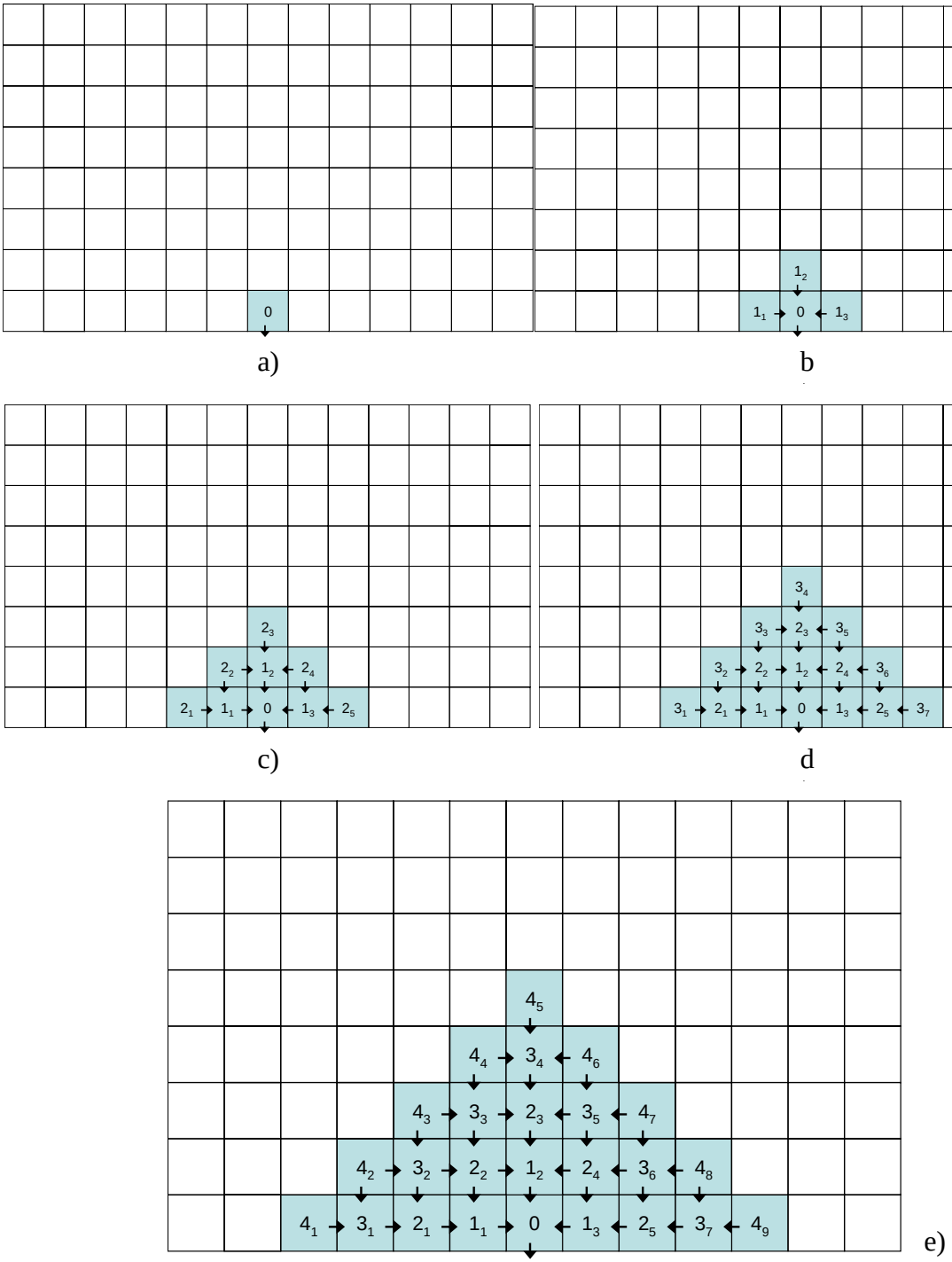

Figure 5: Pattern obtained with a linear response function. The pattern grows at each stop from the center. Boxes are ranked in a radial fashion from the cell 0 at the bottom-center, to the periphery, and the indices are from the left to the right. Arrows represent the net fluxes between the boxes. Blue color represents pumping

boxes. A rough idea of the length of each horizontal and vertical arrow can be given by $-\cos(\theta)/rank$ and $-\sin(\theta)/rank$ respectively, with up-right positive direction, and θ being the angle with the horizontal centered on box 0. a) - e) water is supplied everywhere. Box 0 has a hole in it.

What happens now with the quadratic response function? Previously, in the example of Figure 3b with the quadratic response function, we noticed the presence of a threshold of the water supply above which the flux becomes high enough so only one valve ends opened and the other tends to close up. The box goes through this threshold if the value of the water supply increases, increasing in turn the out flux. In the case of our lattice of boxes, the water supply for one box includes also the quantity of water received from the neighbors. Let us assume, for simplicity, that once a box receives more than one unit of flux (for example one box with two outward fluxes sends half a unit of flux per side), the total amount of water received (water supply + sum of incoming fluxes from the neighbors) can create a sufficiently large net flux with another downstream box so the system is above the threshold, making the pump with the largest net flux to work harder and the others to shut down: the box becomes polar.

Let us see step by step on the

Figure 6 the pattern obtained with a quadratic response function. For a better understanding, they are three steps to repeat as a loop: first, establish the zone in which boxes do not have the same water level to decide the orientation of the fluxes; second, find the boxes receiving water from more than one neighbor; third, set a polarity to these boxes and reorient the arrows of all the other boxes according to the changes due to the new polar boxes. I will principally deal with the left half of the lattice since it holds for the right half by symmetry.

In a) one starts supplying the water into all the boxes, and box 0 remains with a lower level of water due to its hole. b) As a result water from boxes 1_1, 1_2 and 1_3 flows into box 0. One notices that box 0 receives water from more than one box so it becomes polar. c) In turn water level decreases in boxes 1_i and now boxes 2_i flow into box 1_i. Boxes 1_i can become polar. d) Since boxes 2_i lose water into boxes 1_i their water level is lower than boxes 3_i. Therefore boxes 3_i start sending water into boxes 2_i. e) Boxes 21, 23 and 25 receive enough water to become polar. One can see now the emergence of preferential paths of water. As seen previously, a box with quadratic response function under the threshold gives a behavior similar to the one with linear response function. Knowing that, one can see that the outward flux of box 33 should be roughly equal to the sum of the two outward fluxes of box 22. Therefore one can conclude that they have the same water level, and

thus there is no flux between them. Same thing happens for boxes 22 and 32. f) Now that 3i boxes lose water, their levels become low and boxes 4i start pumping water toward them. Boxes 32 and 33 receive both 1 unit of flux. But the symmetry is broken when looking at the surrounding boxes of 32 and 33. Box 34 receives 2 units of water though box 31 receives 1.5, which means that box 34 has a higher level of water than box 31. Due to this level difference, box 44 will actually send more water in box 33, because the level difference is advantageous, than in box 34. Symmetrically, box 42 will actually send more water in box 32 than in box 31. But due to the higher water level in boxes 34 than in 31, box 44 will send more water in box 33 than box 42 will send in box 32. As a result both boxes receive more than one unit of flux, but box 33 receives more water than box 32, allowing it to become polar first. Box 31 receives also enough water to become polar. g) We just met the reasons why preferential path can branch, and it is greatly helped by symmetry breaking. Now that new polar boxes appeared, other boxes reorient their fluxes toward them. h) Boxes 5i start pumping toward boxes 4i. One easily sees that boxes 41, 43 and 45 have the required conditions to become polar. i) If we continue using the previous rules the tips of the water preferential paths keeps on bifurcate and paths elongate until the pattern fills the whole lattice.

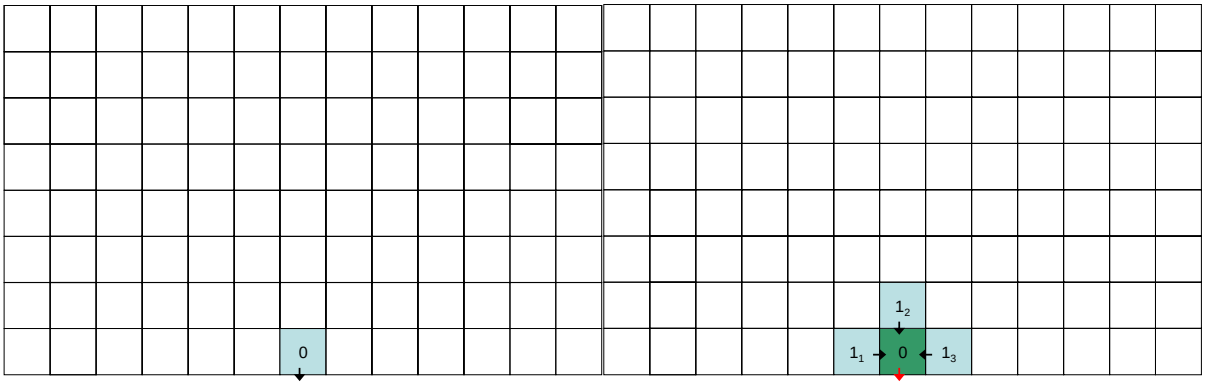

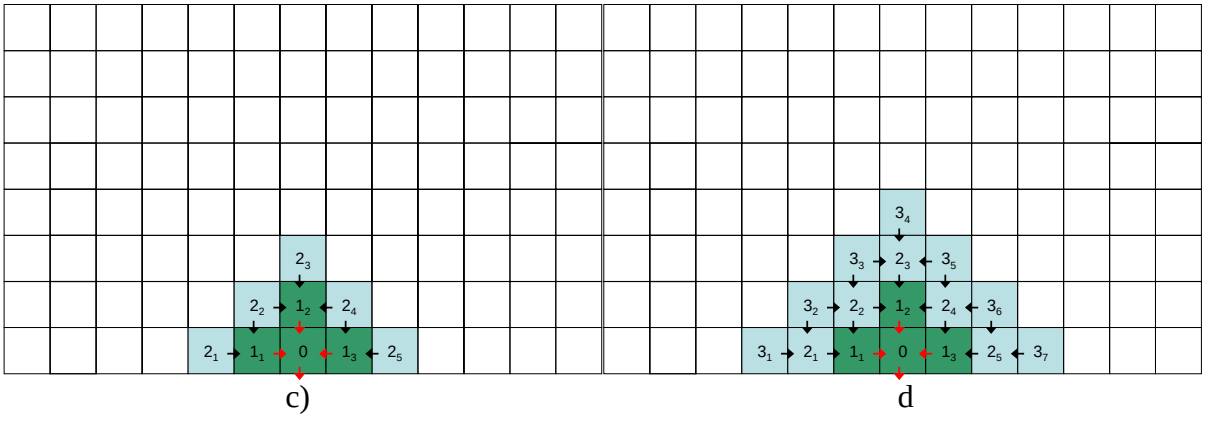

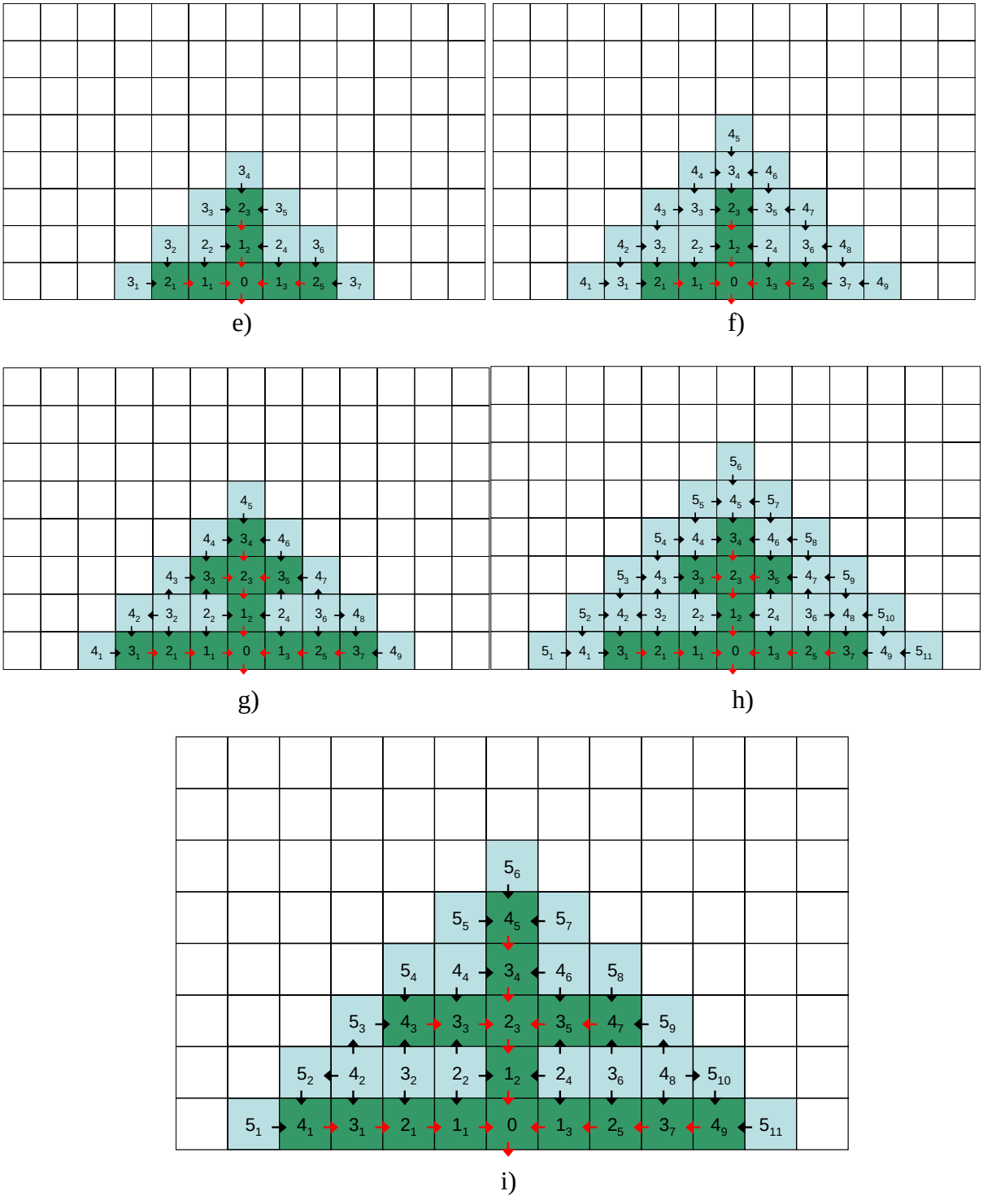

Figure 6 : Pattern obtained with a quadratic response function. The pattern grows at each stop from the center. Boxes are numerated in a radial fashion from the cell 0 at the bottom-center, to the periphery, and the indices are from the left to the right. Arrows represent the net fluxes between the boxes. Blue color represents non polar boxes and black arrows are their fluxes. Green color represents polar boxes and red arrows are their only outward flux. a) - i) water is supplied everywhere. Box 0 has a hole in it.

It is clear that, although the tip of the preferential path elongates and bifurcates it does not mean that boxes are moving. It means that, from near to near as we saw, the state of the boxes will change from non polar to polar, creating the preferential path where water flows better, and where the tip is the last box which became polar. The tip is the place where the transition between these two states occurs.

The understanding of the behavior at a microscopic scale (one box) is very enlightening for the comprehension of a much more complicated behavior at a macroscopic scale (many boxes).

Finally one can see the difference between the self enhancement of the flux and canalization. Canalization is a flux self enhancement process, but flux self enhancement is not necessarily canalization. For example, linear response function does not give any preferential paths; therefore it is not a canalization process, although it does flux self enhancement. Quadratic response function does give preferential paths; therefore it is a canalization process as well as it is a self enhancement process. Canalization does not occur in any flux self enhancements. Conditions of occurrence are discussed in Appendix B.

Now that we saw what becomes of a lattice of boxes with water and pumps, let us, at last, investigate models of canalization based on what we saw previously and extend it to the case of leaves. Boxes become cells, water becomes the auxin, pumps become auxin efflux carriers PIN1 and the response function becomes what the cell does with its auxin.

In the first article included in this thesis I deal with models based on flux self enhancement. I verify whether this process, transposed to a hormone and its carriers, can create an acceptable pattern and the conditions of emergence.

In the second paper I extend a model so that it can create a reticulate network by adding a parsimonious change in the way an evolutionary jump could do.

All reference numberc (figures numbers, tables…) are internal to each article.

- First article -

Self-organization of the vascular system in plant leaves: Inter-dependent dynamics of auxin flux and carrier proteins.

Francois G. Feugier, A. Mochizuki, Y. Iwasa

Abstract

The vegetative hormone Auxin is involved in vascular tissues formation throughout the plant. Trans-membrane carrier proteins transporting auxin from cell to cell and distributed asymmetrically around each cell give to auxin a polarized movement in tissues, creating streams of auxin that presume future vascular bundles. According to the canalization hypothesis, auxin transport ability of cells is thought to increase with auxin flux, resulting in the self-enhancement of this flux along auxin paths. In this study we evaluate a series of models based on canalization hypothesis using carrier proteins, under different assumptions concerning auxin flux formation and carrier protein dynamics. Simulations are run on a hexagonal lattice with uniform auxin production. A single cell located in the margin of the lattice indicates the petiole, and acts as an auxin sink. The main results are: (1) We obtain branching auxin distribution patterns. (2) The type of self-enhancement described by the functional form of the carrier proteins regulation responding to the auxin flux intensity in different parts of a cell, has a strong effect on the possibility of generating the branching patterns. For response functions with acceleration in the increase of carrier protein numbers compared to the auxin flux, branching patterns are likely to be generated. For linear or decelerating response functions, no branching patterns are formed. (3) When branching patterns are formed, auxin distribution greatly differs between the case in which the number of carrier proteins in different parts of a cell are regulated independently, and the case in which different parts of a cell compete for a limited number of carrier proteins. In the former case, the auxin level is lower in veins than in the surrounding tissue, while in the latter, the auxin is present in greater abundance in veins. These results suggest that canalization is a good candidate for describing plant vein pattern formation.

1. Introduction

The self-assembled vascular network of higher plants displays very diverse patterns, such as parallel veins, branching veins and reticulated networks. One of the principal actors in the development of those structures is the phytohormone auxin (Jacobs, 1952; Sachs, 1975; Mitchison, 1981; Uggla et al., 1996; Sieburth, 1999; Avsian-Kretchmer et al., 2002; Fukuda, 2004). Applying ectopic auxin to vegetative tissue can initiate the development of vascular bundles (Sachs, 1975). To understand the mechanisms behind this vascular tissue formation with the action of auxin, molecular biologists created many mutants which exhibited abnormal venation (Carland et al., 1999; Berleth et al., 2000; Deyholos et al., 2000; Steynen and Schultz, 2003). Auxin is a particular hormone transported in a polar fashion by a protein named PIN1 capable of driving auxin out of the cell (Mitchison, 1980b, 1981; Sachs, 1991; Goldsmith, 1997; Berleth et al., 2000; Morris, 2000). Auxin entering a cell from its apical side is not pumped back toward the side of entry, but is transported out by the efflux protein PIN1 present in the membrane at the basal side of the cell. Inhibiting PIN1 dramatically changes the shape of the vascular network (Mattson et al., 1999).

The canalization hypothesis (Sachs, 1975, 1981, 1991) states that cells with a higher flux of auxin than their neighbors become specialized in auxin transport, and turn into an auxin sink for normal surrounding cells. At this point, it remains unclear what triggers this shift in the cell behavior, but the result would create preferential paths which lead auxin toward the petiole.

A similar self-organization process of network pattern formation has been discussed by Honda and Yoshizato (1997) as well as Kobayashi (2000). These discussions concern the formation of blood vessel networks in the yolk of chicken eggs. They start within a population of non-joined cells, between which blood can circulate forming a network of fine vessels. If one path (e.g. vessel) is wider than other competing paths, then the flux through this path increases relative to the other competing paths. The result is a positive feedback: increased flux stimulates a broadening in the pathways' diameter, which in turn further enhances flux rate. In contrast, narrow paths with a weak flux, will decrease in diameter and eventually disappear. This model is somehow similar to the self-organization of leaf vein pattern formation, generated by the action of auxin, except that the blood vessel network of Honda and Yoshizato's model assumed no polarized cellular transport of blood (i.e. only passive isotropic blood movement outside of the cells).

Mitchison proposed a similar vein formation model (Mitchison, 1980a) based on Sachs' canalization hypothesis, with isotropic auxin movements between cells. He extended this model (Mitchison, 1981) by adding anisotropy in auxin transport. In his model, cells exchange auxin with their neighbors. They increase the permeability of their plasma membrane on the side where the net flux of auxin with a neighboring cell, through the membrane, is positive and large. Mitchison performed simulations in a small square lattice of size 4 cells by 5 cells. In this model, the top row of cells was linked to an auxin source of a fixed concentration, and the bottom row was linked to a sink of zero auxin concentration. Starting with a laminar flow of auxin from top to bottom, Mitchison demonstrated that a small perturbation grows to form a preferential path of auxin. Subsequently auxin supplied in the top margin of the lattice first flows into the preferential path, and then streams down to the sink. To create a preferential auxin path, Mitchison argued that auxin concentration in the cells of the path must be lower than concentration in adjacent cells in order to create an inward flux of auxin into the path. To achieve this, he assumed that the permeability of membranes regions increases as a quadratic function of auxin flux passing through it. He reported neither branching patterns nor a network of veins, probably because the lattice size adopted in his numerical analyses of the model was too small to show these phenomena.

In this paper we consider a hexagonal lattice of about 3000 cells, which is sufficiently large to study the formation of two-dimensional patterns. In our model, auxin is produced in all cells in the lattice and flows out of the lattice through a sink corresponding to the petiole. We consider the abundance of efflux carrier proteins such as PIN1, and assume that they change their abundance in response to the auxin net flux. We explore nine different functional forms that describe the dependence of carrier protein abundance on the flux. We also examine two different ways of controlling carrier protein numbers PIN1 and two types of auxin transport reaction kinetics by PIN1. Finally we identify conditions in which branching veins can be formed.

2. Self-organization model for vein formation

Mitchison (1981) considered the external movement of auxin with changes in membranes permeability from one cell to another and also the internal diffusion of auxin between different sides of a cell. Here we simplify Mitchison's model by assuming that auxin concentration is uniform within each cell. We consider a hexagonal lattice of cells in which a cell i has a

concentration Ai of auxin, a concentrations c_i of efflux carrier proteins free in cytoplasm, and a concentration $P_{i,j}$ of efflux carrier proteins embedded in the membrane on side j (j = 1,2,…,6) and active as carriers. We assume that cells use the net flux of auxin going through each side of their membrane as a cue to produce or to reallocate the carrier proteins appropriately.

2.1. Cell-to-cell auxin flux

Concerning the auxin flux from cell i to cell on side j, the simplest assumption is a linear form derived from the mass action law between auxin and carrier proteins:

Linear flux:

$$J_{i,j} = \frac{1}{2}\alpha\left(A_i P_{i,j} - A_j P_{j,i}\right), \tag{1a}$$

where $J_{i,j}$ is the net flux of auxin from cell i to cell j, α is the efficiency of a carrier protein. This equation is derived from the following argument. A single carrier protein in cell i causes efflux αA_i of auxin. The side of cell i facing cell j contains $P_{i,j}$ carrier proteins, and hence the auxin efflux from cell i to the intercellular space between i and j is $\alpha A_i P_{i,j}$. Auxin moving out of the cell into the intercellular space will randomly enter the next cell or return to the cell it originated from. If decay of auxin is neglected, half of the auxin efflux is effectively pumped into the neighboring cell j. Considering a similar process caused by carrier proteins in cell j in the side facing to cell i, we obtain Eq. (1a) as the net flux of auxin.

Since carriers are enzymes and auxin is substrate, we also investigated a Michaelis–Menten form for the reaction of auxin transport out of the cell. Hence the rate of transport would saturate for a high auxin concentration, as follows:

Saturating flux:

$$J_{i,j} = \frac{1}{2}\alpha\left(\frac{A_i}{k + A_i} P_{i,j} - \frac{A_j}{k + A_j} P_{j,i}\right), \tag{1b}$$

where α is the maximum speed of the transport reaction achieved when auxin concentration is very high. The Michaelis-Menten constant *k* indicates the auxin concentration achieving half of the maximum speed. If the auxin concentration is high enough to saturate the carriers, the total amount of auxin transported through the carriers on one side of the cell is close to $\alpha P_{i,j}$.

2.2. Dynamics of carrier protein concentrations

We consider two types of dynamics for the carriers. First, we assume that carriers of different sides of a cell are regulated independently:

Independent regulation model:

$$\frac{dP_{i,j}}{dt} = \lambda\left(\varphi\left(J_{i,j}\right) + q_m - P_{i,j}\right), \tag{2}$$

where λ is the turnover rate at which the carrier protein abundance responds to the auxin flux, q_m is the minimum density of carriers always embedded in the plasma membrane, $\varphi\left(J_{i,j}\right)$ is an increasing function of flux $J_{i,j}$ describing the response of the cell to the flux, by producing new carrier proteins or by allocating existing free proteins within the cytoplasm to the cell membrane. We will examine different possible functions for $\varphi\left(J_{i,j}\right)$ later.

An alternative assumption is that the number of carrier proteins per cell is fixed, or changes very slowly over time (Geldner et al., 2001). In this case, different sides of a cell must compete with each other for allocation of free carrier proteins. We consider the following dynamics of a free carrier proteins pool and the carrier proteins on different sides of the cell:

Reallocation model:

$$\frac{d\psi_i}{dt} = \lambda\left(\sum_{j=1}^{n} P_{i,j} - \psi_i \sum_{j=1}^{n}\left(\varphi\left(J_{i,j}\right) + q_a\right)\right), \tag{3a}$$

$$\frac{dP_{i,j}}{dt} = \lambda\left(\psi_i\left(\varphi\left(J_{i,j}\right) + q_a\right) - P_{i,j}\right), \tag{3b}$$

Here ψ_i is the abundance of free and inactive carrier proteins located in a cytoplasm compartment. Carrier proteins leave the cell membrane by mass action law to join the free carrier pool and are allocated from the free pool to the cell membrane with a rate depending on $\varphi(J_{i,j})$. q_a is the minimum carrier allocation value when there is no flux. Under the Reallocation model the number of carrier proteins is fixed and thus

$$\frac{d\psi_i}{dt} = -\sum_{j=1}^{n} \frac{dP_{i,j}}{dt}.$$

2.3. Auxin production rate

We assume that in the beginning stages of vein formation, cells contain some auxin and are able to produce it. Only one cell, located at the boundary of the domain, is the auxin sink and has its concentration of auxin set to zero. It represents the petiole of the leaf, through which auxin is flushed away.

We assume two steps in auxin production. First, let S_i be the concentration in cell *i* of a hypothetical enzyme that is responsible for synthesizing auxin. The production of S_i is inhibited by auxin and follows Eq. (4).

$$\frac{dS_i}{dt} = s\left[1 - \frac{A_i}{A_{eq}}\right]_+ - \delta S_i, \tag{4}$$

where $[x]_+ = x$ for $x > 0$ and $[x]_+ = 0$ for $x \le 0$. s is the maximum rate at which the auxin synthesizing enzymes S_i are produced, A_{eq} is the threshold auxin concentration such that if $A_i > A_{eq}$, S_i production is shut down, δ is the decay rate of S_i. Second, auxin in cell *i* is synthesized by S_i and follows the dynamics of Eq. (5).

$$\frac{dA_i}{dt} = \varepsilon S_i - \sum_{j=1}^{n} J_{i,j}, \tag{5}$$

where ε is the efficiency of the auxin synthesizing enzyme S_i.

2.4. Response functions

The response function φ, in Eqs. (2) and (3), increases with auxin flux *J*. At this point in time, sufficient knowledge of biological molecular processes is unavailable. Hence, we examine many possible φ functions which differ in the manner that they increase with *J*.

We consider nine functions of carrier protein production, or carrier protein reallocation, as candidates for the response to the auxin flux (as given in Table 1 and illustrated in Fig. 1). We assume $\varphi = 0$ if $J_{i,j}$ is negative, and we consider φ to be as in Table 1 when the net flux $J_{i,j}$ is positive. In other terms, the cell reacts only if the quantity of auxin going out through its membrane is larger than the quantity of auxin received from outside.

For the (1) *linear function*, the production or allocation of carrier proteins increases in proportion to the flux. For the (2) *square function*, the production or allocation of carrier proteins increases in proportion to square flux. (3) *Curvilinear function* has a derivative equal to zero at *J* = 0, behaving like a square function when *J* is small, but increases linearly with *J* when *J* is large. For the (4) *shifted linear function*, there is no carrier production or allocation if *J* is smaller than *b*, and production or reallocation increases linearly with *J* otherwise.

The production or reallocation of carrier proteins is an increasing function of the flux *J* and is given by $\varphi(J)$ in Eq. (2). These are classified in four groups based on the behavior of $\varphi(J)/J$. *a*, *b*, *h* and *k* are parameters.

For the (5) *square root function*, the production or reallocation of carrier proteins increases with *J*, but the rate of increase becomes slower for a larger *J*. For the (6) *saturating function*, the production or reallocation of carrier proteins increases rapidly when the flux is low and saturates to an asymptote when the flux is high. (7) *Divergent S-function* has a derivative equal zero at *J* = 0, and behaves like a square root function when J is large. (8) S-shape function has a derivative equal zero at *J* = 0. The production or allocation of carrier proteins is low for a small *J*, accelerates when *J* becomes larger, and saturates for a large *J*. Finally, with (9) step function, neither carrier protein production nor reallocation occurs if *J* is smaller than *b*, but carrier production or reallocation occurs at a constant rate when *J* is greater than *b*.

Table 1
Nine response functions.

Linear	(1) Linear function	$\varphi = aJ$
Accelerating	(2) Square function	$\varphi = aJ^2$
	(3) Curvilinear function	$\varphi = \dfrac{aJ^2}{1+J}$
	(4) Shifted linear function	$\varphi = a[J-b]_+$
Decelerating	(5) Square root function	$\varphi = a\sqrt{J}$
	(6) Saturating function	$\varphi = \dfrac{aJ}{k+J}$
S-like	(7) Divergent S-function	$\varphi = \dfrac{aJ^2\sqrt{J}}{k+J^2}$
	(8) S-shape function	$\varphi = \dfrac{aJ^2}{k+J^2}$
	(9) Step function	$\varphi = \begin{cases} h & \text{if } J \geqslant b \\ 0 & \text{if } J < b \end{cases}$

Among these nine functions, (2) square, (3) curvilinear, and (4) shifted linear functions share a common feature. The function value is relatively small for a small *J* and rapidly increases beyond some threshold. Opposite to the previous are the cases for (5) square root function and (6) saturating function, where the function is rather high for a small *J*, but increases slower as *J* becomes large. (7) Divergent S-function and (8) S-shape function contain a mixture of the two previous groups. The function is rather small for a small *J*, increases as *J* becomes larger, and finally the rate of increase diminishes for a high *J*. (9) Step function has a similar property.

By noting the behavior of the ratio $\varphi(J)/J$ these nine functions can be classified into four types: For response function (1), $\varphi(J)/J$ is constant. We call this function linear response function. For response functions (2)–(4), $\varphi(J)/J$ increases with *J*. We call these responses accelerating response functions. For response functions (5) and (6), $\varphi(J)/J$ decreases with *J*. We call these responses decelerating response functions. Finally, for response functions (7)–(9), $\varphi(J)/J$ is small for a small *J*, then becomes large for an intermediate *J*, and then becomes smaller for a large *J*. We call these responses S-like response functions.

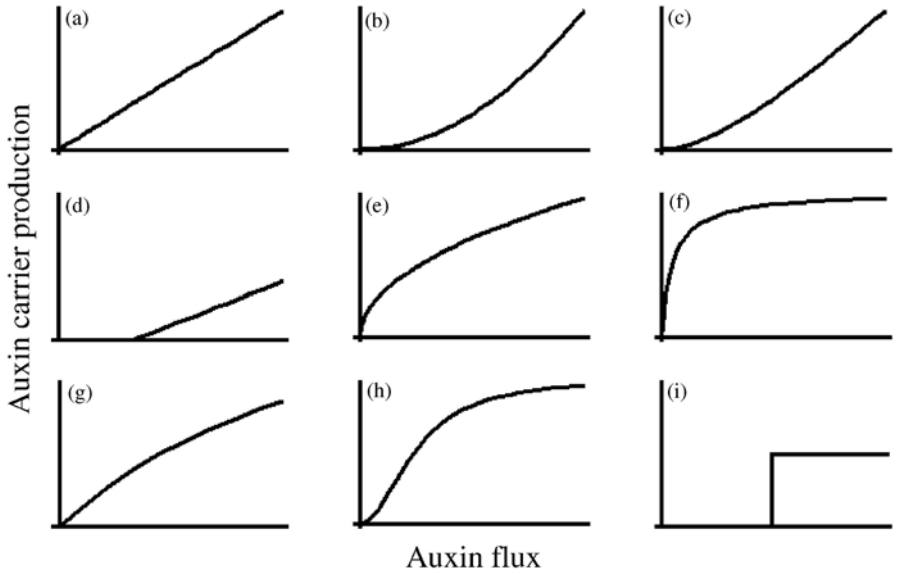

Fig. 1. Different protein production response according to the auxin flux. (a) Linear function, (b) square function, (c) curvilinear function, (d) shifted linear function, (e) square root function, (f) saturating function, (g) divergent ‘‘S’’ function, (h) S-shape function, (i) step function. Horizontal axis is for auxin flux.

3. Numerical analyses

3.1. Computer simulations

We performed the simulations on a hexagonal lattice of fixed size, consisting of 2912 cells, plus one playing the role of the auxin sink, all arranged inside an elliptic-shaped domain imitating a leaf primordium. Since we are mostly interested in the conditions of vein formation we did not perform the numerical analysis on a growing domain.

Each cell has 6 neighbors, except those at the boundary of the leaf/domain. Cells having one or more sides on the boundary cannot exchange auxin across it. The sink cell corresponds to the petiole of the leaf. Its auxin concentration is fixed at 0 throughout the simulations.

We also performed simulations on a smaller lattice of 230 cells, plus one sink, in order to increase spatial resolution scale, to appreciate the qualitative distribution of carrier proteins and orientation of the mean fluxes of cells in the principal patterns.

Initial concentration of auxin for all the cells is $A_i = A_{eq}$. A_{eq} is set to different values between simulations to give the least ambiguous results. We initialize carrier protein abundance to a constant, for all useable sides of all cells ($P_{i,j} = 0.1$). This initial condition corresponds to the

equilibrium value of carrier protein concentration in the absence of auxin flux; as we assume q_m = 0.1 for the independent regulation model (Eq. (2)) and ψ_i = 2 and q_a = 0.05 for the reallocation model (Eqs. (3a,b)).

The simulations were stopped: when the variables became extremely large; when the spatial pattern, and all the variables, became stationary; when the pattern was static, although auxin was still accumulating; or when leaking (Table 2) was observed before the pattern could be disturbed. We explored a wide range of parameters and attempted to grasp all the different typical spatial patterns (see Section 3.2). We especially examined the parameter range which generates the different branching patterns (Table 2).

3.2. Typical patterns

For an explanation of the different computer simulation results, we introduced a terminology listed in Table 2.

Through the simulations, with all our assumptions in a wide range of parameters, the model generated several typical spatial patterns, which are as follows:

(a) *Laminar orientation pattern*: The mean flux (Table 2) of all the cells is oriented toward the sink, irrespective of their distance from it. No veins (Table 2) are formed, and cellular concentration of auxin within the lattice remains uniform (Fig. 2a); or an increasing gradient toward the sink can occur, with total concentration stabilized (Fig. 2b); also displayed was an increasing gradient toward the sink, with an indefinite accumulation of auxin over time (Fig. 2b).

(b) *V-pattern*: Cellular mean auxin flux is oriented parallel to the lattice sector lines (Table 2) to which they are the closest. Cells on the bisectrix of the sector lines are oriented toward the sink, and have a higher auxin concentration to that of their neighbors (Fig. 2c).

(c) *Branching pattern*: Veins grow and bifurcate from the sink to the periphery without forming closed loops. Auxin concentration is higher in veins than in the surrounding cells (Fig. 2d).

(d) *Reversed branching pattern*: This is also a branching pattern, but auxin levels are lower in the veins than in the surrounding tissues (Fig. 2e).

(e) *Leaking pattern*: This pattern results from venous auxin leakage (Table 2). The total auxin concentration can keep increasing with time. Once leaking starts, waves of auxin move across the lattice destroying any pattern established.

Table 2 Terminologies used in describing the results

Mean flux and orientation/polarization of a cell: The vector having the carrier protein concentrations of the 6 sides of the cell as coordinates. If the cell has a high concentration of carriers on one side only and just the basic concentration of carriers on the other sides, then the cell is strongly oriented (in one direction), and the mean flux shows the direction. Preferential path/vein: A line of cells in which auxin flux is much higher than in surrounding cells and homogeneously oriented to form a stream. The downstream side of each cell is richer in carrier proteins than the other sides. Auxin concentration (not the flux) can be either higher or lower than in the surrounding tissues. Sector lines: The straight lines of slope 0, $-\sqrt{3}$ and $+\sqrt{3}$ separating the hexagonal lattice into 6 equal sectors. Leaking: Initially veins are formed, and then leaking starts. A vein cell suddenly starts pumping auxin out to the surrounding (non-vein) cells.

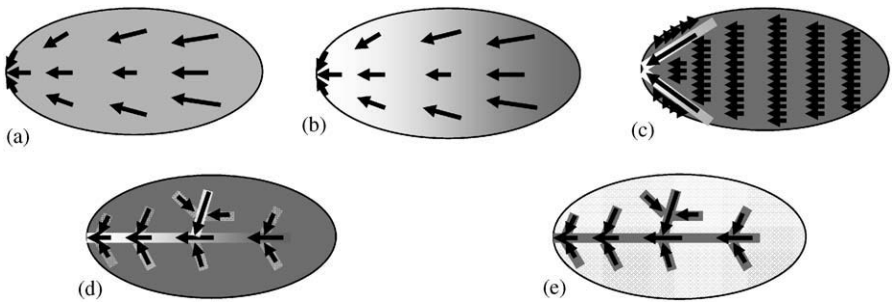

Fig. 2. Typical patterns observed with the models. (a) Laminar orientation without gradient of auxin, (b) laminar orientation with gradient of auxin, (c) V-pattern, (d) reversed branching pattern, (e) branching pattern. Light gray indicates high auxin concentration and dark gray low auxin concentration.

4. Results

We carried out computer simulations of all the combinations, of (1) the linear flux versus saturating flux, (2) independent carrier regulation versus competition for free carriers, and (3) all the nine response functions to the fluxes, i.e. $2 \times 2 \times 9 = 36$ cases in total. In the following section, we explain the results using four main categories corresponding to the four possible combinations of auxin flux dynamics and pump regulation, and in each category we describe the results obtained with the different response functions.

4.1. Linear flux and independent carrier protein regulation

We first consider the case in which the flux is non-saturating (Eq. (1a)) and the carrier protein concentrations are regulated independently (Eq. (2)).

The results greatly depend on the choice of response function $\varphi(J)$. For the linear response function (1), no preferential path (Table 2) is formed but we observe a laminar orientation of the cells' mean flux toward the sink as seen in Fig. 3a.

For accelerating response functions ((2)–(4)) and the S-like response functions ((7)–(9)), the model can create veins and bifurcations if A_{eq} is sufficiently high, giving rise to a reverse branching pattern (Figs. 3c and 4a, b). For the accelerating response functions, we observed that cells belonging to a vein are strongly polarized containing most carrier proteins in a single, downstream side of the cell. Also we often observed for these accelerating functions an extremely rapid increase followed by a rapid decrease in the carrier proteins concentrations of cells near the sink (see appendix *A* in third part for details), making simulations impossible for higher values of A_{eq}. The auxin concentration was also observed to be lower in the veins than in the surrounding tissue.

For S-like response functions ((7)–(9)), the model initially creates veins. However, if the auxin flux is high enough, veins begin to bifurcate, and cells at the bifurcation points start leaking (Fig. 3f). Leaking destroys all the established vein patterns.

In contrast, with decelerating response functions ((5) and (6)), the model displayed paths of high auxin concentration as a V-pattern, but no branching of paths was observed (Figs. 3b and 4c, d). Furthermore, cells with a high auxin concentration are not strongly polarized and send out the

hormone through two sides. Cells between the high concentration paths pump out auxin through their three sides which face in the direction of the sink (Fig. 4c, d).

4.2. Saturating flux and independent carrier protein regulation

If we adopt the Michaelis–Menten saturating flux, as in Eq. (1b), results of the 9 different response functions $\varphi(J)$ are as follows:

The linear response function gives laminar orientation (Fig. 3a) as in the previous section.

If α is too small, no pattern occurs for the other response functions. Therefore we set α high enough for a pattern to develop. Accelerating response functions ((2)–(4)) generate reverse branching patterns (Figs. 3c and 4a, b). We still have an extremely rapid increase of carrier protein concentrations followed by a rapid decrease causing simulations to stop even for a very small time step. The saturating response function (6) resulted in a V-pattern (same as Figs. 3b and 4c, d). Auxin continues to accumulate over time, in the two paths leading to the sink, when A_{eq} is high. For S-like response functions ((7)–(9)), reverse branching veins are produced first (Figs. 3c and 4a, b), and followed by leaking after veins bifurcate (Fig. 3f). Finally, the square root response function (5) gives irregular, unpredictable, but symmetric patterns (Fig. 3e). Groups of cells become polarized toward the sink, while others are polarized toward the opposite direction. No preferential paths are formed as each cell has several sides with a high carrier protein concentration.

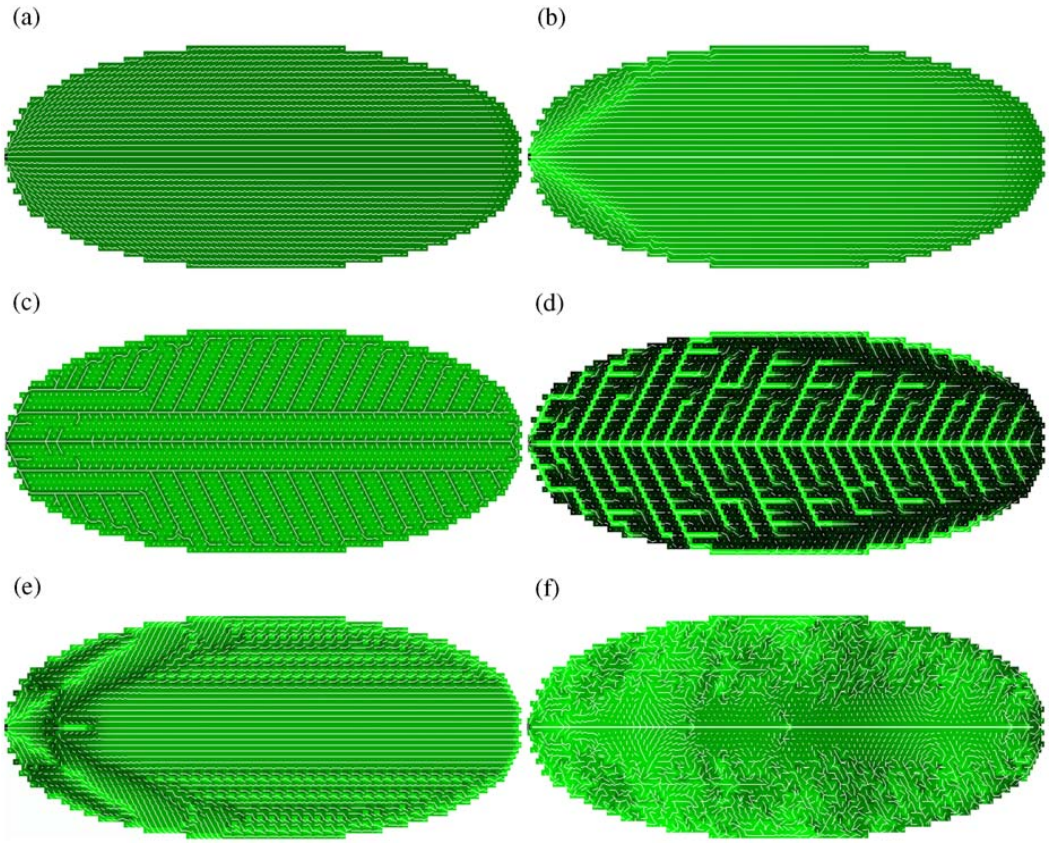

Fig. 3. Results of the numerical analysis. The number of cells in the lattice is 2912. The leftmost cell of the lattices is the sink of auxin, corresponding to the petiole. The white lines starting from the center of each cell indicate the orientation of the mean flux of the cell. Auxin level is represented by density plot. Light indicates higher level and dark indicates lower level. (a) Laminar orientation obtained with linear flux (Eq. (1a)), independent carrier protein regulation (Eq. (2)) and linear response function to the auxin flux ((1) in Table 1). A_{eq} **= 2 and** s **= 0.3. (b) V-pattern obtained with linear flux (Eq. (1a)), independent carrier protein regulation (Eq. (2)) and saturating response function (6).** A_{eq} **= 2,** s **= 0.2 and** h **= 1. (c) Reverse branching obtained with linear flux (Eq. (1a)), independent carrier protein regulation (Eq. (2)) and curvilinear response function to the auxin flux (3).** A_{eq} **= 3.5,** s **= 0.7,** h **= 1. (d) Branching pattern obtained with linear flux (Eq. (1a)), carrier protein reallocation (Eqs. (3a) and (3b)) and curvilinear response function to the auxin flux (3).** A_{eq} **= 0.7,** s **= 0.18,** h **= 1,** α **= 6 and** k **= 0.05. (e) Chaotic pattern obtained with saturating flux (Eq. (1b)), independent carrier protein regulation (Eq. (2)) and the square root response function to the auxin flux (2).** A_{eq} **= 1.96,** s **= 0.2,** k **= 1. (f) Leaking pattern obtained with linear flux (Eq. (1a)), independent carrier protein regulation (Eq. (2)) and the ‘‘S’’ shape response function to the auxin flux (8)** A_{eq} **= 1.15,** s **= 0.17 and** h **= 1. In all the simulations,** a **= 1,** α **= 2,** δ **= 1,** q_m **= 0.1,** q_a **= 0.05,** ψ_i **= 2,** λ **= 1 and** ε **= 1 unless stated otherwise.**

4.3. Linear flux and carrier protein reallocation

Now let us consider the case in which cells contain a fixed number of carrier proteins, allocating them to any side according to auxin fluxes.

Response function (1) gives a laminar orientation with an auxin gradient increasing toward the sink. The spatial patterns are similar to those described in the previous sections.

The most striking difference between the results of the previous two sections and the following two sections is the spatial distribution of auxin. For the accelerating response functions ((2)–(4)), veins include higher levels of auxin than in the surrounding tissues and have an increasing auxin concentration gradient as we move along a vein, from the tip to the sink; at equilibrium, auxin level is stabilized to a finite value (Fig. 3d).

Decelerating response functions ((5) and (6)) generate again the V-pattern displayed in Figs. 3b and 4c, d. Auxin levels increase from the tips of the V-shape to the sink.

S-like response functions ((7)–(9)) produce veins initially for a small A_{eq} (Fig. 3d), and following the branching process, leaking occurs. In the present case, when a vein cell starts leaking, it pumps auxin into adjacent non-vein cells, which in turn, pump auxin back into the neighboring not yet leaking vein cells. Subsequently these adjacent vein cells start leaking. When A_{eq} is not too large, this chain reaction can produce thicker veins. Auxin accumulates in the lattice until the leaking stops spreading or fills the entire leaf. When A_{eq} is large the model does not start with a branching pattern and generates only a V-patterns. No destruction of the pattern occurs and auxin levels are stabilized to a finite value.

When k is large, well-defined veins quickly form before any leaking occurs, even for high values of A_{eq}.

4.4. Saturating flux and carrier protein reallocation

In all the cases, we observed the unlimited accumulation of auxin over time in veins, which is due to the saturating flux function.

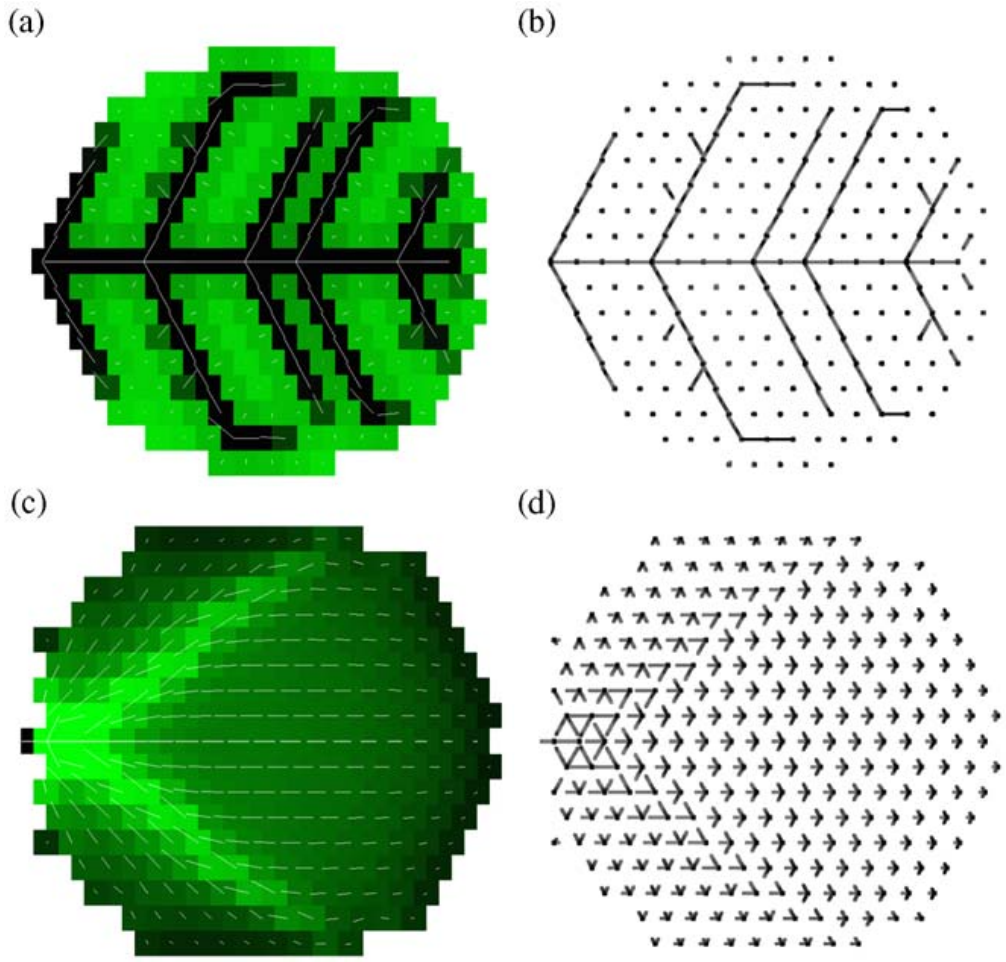

Fig. 4. Contrasts between auxin levels, auxin fluxes and carrier protein concentrations, in the case of strongly polarized and weakly polarized cells. The number of cells in the lattice is 230. The leftmost cell in the lattices is the sink of auxin, corresponding to the petiole. On the left, parts (a) and (c), auxin level is represented by density plot. Light indicates higher levels and dark indicates lower levels. Mean auxin fluxes of cells are indicated by white lines starting from the center of each cell. On the right, parts (b) and (d), the concentrations of the carrier proteins on each of the six sides of the cells are indicated by the black lines starting fromthe center of each cell. For all parts (a, b, c and d), long white or black lines indicate respectively high mean auxin flux, or high carrier protein concentration on the corresponding side. (a) and (b) Linear flux, independent carrier protein regulation, square response function, A_{eq} = 2.44, s = 0.55, q_m = 0.1, a = 1, α = 2. In (b) the cells exhibit only one side with a dominant carrier protein concentration. Cells belonging to a vein have only one carrier with a high concentration oriented downstream to the sink, and the other carriers to the minimum value; hence cells are strongly polarized. The mean fluxes are well superposed to the most abundant carrier protein. (c) and (d) Linear flux, independent carrier protein regulation, square root response function A_{eq} = 2, s = 0.3, q_m = 0.1, a = 1, α = 2. The mean fluxes in (c) are oriented toward the base of the leaf and not preferentially toward the two lines rich in auxin. Carrier protein concentrations in (d) show that each cell has

more than one side rich in carrier proteins, hence cells are not strongly polarized. Other parameters are: a = 1, δ = 1, λ = 1 and ε = 1.

Consequently veins have a higher auxin concentration than the surrounding cells. Response functions (1), (5) and (6) generated qualitatively similar patterns as described for these functions in Section 4.1, and response function (2)–(4) and (7)–(9) generated patterns similar to those described in Section 4.3. Although accelerating functions in Section 4.1 often gave rise to an extremely rapid increase followed by sudden decrease in carrier protein abundance, the simulations using these functions in this section did not exhibited this feature.

5. Discussion

We have studied the conditions in which the self-organization of a vascular system-like pattern can be achieved by interrelated dynamics of auxin flux and carrier proteins. This is based on the hypothesis proposed by Sachs (1975) and studied by Mitchison (1981). We observed that several assumptions of the model have strong effects on the possibility of developing vein patterns similar to those observed in real plant leaves.

First, the model can generate stable inhomogeneous distributions of auxin, resulting in pathways that branch and avoid collision. These pathways may have either lower or higher concentrations of auxin relative to surrounding cells.

Second, the likelihood of obtaining veins is very sensitive to the regulation of carrier protein concentrations by auxin flux as described by $\varphi(J)$. The accelerating and S-like response functions (in Table 1 and shown in Fig. 1b, c, d, g, h and i) can give rise to a pattern of branching veins. A linear response function can also maintain the pattern once it is created, such as response functions (2) and (3). In contrast, for the decelerating response functions (shown in Fig. 2e, f), the model generates mostly V-patterns that do not branch. The accelerating and S-like response functions differ from the decelerating response functions by the behavior of $\varphi(J)/J$ near the origin.

Third, when branching veins are formed, there are two distinct cases concerning auxin concentration in veins. In reversed branching patterns, such as Figs. 3c and 4a, b, the concentration of auxin is lower within veins than in the surrounding tissues. This can occur when the number of

carrier proteins in any region of the cell's membrane is regulated independently of the number of proteins in other regions of the cell. On the other hand, if carrier protein regulation is achieved mainly by competition for the allocation of free carrier proteins, where an increase of carrier proteins in a portion of the cell's membrane tends to inhibit the increase of the number of carrier proteins in other regions of the same cell's membrane, whilst the total number of proteins is fixed, then non-reversed branching patterns are likely to be formed. This is demonstrated by Fig. 3d, which corresponds to carrier protein Eqs. (3a) and (3b). Although the veins are richer in auxin, they do not exhibit leaking if the accelerating response functions ((2)–(4)) are adopted.

Fourth, compared with the choices of response function and carrier protein regulation, the choice of linear or saturating flux as a function of auxin levels in two adjacent cells, i.e. the choice between Eqs. (1a) and (1b), does not have a strong influence on the formation of vein patterns.

Fifth, there are many patterns that show leaking. This can occur if a vein system is formed, and if the response functions is of S-like type ((7)–(9)).

5.1. Leaking

In instances where leaking occurs, a pulse will ‘‘push’’ away auxin from the vein, creating a wave with no preferential direction which starts from the leaking site and spreads among the normal cells.

Furthermore, we often observed the formation of small cycles, or rings, of three or four cells with circulating auxin, creating self-enhanced isolated systems. This is consistent with Sachs' observations on fragments of radish (explained in Mitchison 1981). When auxin is applied to one side of the fragment, the opposite side presents these kinds of vascular cell cycles. This type of vein formation, caused by pulsing auxin out from the extremity of an elongating vein is not likely to create well-structured branching veins. To drive the auxin flushing tip of an elongating vein toward the right direction (i.e. an auxin sink), cells receiving auxin from the tip of this vein need to be ‘‘partially induced’’ in some direction (Sachs, 1991) in order to lead this vein's auxin flow correctly. Otherwise, the vein wanders and can eventually meet itself, creating a ring with circulating auxin.

5.2. Response function and branching

We observed that the branching vein formation critically depends on the choice of response function $\varphi(J)$. Concerning the reason why $\varphi(J)$ determines the formation of branching, we may develop the following intuitive argument: Considering a cell that receives a strong flux from one of its neighbors, and has 5 other neighbors which are almost equivalent to each other. The focal cell tends to move carrier proteins into the 5 portions of the plasma membrane which are in contact with its neighbors, to redistribute the received flux among the five neighboring cells. Then we ask whether all of these 5 portions tend to equilibrate their outgoing auxin flux or if one of them monopolizes the total flux. If the response function increases faster than linear, then one that happens to have slightly more carrier proteins than the others will have a higher flux. It will tend to increase its carrier protein concentration more than proportionally, resulting in the monopoly of the auxin flux (se appendix *B* in third part for analysis). A preferential auxin path emerges, and possibly a branching pattern (Figs. 3c, d and 4a, b). In the carrier reallocation model the monopoly is reinforced by competition for free carrier proteins.

5.3. Higher auxin concentration in veins

In the case of carrier reallocation model, total carrier protein abundance is constant. For a strongly oriented cell, all the carrier proteins are present on one side. Thus the outgoing flux is proportional only to the internal auxin concentration since carrier concentration on that side becomes constant. This allows an increase of cellular auxin concentration. Subsequently we obtain a branching pattern in which vein cells have a higher concentration of auxin than normal cells.

This result is consistent with experimental observations (Uggla et al., 1996; Avsian-Kretchmer et al., 2002; Mattson et al., 2003). It seems that a higher concentration of auxin in the pre-procambial cells is necessary for correct orientation of cell division (Petrasek et al., 2002). Note that this is contrary to the expectation of Mitchison (1981) who stated that the auxin concentration needs to be lower in the preferential path than in the surrounding tissue, as seen in reversed branching patterns.

According to our study, branching patterns are formed when carrier proteins are regulated by competition between regions of a cell membrane, as given by the reallocation model (Eqs. (3a)

and (3b)), whilst reverse branching patterns are formed when carrier proteins in different regions of the cell membrane are regulated independently of the others (Eq. (2)). Hence the experimental results suggest that the carrier protein should be regulated by competition as given by Eqs. (3a,b), which is consistent with another observation that the total number of proteins within a cell changes very slowly (Geldner et al., 2001). The rapid turnover between different parts of a cell needs to be tested by more direct experiments.

The theoretical study in this paper is just a beginning of a more comprehensive modeling of the phenomena. There are several points we need to address in future studies. First we could find conditions in which branching veins are formed and why in our study we found no closed loops, although loops are formed in the network of some plant leaves. Second there are many mutants of vein pattern formation, especially in Arabidopsis. Some of these mutants show discontinuous veins (Carland et al., 1999; Deyholos et al., 2000; Koizumi et al., 2000) which seem to be difficult to produce using the model studied in this paper. The reason may be that we consider a global and uniform auxin production, and not, for instance, only in the margin. Tohya and Mochizuki (in press) recently developed a reaction–diffusion model that is able to explain the formation of discontinuous veins. Fujita and Mochizuki (in press) studied the pattern formation produced by auxin and its carrier protein, and found patch-like network patterns. Couder et al. (2002) proposed tensorial field cracks formation as a potentially useful model for leaf vein development (Couder et al., 2002; Bohn et al., 2002). We need to examine how these different theories might be related to the formation of vein networks in plants. Finally the leaf pattern formation of real plants occurs on a dynamically growing region. Modeling vein formation in a growing domain, incorporating knowledge of molecular biology, is an important future problem of theoretical biology.

Acknowledgment

This work has been done with an exchange program for Japanese and French doctoral students entitled Collège Doctorale Franco-Japonais. The work has also received the support of a grant-in-aid for scientific research of JSPS to YI. FGF would like to thank his French co-Director, Professor Jacob Koella, for his kind advice; and Shôko Sakurai for her support.

All figures, except in the appendices, are from Feugier, Francois G., Mochizuki, A., Iwasa, Y., 2005. Self-organization of the vascular system in plant leaves: Inter-dependent dynamics of auxin flux and carrier proteins. Journal of Theoretical Biology 236 (2005) 366–375.

References

Aloni, R., 2001. Foliar and axial aspects of vascular differentiation: hypotheses and evidence. J Plant Growth Regul 20, 22–34.

Aloni, R., Schwalm, K., Langhans, M., Ullrich, C.I., 2003. Gradual shifts in sites of free-auxin production during leaf-primordium development and their role in vascular differentiation and leaf morphogenesis in Arabidopsis. Planta 216, 841–853.

Avsian-Kretchmer, O., Cheng, J.-C., Chen, L.J., Moctezuma, E., Sung, Z.R., 2002. Indole acetic acid distribution coincides with vascular differentiation pattern during Arabidopsis leaf ontogeny. Plant Physiol 130, 199–209.

Bohn, S., Andreotti, B., Douady, S., Munzinger, J., Couder, Y., 2002. Constitutive property of the local organization of leaf venation networks. Phys. Rev. E 65 art no. 061914.

Carland, F.M., Nelson, T., 2004. COTYLEDON VASCULAR PATTERN2-mediated inositol (1,4,5) triphosphate signal transduction is essential for closed venation patterns of Arabidopsis foliar organs. Plant Cell 16, 1263–1275.

Couder, Y., Pauchard, L., Allain, C., Adda-Bedia, M., Douady, S., 2002. The leaf venation as formed in a tensorial field. Eur. Phys. J. B 28, 135–138.

Deyholos, M.K., Cordner, G., Beebe, D., Sieburth, L.E., 2000. The SCARFACE gene is required for cotyledon and leaf vein patterning. Development 127, 3205–3213.

Feugier, F.G., Mochizuki, A., Iwasa, Y., 2005. Self-organization of the vascular system of plant leaves: Inter-dependant dynamics of auxin flux and carrier proteins. J. Theor. Biol. 236, 366–375.

Fujita, H., Mochizuki, A., 2006. Pattern formation of leaf veins by the positive feedback regulation between auxin flow and auxin efflux carrier. J. Theor. Biol., (in press).

Fukuda, H., 2004. Signals that control plant vascular cell differentiation. Nat. Rev. Mol. Cell Biol. 5, 379–391.

Foster, A.S., Gifford Jr., E.M., 1974. Comparative Morphology of Vascular Plants. W.H. Freeman and Company, San Francisco.

Goldsmith, M., 1977. The polar transport of auxin. Annu. Rev. Plant Physiol. 28, 349–378.

Jacobs, W.P., 1952. The role of auxin in the differentiation of xylem around a wound. Am. J. Bot. 39, 327–337.

Jönsson, H., Heisler, M.G., Shapiro, B.E., Meyerowitz, E.M., Mjolsness, E., 2006. An auxin-driven polarized transport model for phyllotaxis. Proc. Natl. Acad. Sci. USA 103 (5), 1633–1638.

Koizumi, K., Sugiyama, M., Fukuda, H., 2000. A series of novel mutants of Arabidopsis thaliana that are defective in the formation of continuous vascular network: calling the auxin signal flow canalization hypothesis into question. Development 1127, 3197–3204.

Koizumi, K., Naramoto, S., Sawa, S., Yahara, N., Ueda, T., Nakano, A., Sugiyama, M., Fukuda, H., 2005. VAN3 ARF–GAP-mediated vesicle transport is involved in leaf vascular network formation. Development 132, 1699–1711.

Mattson, J., Sung, Z.R., Berleth, T., 1999. Responses of plant vascular systems to auxin transport inhibition. Development 126, 2979–2991.

Mattson, J., Ckurshumova, W., Berleth, T., 2003. Auxin signaling in Arabidopsis leaf vascular development. Plant Physiol 131, 1327–1339.

Mitchison, G.J., 1980a. A model for vein formation in higher plants. Proc. R. Soc. London B 207, 79–109.

Mitchison, G.J., 1980b. The dynamics of auxin transport. Proc. R. Soc. London B 209, 489–511.

Mitchison, G.J., 1981. The polar transport of auxin and vein pattern in plants. Philos. Trans. R. Soc. London B 295, 461–471.

Morris, D.A., 2000. Transmembrane auxin carrier systems-dynamic regulators of polar auxin transport. Plant Growth Regul. 32, 161–172.

Motose, H., Sugiyama, M., Fukuda, H., 2004. A proteoglycan mediates inductive interaction during plant vascular development. Nature 429, 873–878.

Paciorek, T., Zazimalova, E., Ruthardt, N., Petrasek, J., Stierhof, Y.-D., Kleine-Vehn, J., Morris, D.A., Emans, N., Jurgens, G., Geldner, N., Friml, J., 2005. Auxin inhibits endocytosis and promotes its own efflux from cells. Nature 435, 1251–1256.

Pyo, H., Demura, T., Fukuda, H., 2004. Gradual shifts in sites of free-auxin production during leaf-primordium development and their role in vascular differentiation and leaf morphogenesis in Arabidopsis. Plant Cell Physiol 45 (10), 1529–1536.

Rolland-Lagan, A.-G., Prusinkiewicz, P., 2005. Reviewing models of auxin canalization in the context of leaf vein pattern formation in Arabidopsis. Plant J. 44, 854–865.

Runions, A., Fuhrer, M., Lane, B., Federl, P., Rolland-Lagan, A.-G., Prusinkiewicz, P., 2005. Modeling and visualization of leaf venation patterns. ACM Trans. Graphics 24 (3), 702–711.

Sachs, T., 1975. The control of the differentiation of vascular networks. Ann. Bot. 39, 197–204.

Sachs, T., 1981. The control of the patterned differentiation of vascular tissues. Adv. Bot. Res. 9, 152–162.

Sachs, T., 1989. The development of vascular networks during leaf development. Curr. Top. Plant Biochem. Physiol. 8, 168–183.

Sachs, T., 1991. Cell polarity and tissue patterning in plants. Dev. Suppl. 1, 83–93.

Sack, L., Cowan, P.D., Holbrook, N.M., 2003. The major vein of the mesomorphic leaves revisited: tests for conductive overload in Acer saccharum (Aceraceae) and Quercus rubra (Fagaceae). Am. J. Bot. 90 (1), 32–39.

Scarpella, E., Francis, P., Berleth, T., 2004. Stage-specific markers define early steps of procambium development in Arabidopsis leaves and correlate termination of vein formation with mesophyl differentiation. Development 131, 3445–3455.

Sieburth, L.E., 1999. Auxin is required for leaf vein pattern in Arabidopsis. Plant Physiol 121, 1179–1190.

Smith, R.S., Guyomarc'h, S., Mandel, T., Reinhardt, D., Kuhlemeier, C., Prusinkiewicz, P., 2006. A plausible model of phyllotaxis. Proc. Natl. Acad. Sci. USA 103 (5), 1301–1306.

Steynen, Q.J., Schultz, E.A., 2003. The FORKED genes are essential for distal vein meeting in Arabidopsis. Development 130, 4695–4708.

Uggla, C., Moritz, T., Sandberg, G., Sundberg, B., 1996. Auxin as a positional signal in pattern formation in plants. Proc. Natl Acad. Sci. USA 93, 9282–9286.

- Second article -

How canalization can make loops: A new model of reticulated leaf vascular pattern formation

François G. Feugier, Yoh Iwasa

Abstract

Formation of the vascular system in plant leaves can be explained by the canalization hypothesis which states that veins are formed in an initially homogeneous field by a self-organizing process between the plant hormone auxin and auxin carrier proteins. Previous models of canalization can generate vein patterns with branching but fail to generate vein patterns with closed loops. However, closed vein loops are commonly observed in plant leaves and are important in making them robust to herbivore attacks and physical damage. Here we propose a new model which generates a vein system with closed loops. We postulate that the ‘‘flux bifurcator’’ level is enhanced in cells with a high auxin flux and that it causes reallocation of auxin carriers toward neighbouring cells also having a high bifurcator level. This causes the auxin flux to bifurcate, allowing vein tips to attach to other veins creating vein loops. We explore several alternative functional forms for the flux bifurcator affecting the reallocation of efflux carriers and examine parameter dependence of the resulting vein pattern.

1. Introduction

In multicellular organisms it is of crucial importance to distribute the nutrients and oxygen each cell needs to survive. This can be achieved by simple diffusion when the organism is small and/or thin and the resources are easily accessible (for instance algae). However, for many terrestrial plants this can be achieved more efficiently by using a network of tubes. In leaves of higher plants very diverse shapes of vascular systems are observed ranging from long parallel major veins interconnected by short secondary veins in monocotyledons, through open branching in ferns, to reticulated networks in the dicotyledons (Foster and Gifford, 1974).

Reticulated networks may have a robustness advantage against damage due to their redundancies—even when physical damage occurs, fluids can use a different path so the whole leaf is still well supplied (Sack et al., 2003). This gives the leaves more resistance to herbivores and pathogens. The vascular system is formed by a self-assembly process involving complex interactions which are still not well understood. Nevertheless, it is well known that the plant hormone auxin is involved in this process (Jacobs, 1952; Mitchison, 1981; Uggla et al., 1996; Mattson et al., 1999; Sieburth, 1999; Avsian-Kretchmer et al., 2002; Aloni et al., 2003; Fukuda, 2004).

Auxin is produced in the shoots of the plant and is transported at constant speed through the whole plant toward the roots (Goldsmith, 1977). This transportation of auxin depends on a trans-membrane efflux carrier protein called PIN1 (Sachs, 1991; Morris, 2000). Auxin can enter passively into the cell but needs PIN1 to leave it. It has been observed that the position of PIN1 proteins in the cell membrane is not uniform but polar and, moreover, depends on the presence of auxin (Paciorek et al., 2005).

This gives auxin a polar movement in plant organs. Recent works show that auxin can increase the concentration of PIN1 in the membrane to enhance its own efflux from the cell (Paciorek et al., 2005).

Sachs (1981, 1991) proposed a canalization hypothesis which suggests that the paths of auxin flux are formed by a self-organization process in which cells become polarized toward the auxin flux they experience, and that the auxin paths thus formed become vascular bundles later. Mitchison (1980a,b, 1981) studied a model based on the self-enhancement of the flux and showed the formation of preferential paths of auxin flows. His model predicts lower auxin concentration in

the formed paths than in the surrounding cells which is inconsistent with recent experiments suggesting a higher concentration of auxin inside files of cells, presaging the formation of vascular bundles (Uggla et al., 1996; Avsian-Kretchmer et al., 2002; Mattson et al., 2003).

Feugier et al. (2005) studied models of leaf vein formation based on canalization. In their models cell-tocell transportation of auxin is polarized due to redistribution of auxin carriers within each cell. They considered a series of models with different assumptions concerning auxin flux formation under given carrier protein dynamics (and vice versa) on a hexagonal lattice with uniform auxin production in which a cell located in the margin of the lattice, indicating the petiole of a leaf, acts as an auxin sink. The carrier protein concentration in the membrane on different sides of a cell increases with the intensity of the auxin outflux on that side. Branching veins are only likely to form if the carrier protein concentration increases in an accelerating fashion with respect to the auxin flux (Feugier et al., 2005). Feugier et al. also demonstrated that different sides of a cell need to compete for the allocation of carrier proteins in order to explain experimental observations of higher auxin concentrations in the paths than the surrounding cells. If the amount of carrier proteins on different sides of a cell's membrane is regulated independently the auxin concentration in the final pattern is lower in the paths than in the surrounding cells.

However, no loops were produced in the open branching patterns obtained by Feugier et al. (2005). An auxin preferential path can repeatedly bifurcate, resulting eventually in a branching vein system, but cannot attach to another one to create an area enclosed by veins. Fujita and Mochizuki (2006) modeled the canalization hypothesis with auxin and auxin carriers but they also failed to generate patterns with vein loops.

Among ferns we find species in which leaves have no loops (open venation) although other species exhibit reticulate venation (Foster and Gifford, 1974). Experiments with Arabidopsis found mutant plants with open branching venation but no closed loops of veins (Steynen et al., 2003; Carland and Nelson, 2004; Motose et al., 2004). This suggests that there might be an additional process working to connect veins and to make closed loops that is not involved in vein formation itself. Furthermore, mutants showing discontinuous venation (Deyholos et al., 2000; Koizumi et al., 2000, 2005) suggest that simple canalization mechanism may not be enough to explain vascular formation in plant leaves.

The difficulty of forming a closed loop of veins (i.e. a closed loop of auxin preferential paths) in canalization models can be illustrated by considering the way a loop is formed. In the leaf

of Arabidopsis, a loop is formed when the tip of a vein is attached with another older vein (Scarpella et al., 2004, p. 3447, caption to Fig. 1). When this occurs we believe the flux of auxin bifurcates at the connection point of the vein (Fig. 1) giving a domain of cells enclosed by a loop of veins. The cell at that point has two faces with a positive outflux of auxin, creating as a result a flux bifurcation.

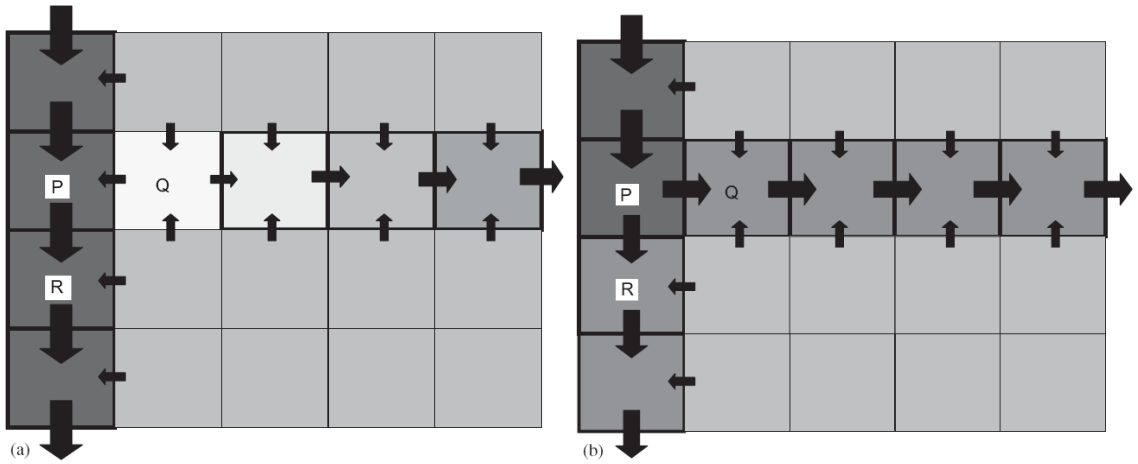

Fig. 1. Difference between no vein junction and vein junction. Arrows show the auxin flux direction and size indicates auxin flux strength. Gray background indicates the concentration of auxin in the cell. Light gray: low level; dark gray: high level. (a) Without flux bifurcator. Cell P is sending auxin only to cell R. Cell Q receives no flux from cell P, and the flux does not bifurcate. The vein ending by the cell Q may stop its progression in this situation or make a u-turn and continue growing elsewhere. (b) With flux bifurcator. Cell P makes the flux bifurcation and has outflux to cell R and to cell Q.

On the other hand, a cell with only one outflux of auxin but several influxes, creates a flux junction. According to a study of the shape of the response function in canalization models (Feugier et al., 2005) auxin preferential paths can be formed only when each cell has a single side in which auxin carriers are concentrated, which corresponds to accelerating response functions. On the other hand, if we choose response functions that allow two or more faces having auxin carriers then preferential paths and hence branching patterns will not be formed. In models with an accelerating response function, when branching patterns are formed the streams of auxin can merge but cannot bifurcate. As a consequence loops of veins and reticulate venations are difficult to form.

In this paper, we introduce a new model which is able to create preferential paths of auxin which can form closed loops. In each cell we consider a variable named auxin ‘‘flux-bifurcator’’ that describes a process making possible to attach the tip of a preferential path to the side of another path by allowing the cell at the connection point to share its auxin flux.

2. Model

In the model studied by Feugier et al. (2005), carrier protein allocation can increase in response to auxin outflux. Here we add a new variable to the model. It allows a cell already having a strong flux on one side to reallocate carriers to another side without flux but facing an incoming vein tip. We call this variable the ‘‘flux bifurcator’’. A high level of this variable in a cell indicates that the cell experiences a high outflux and hence is likely to be part of a vein. When two cells both having high levels of flux-bifurcator are adjacent, the reallocation of auxin carriers toward the adjacent cell can start, even in the absence of auxin flux between them (Fig. 1a and b). The flux-bifurcator may not be a single molecule, but a process including a number of genes and proteins.

We consider a cell i with a concentration A_i of auxin, and concentrations P_{ij} of carrier proteins on the side facing its neighboring cell j. Auxin can leave cell i to enter a neighboring cell j by going through carrier proteins P_{ij}. Reciprocally, auxin can leave cell j through carrier proteins P_{ji} to enter cell i. Auxin meets carrier proteins by mass action law. The resulting net flux of auxin J_{ij} leaving cells i and entering cell j is defined as:

$$J_{ij} = \frac{1}{2}\alpha\left(A_i P_{ij} - A_j P_{ji}\right), \tag{1}$$

where a is efficiency of the carrier proteins. Each cell produces auxin and in the absence of flux J has concentration Aeq at which auxin production equals auxin decay. The dynamics of auxin concentration A_i in cell i surrounded by n neighbors follows:

$$\frac{dA_i}{dt} = r\left(1 - \frac{A_i}{A_{eq}}\right) - \sum_{j=1}^{n} J_{ij}\,, \tag{2}$$

where r is the maximum production rate and r/A_{eq} is the destruction rate.

Let B_i be the flux-bifurcator level in cell i. We assume that the flux-bifurcator is activated in proportion to the sum of the carrier allocation strengths on different sides of cell i and that the strength of carrier protein allocation is the square of the magnitude of the auxin outflux (see below). Dynamics of the flux-bifurcator level are

$$\frac{dB_i}{dt} = \lambda\left(\sum_{j=1}^{n}\left[J_{ij}\right]_+^2 - B_i\right), \tag{3}$$

where λ is the reaction speed, $[x]_+ = x$ if $x \geq 0$ and $[x]_+ = 0$ if $x < 0$.

Carrier proteins in a cell i are allocated to different sides according to two forces. The first is pure canalization which is proportional to $\left[J_{ij}\right]_+^2$ on the side facing neighboring cell j. The second is caused by the flux-bifurcator level B_j of neighboring cell j combined with the focal cell's flux-bifurcator level B_i. The cell i will allocate carrier proteins on a second side only if both B_j and B_i are sufficiently large. Carrier protein dynamics are defined as

$$\frac{dP_{ij}}{dt} = \psi\left(\left[J_{ij}\right]_+^2 + \eta\left(B_i, B_j\right) + q\right) - \delta P_{ij}, \tag{4}$$

where $\psi = T - \sum_{j=1}^{n} P_{ij}$ is the amount of free carriers and T is the total amount of carriers in cell i. B_i and B_j are the flux-bifurcator levels in cells i and j, respectively. $\eta\left(B_i, B_j\right)$ is the term for the interaction between B_i and B_j of two neighboring cells. We call $\eta\left(B_i, B_j\right)$ the ''cell coupling function''. $\eta\left(B_i, B_j\right)$ increases both with B_i and with B_j. We will examine several alternative forms for this. q is the background allocation of carriers and δ is the rate at which allocated carriers return to the free carriers pool.

Except for flux-bifurcator in Eq. (3) and the cell-coupling function in Eq. (4), this model is similar to the ''reallocation model'' (Eqs. (3a,b)) with ''Linear flux'' (Eq. (1a)) and the

‘‘accelerating square response function’’ in Feugier et al. (2005). Additional minor changes are: auxin is produced in one step instead of two steps; auxin can be decomposed

(i.e. the first term of Eq. (2) can be negative).

3. Simulations

Most simulations were done on an elliptic domain containing 4042 cells with hexagonal neighborhood. One of the cells at the border of the lattice was a sink of auxin and played the role of a vein connected to the petiole of the leaf. The auxin concentration at the sink was fixed at 0 throughout the simulations. Cells at the margin of the domain have less than six neighbors and only exchanged auxin toward sides with a neighboring cell. Initial concentration of auxin for all the cells was $A_i = A_{eq} + \varepsilon$ where ε was a small amount of random noise added during the simulations.

We used the Euler method with a time step of 0.01. The simulations were stopped either when the spatial pattern became stationary or when the patterns were thought to be non-convergent. We examined the parameter range for which different choices of $\eta(B_i, B_j)$ generated different branching patterns. In all the simulations: $\alpha = 1$, $a = 1.2$, $A_{eq} = 2.2$, $\delta = 1$, $\lambda = 1$, $k_1 = 0.3$, $k_2 = 1$, $r = 2$, $T = 4$ and $q = 1/6$ unless stated otherwise. a, k_1 and k_2 are defined later. By this choice of q half of the total carrier proteins are allocated in the absence of auxin flux.

4. Results: vein patterns

When the simulations start, preferential paths of auxin emerge from the cells near to the sink and begin to grow. Auxin flows into a path by the sides but especially around its tip, and is transported toward the sink in the path. Then the path elongates slowly for as long as enough auxin enters its tip.

The model in the absence of flux-bifurcator is given by $\eta(B_i, B_j) = 0$ in Eq. (4), and is similar to the one studied by Feugier et al. (2005) and shown in their Fig. 3d. The result is illustrated in Fig. 2a. No closed vein loops were formed.

4.1. Alternative choices of the cell coupling function

The simplest cell-coupling function is the product of flux-bifurcator levels in two adjacent cells:

$$\eta\left(B_i, B_j\right) = aB_iB_j\,, \tag{5}$$

where a is the strength of the coupling. If two adjacent cells both have a high bifurcator level it is likely that both are vein cells. Using the additional Eq. (5) term in Eq. (4) might help in forming loop of veins in a situation illustrated in Fig. 1. According to the simulation results, however, the model with Eq. (5) is not promising. Veins start growing from the sink, but at some distance from it veins stop growing, then shrink, then grow again. The pattern shows oscillations and does not converge. This anomalous behavior can be explained by a sensitive dependence of the coupling term η on the flux. Consider two consecutive cells *i* and *j* in a linear vein along which auxin flows. The term for canalization in Eq. (4) is proportional to $\left[J_{ij}\right]_+^2$, as well as the bifurcator level given by Eq. (3). Since they experience approximately the same outflux the product of both flux-bifurcator levels in the coupling function from Eq. (5) is proportional to $\left[J_{ij}\right]_+^4$. Hence carrier allocation dynamics given by Eq. (4) will be driven by canalization for low value of the flux $\left[J_{ij}\right]_+$ but for larger values of $\left[J_{ij}\right]_+$ the coupling function η dominates in Eq. (4).

While η dominates level of carriers becomes very large and as a result auxin is flushed out from the cell. Then the flux diminishes again because of low auxin concentration and canalization dominates the dynamics again. This switching makes the flux going back and forth and the vein system stops growing. We therefore need a canalization term and a coupling function of the same order with respect to $\left[J_{ij}\right]_+$.

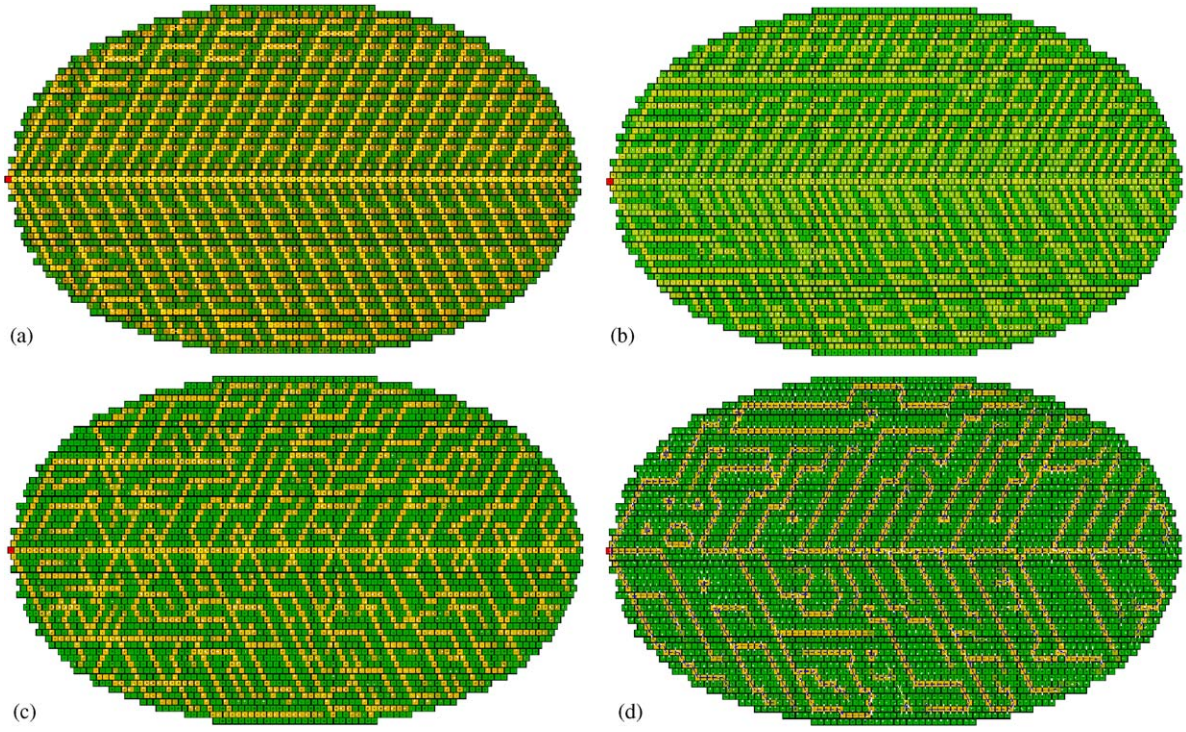

Fig. 2. Resulting pattern for different functions $\eta(B_i, B_j)$. (a) Pure canalization, $\eta(B_i, B_j) = 0$. The pattern includes only branching veins without loops. (b) $\eta(B_i, B_j)$ is as Eq. (6). Loops are observed but carriers are allocated against the flux. (c) $\eta(B_i, B_j)$ is as Eq. (7). We observe loops with correct carrier allocation. (d) $\eta(B_i, B_j)$ is as Eq. (7). Discontinuous veins are formed for different values of λ and k_2. Green color is auxin concentration and red color is flux-bifurcator level. Yellow is the result of high auxin concentration and high flux-bifurcator level. Cells have hexagonal neighborhood although they are displayed as squares. In all the figures the parameters are a = 1.2, α = 1, A_{eq} = 2.2, δ = 1, k_1 = 0.3, k_2 = 1, r = 2, λ = 1 except for (b) where A_{eq} = 3.5 and (d) where λ = 0.08 and k_2 = 1.95.

To mitigate instability observed for the model with the cell coupling function from Eq. (5) we studied the model with the following coupling function:

$$\eta(B_i, B_j) = aB_i \frac{B_j}{k_1 + B_j}, \tag{6}$$

where k1 is the half saturation constant. Now, for large values of B_j the cell-coupling function Z is proportional to B_i instead of B_i^2 in Eq. (5) (i.e. $\left[J_{ij}\right]_+^2$ instead of $\left[J_{ij}\right]_+^4$). Using Eq. (6) the instability described above disappears and we observe the formation of veins and loop connections (Fig. 2b).

We note that in the model with Eq. (6) veins are formed for an equilibrium value of auxin much greater than is the case without the η term. For example, in Fig. 2b we used A_{eq} = 3.5, compared with A_{eq} = 2.2 in Fig. 2a, so veins with loops could be formed. This implies that the η term given in Eq. (6) acts as an inhibitor of vein formation. The η term makes vein cells reallocate carriers to any side facing adjacent vein cells, even the sides with auxin influx. As a consequence carriers allocated to the upstream face of the vein cell make flux more difficult to form than the model without the η term.

To suppress this unrealistic reallocation of carriers, we multiply Eq. (6) by a new factor:

$$\eta\left(B_i, B_j\right) = aB_i \frac{B_j}{k_1 + B_j} \frac{k_2}{k_2 + \left[-J_{ij}\right]_+}, \qquad (7)$$

where k_1 and k_2 are half saturation constants and J_{ij} is the net flux from cell *j* entering cell *i*. The last factor is 1 if there is no incoming auxin flux ($J_{ij} \geq 0$ so $\left[-J_{ij}\right]_+$ is 0) but it is very small if there is a strong incoming flux ($J_{ij} < 0$ so $\left[-J_{ij}\right]_+$ large). The model with Eq. (7) shows branching veins in the same range of parameters as the model without the flux-bifurcator term. In addition, the model can generate closed loops if parameters are chosen appropriately. The resulting pattern is shown in Fig. 2c and a magnification of an area of flux bifurcation with the value of variables is shown in Fig. 3. The document Supp.1 is a movie of a simulation published as supplementary material available on the web page of the JTB. It shows the formation of preferential paths and the spontaneous connection process. One representation of the behavior of the auxin fluxes in such a reticulate network we obtain is shown in Fig. 4.

We have also examined the η function from Eq. (5) multiplied by factor $k_2 / \left(k_2 + \left[-J_{ij}\right]_+\right)$. We observed more pronounced oscillations than resulted from Eq. (5) alone, followed by explosion in the variables.

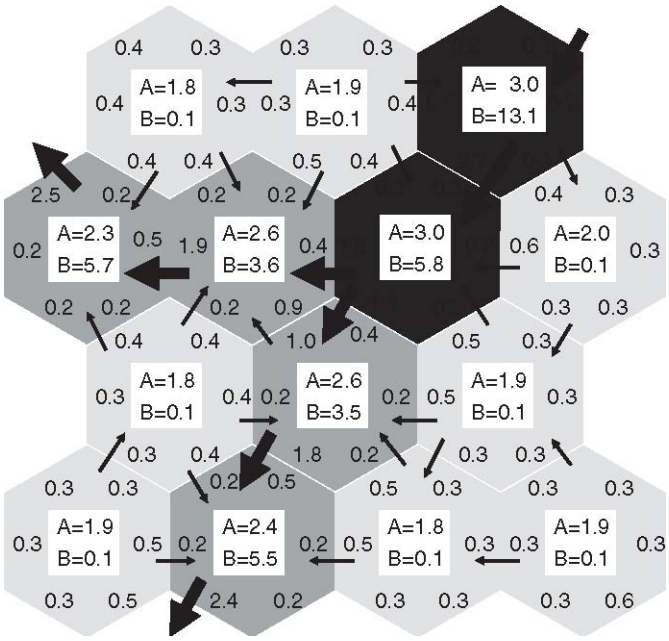

Fig. 3. Magnification of an area of flux bifurcation. In each cell concentration of auxin is shown by the letter ‘‘A’’ and level of flux-bifurcator is shown by the letter ‘‘B’’. Numbers near each side of a cell indicate carrier protein concentration on that side. Arrows show the direction of the auxin flux and their thickness indicates approximately the strength of the flux. Dark background shows a high auxin concentration and light shows low auxin concentration. The preferential path has a higher concentration of auxin and higher level of flux-bifurcator than the surrounding normal cells. Parameters used are the same as the simulation in Fig. 2c.

Hence, in the rest of the paper we adopt Eq. (7) together with Eqs. (2–4) as the model for generating the reticulate vein system.

The pattern generated by the model with Eq. (7) has loops as well as free ending veins. Indeed, some veins can remain stably free ending in the equilibrium pattern without attaching to the side of another vein. This mixed type of vein patterning is consistent with experimental observation in *Arabidopsis thaliana* (Scarpella et al., 2004).

4.2. Parameter dependence

To study the parameter dependence of the pattern, we chose a standard set of parameters giving the best pattern and examined the changes in this standard pattern in response to modifying parameters. Each of the eight parameters was increased or decreased by 20% one by one around its reference value with the other parameters fixed. Here we ran the simulation in a small lattice of

square shape with 263 cells having a hexagonal neighborhood, representing some small area of a leaf.

The typical patterns generated are shown in Fig. 5, where Fig. 5d is the reference pattern, and the parameter dependence is summarized in Table 1. The parameters can be sorted into four categories depending on the effect they have on the reference pattern.

Increasing any parameter in the first category (a, r and k_1) increased the number of veins and decreased the space between them (Fig. 5e), while a decrease in these parameters had the reverse effect (Fig. 5b–d).

In the second category, A_{eq} and α had an especially strong effect on the number of veins, and increasing them produced a pattern with many veins fused together which we call ‘‘densely packed veins’’ (Fig. 5f). Decreasing them produced ‘‘no veins’’ (Fig. 5a).

In contrast to the two previous categories, an increase in either parameter of the third category (k_2 and δ) decreased the number of veins in the resulting pattern and increased the space between them (Fig. 5b,c). A decrease produced the reversed effect (Fig. 5e).

Finally, a change of 20% in any direction in the forth category λ did not significantly change the number of veins formed but the resulting pattern had a different disposition (Fig. 5d).

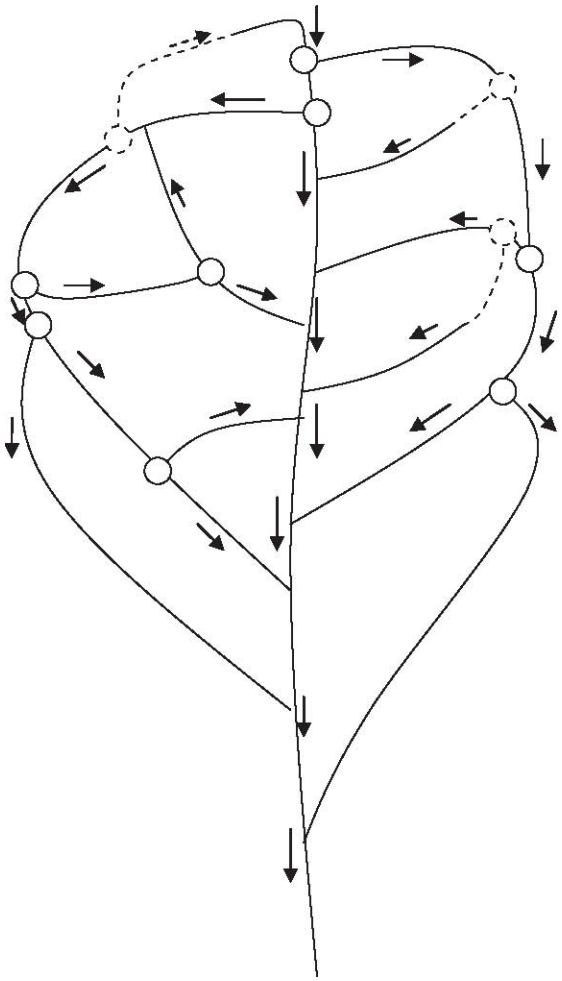

Fig. 4. Scheme illustrating the principle of flux-junctions/flux-bifurcations in a reticulate network. Arrows indicate the direction of the auxin net fluxes; nodes with a circle correspond to a flux bifurcation, otherwise they correspond to flux junctions. Eventually freely ending veins can reconnect later on during development (dashed), creating new flux bifurcation nodes. Other configurations of the flux bifurcations are possible but their number has to equal the number of empty loops.

4.3. Pattern with discontinuous veins

Some mutants of *Arabidopsis thaliana* show a leaf pattern with discontinuous veins (Deyholos et al., 2000; Koizumi et al., 2000, 2005). We examined whether the model with the flux-bifurcator can produce discontinuous vein patterns, as found in these *A. thaliana* mutants. We found that setting very low values of the flux-bifurcator's production speed λ is enough to create discontinuous veins. Increasing k_2 at the same time enhances the phenomenon (Fig. 2d).

Veins start growing and bifurcating, but as they become longer they lose their connection to the vein from which they emerged earlier. The disconnected end shrinks and forms a small cycle of veins playing the role of a sink while the other end stops growing when the auxin concentration landscape is no more favorable.

5. Discussion

We have demonstrated that a canalization-based model can generate a reticulated network of veins by adding a new process to the dynamics of auxin carriers. This process, which we called ‘‘flux-bifurcator’’, allows a cell to share its auxin outflux between two adjacent cells. The typical behavior of the auxin flux throughout a reticulated network that we obtained is illustrated in Fig. 4, where arrows indicate direction of the flux. Note that there is no point at which flux vanishes—no arrows of opposite directions in the same auxin path, contrary to the proposition of Sachs (1975, 1989) on the existence of non-polar strands in reticulate networks. There are neither three arrows emerging from, nor converging to one node. Later, on the tracks of the preferential paths of auxin, cells will differentiate into procambium and eventually give the xylem and the phloem in which fluids will flow independently from the direction of the former auxin flows.

Bifurcations are formed when the tip of a growing vein reaches a cell Q (cf. Fig. 1) which is on the side of another vein cell P, Q will slowly start pumping auxin toward that tip, stronger than toward P. By doing so, Q’s level of bifurcator will increase whilst its auxin concentration will decrease. This new high level of bifurcator will be perceived by P and reallocation of carriers in P will start toward Q, as well as reallocation in Q will start toward P (since both P and Q have now a high level of bifurcator). But the low auxin concentration of Q will decide that the auxin flux will go from P to Q, so the incoming flux in Q will inhibit carrier allocation toward P. As a result the allocation of carriers in cell P toward cell Q will increase and the flux from P to Q will also increase in turn, creating the bifurcation.

Based on our analysis, the flux-bifurcator needs to have the following properties: [1] Flux-bifurcator level should be enhanced in a cell that experiences a high net outflux of auxin on any of its sides. [2] A cell with a high flux-bifurcator level will inform its adjacent cells that also have a high flux-bifurcator level.

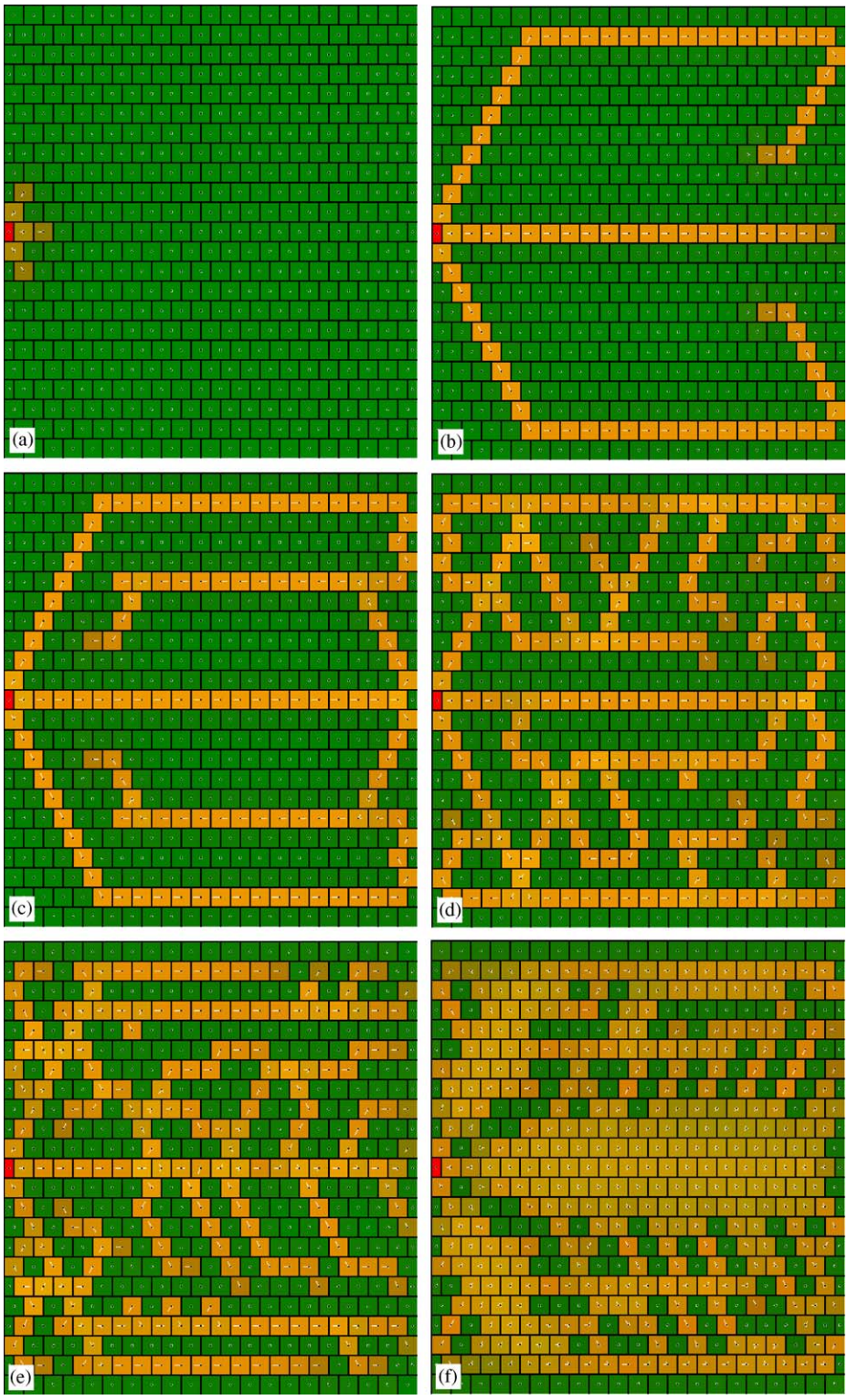

Fig. 5. Parameter dependence of the pattern generated by the model. (a) ‘‘no veins’’; (b) ‘‘very few veins’’; (c) ‘‘fewer veins’’; (d) ‘‘standard’’; (e) ‘‘more veins’’; (f) ‘‘densely packed veins’’. Parameters are: (a) A_{eq} **= 1.76,** α **= 0.8; (b)** k_1 **= 0.24,** δ **= 1.2; (c)** r **= 1.6,** k_2 **= 1.2; (d)** λ **= 0.8,** λ **= 1.2,** a **= 0.92; (e)** r **= 2.4,** δ **= 0.8,** k_2 **= 0.8,** a **= 1.44,** k_1 **= 0.36; (f)** A_{eq} **= 2.64,** α **= 1.2. Other parameters are the same as the standard set. Cells**

have hexagonal neighborhood although they are displayed as squares. The standard pattern (d) was calculated with the following parameters: $a = 1.2$, $\alpha = 1$, $A_{eq} = 2.2$, $\delta = 1$, $k_1 = 0.3$, $k_2 = 1$, $r = 2$, $\lambda = 1$. The lattice has 493 cells plus one for the sink. The white lines starting from the center of the cells indicate the concentration of carrier on each side and therefore give an idea of the strengths of the auxin net fluxes through each cell side.

Table 1 Parameter dependence of the model

Parameters	−20%	+20%	Categories
k_1 r A	"Very few veins" (b) "Fewer veins" (c) "Standard" (d) (slightly fewer)	"More veins" (e)	Few veins to many veins
A_{eq} α	"No veins" (a)	"Densely packed veins" (f)	No veins to densely packed veins
δ k_2	"More veins" (e)	"Very few veins" (b) "Fewer veins" (c)	Many veins to few veins
λ	"Standard" (d) (almost identical)		No change

The letters in parentheses refer to Fig. 5.

[3] The cell that receives such a signal and also has a high flux-bifurcator level starts reallocating PIN1 to the side facing incoming signal. [4] This last process is inhibited on sides having strong incoming auxin net flux. There can be many possible molecular mechanisms to realize a process with these properties, and the flux-bifurcator can be a process including a numerous genes.

In this paper we focused on the connection process instead of geometrical shape of the network. Although the lattice has a pseudo-leaf shape, it is not growing as a real leaf would be during vascular formation. Hence it is difficult to make an interpretation of the geometry of the network. The hierarchical structure should emerge from domain growth and cell division.

Even in a model without a cell coupling term η (i.e. canalization only), and for high A_{eq}, the model sometimes generates a pattern in which the tip of a preferential auxin path comes in contact with a side of another vein. However, in these cases the tip can receive auxin only from the adjacent cells on its sides, not from the vein it touches. As a result, a few cells downstream from the tip have auxin concentrations lower than the equilibrium value (Fig. 1a), and will not differentiate into a vascular system (Uggla et al., 1996; Avsian-Kretchmer et al., 2002; Mattson et al., 2003). After development this leads to an open branching pattern without loops. A loop with a null flux point, as proposed by Sachs (1975, 1989), would give the same result. In contrast, in our model including the flux-bifurcator, auxin concentration in preferential paths is higher than the

equilibrium value (Figs. 1b and 3) and differentiation of cells in the paths can later form a closed network of veins. This suggests that the auxin flux has to experience ‘‘flux junctions’’ as well as ‘‘flux bifurcations’’ in order to create a continuous and closed network (Figs. 2c and 4). Level of flux-bifurcator could also play a role in cell differentiation.

An auxin preferential path gains auxin after a flux junction and loses auxin after a flux bifurcation. A long path, by meeting these successive flux junctions and flux bifurcations, is an irregular succession of low and high auxin concentrations, still higher than the equilibrium value. Depending on species sensitivity to auxin levels, this disparity can lead to a natural transient feature of discontinuous differentiation into xylem, given that speed of differentiation into xylem is suggested to be positively correlated with auxin level (Aloni, 2001; Pyo et al., 2004).

Experiments have shown that some mutant plants with a reticulated venation can lose the ability to produce an initial closed network and hence form an open dichotomous venation (Steynen et al., 2003; Carland and Nelson, 2004; Motose et al., 2004). This too suggests that there exists a specific mechanism to make the connection of veins possible.

In recent experiments Koizumi et al. (2005) have shown that a mutant of VAN3 gene creates a discontinuous vein pattern. They concluded that VAN3 seems to be involved not in auxin transportation but in auxin signal transduction, and that expression of this gene is induced by auxin. The flux-bifurcator model studied in this paper is able to produce discontinuous vein patterns as illustrated in Fig. 2d. VAN3 could be a gene involved in the bifurcator process of our model.

Scarpella et al. (2004) observed that the reticulated network of the leaves of *A. thaliana* is made by free ending veins emerging from older veins and attaching later during the development to create loops. They also reported the absence of procambial islands in their large observation sample which means the network is continuous throughout the development of the leaf. Our model is consistent with these observations since it generates a continuous reticulated network by creation of free ending veins which can attach to older veins later (Figs. 2c, 4 and Supp. 1).

Another hypothesis based on mechanistic processes supposes that pressure among cells during the growth of the leaf induces vein and loop formation in the way that cracks could be formed from a drying gel (Bohn et al., 2002; Couder et al., 2002). There are also other models proposing different ways to form loops, such as moving sources or sinks of auxin (Mitchison, 1980a; Rolland-Lagan and Prusinkiewicz, 2005), or tips connection (Runions et al., 2005), but the flux-bifurcator seems more parsimonious and has a biologically plausible base. Still another

approach is a reaction–diffusion model for leaf vein formation developed by Tohya and Mochizuki (non published results). Their model is able to generate discontinuous veins but no loops. The relationship between our model and Tohya's model needs to be studied further. It is also interesting to notice that some phyllotaxis models (Smith et al., 2006; Jönsson et al., 2006) illustrate a different behavior of the auxin carrier proteins which can be taken into account for the future.

A venation pattern with closed loops would be more resistant to damages. Indeed, if a vein is cut, fluids can use different paths to supply the whole leaf, while in purely open venations damage is lethal for all the part of the leaf above it. For ferns, which produce spores on their leaves, this is dramatic since it results in a net decrease in fertility. Therefore we expect that plants with open venation such as some ferns, and also gymnosperms such as conifers and Gingko, are likely to adopt a strong chemical and/or physical defense against herbivores.

Acknowledgments

This work was done during FGF's stay in Japan under the exchange program of Collège Doctorale Franco-Japonais. The work has also received the support of a Grant-in-Aid for scientific research from JSPS to YI. We thank the following people for their help and comments: H. Fujita, J. Koella, A. Mochizuki, T. Sachs, and T. Yahara.

All figures are from Feugier, Francois G., Iwasa, Y., 2006. How canalization can make loops: A new model of reticulated leaf vascular pattern formation. Journal of Theoretical Biology, 243(2), 235-44.

Appendix. Supplementary materials

Supplementary data associated with this article can be found in the online version at http://www.sciencedirect.com/science?_ob=ArticleURL&_udi=B6WMD-4K3N5S2-2&_user=10&_coverDate=06%2F03%2F2006&_alid=459884156&_rdoc=3&_fmt=summary&_orig=search&_cdi=6932&_sort=d&_docanchor=&view=c&_acct=C000050221&_version=1&_urlVersion=0&_userid=10&md5=898d6281333f0965a4e24bf73d582075

References

Avsian-Kretchmer, O., Cheng, J.-C., Chen, L.J., Moctezuma, E., Sung, Z.R., 2002. Indole acetic acid distribution coincides with vascular differentiation pattern during Arabidopsis leaf ontogeny. Plant Physiol. 130, 199–209.

Bohn, S., Andreotti, B., Douady, S., Munzinger, J., Couder, Y., 2002. Constitutive property of the local organization of leaf venation networks. Phys. Rev. E 65 art no. 061914.

Berleth, T., Mattson, J., Hardtke, C., 2000. Vascular continuity, cell axialisation and auxin. Plant Growth Regulat. 32, 173–185.

Carland, F.M., Berg, B.L., FitzGerald, J.N., Jinamornphongs, S., Nelson, T., Keith, B., 1999. Genetic regulation of vascular tissue patterning in Arabidopsis. Plant Cell 11, 2123–2138.

Couder, Y., Pauchard, L., Allain, C., Adda-Bedia, M., Douady, S., 2002. The leaf venation as formed in a tensorial field. Eur. Phys. J. B 28, 135–138.

Deyholos, M.K., Cordner, G., Beebe, D., Sieburth, L.E., 2000. The SCARFACE gene is required for cotyledon and leaf vein patterning. Development 127, 3205–3213.

Feugier, F.G., Mochizuki, A., Iwasa, Y., 2005. Self-organization of vascular system in plant leaves: inter-dependant dynamics of auxin flux and carrier proteins. J. Theor. Biol. 236, 366–375.

Fujita, H., Mochizuki, A. Pattern formation by the positive feedback regulation between flow of diffusible signal molecule and localization of its carrier. J. Theoret. Biol., in press.

Fukuda, H., 2004. Signals that control plant vascular cell differentiation. Nature Rev. Mol. Cell Biol. 5, 379–391.

Geldner, N., Friml, J., Stierhof, Y.-D., Jürgens, G., Palme, K., 2001. Auxin transport inhibitors block PIN1 cycling and vesicle trafficking. Nature 413, 425–428.

Goldsmith, M., 1997. The polar transport of auxin. Annu. Rev. Plant Physiol. 28, 349–378.

Honda, H., Yoshizato, K., 1997. Formation of the branching pattern of blood vessels in the wall of the avian yolk sac studied by a computer simulation. Dev. Growth Differ. 39, 581–589.

Jacobs, W.P., 1952. The role of auxin in the differentiation of xylem round a wound. Am. J. Bot. 39, 327–337.

Kobayashi, R., 2000. Mathematical models for blood vessel network formation. In: Honda, H. (Ed.), Mathematics and Physics of Biological Pattern Formation. Kyoritsu Publ. Co., Tokyo (in Japanese).

Koizumi, K., Sugiyama, M., Fukuda, H., 2000. A series of novel mutants of Arabidopsis thaliana that are defective in the formation of continuous vascular network: calling the auxin signal flow canalization hypothesis into question. Development 1127, 3197–3204.

Mattson, J., Sung, Z.R., Berleth, T., 1999. Responses of plant vascular systems to auxin transport inhibition. Development 126, 2979–2991.

Mattson, J., Ckurshumova, W., Berleth, T., 2003. Auxin signaling in Arabidopsis leaf vascular development. Plant Physiol. 131, 1327–1339.

Mitchison, G.J., 1980a. A model for vein formation in higher plants. Proc. R. Soc. London 207B, 79–109.

Mitchison, G.J., 1980b. The dynamics of auxin transport. Proc. R. Soc. London 209B, 489–511.

Mitchison, G.J., 1981. The polar transport of auxin and vein pattern in plants. Philos. Trans. R. Soc. London 295B, 461–471.

Morris, D.A., 2000. Transmembrane auxin carrier systems—Dynamic regulators of polar auxin transport. Plant Growth Regulat. 32, 161–172.

Petrasek, J., Elckner, M., Morris, D.A., Zazimalova, E., 2002. Auxin efflux carrier activity and auxin accumulation regulate cell division and polarity in tabacco cells. Planta 216, 302–308.

Sachs, T., 1975. The control of the differentiation of vascular networks. Ann. Bot. 39, 197–204.

Sachs, T., 1981. The control of the patterned differentiation of vascular tissues. Adv. Bot. Res. 9, 152–262.

Sachs, T., 1991. Cell polarity and tissue patterning in plants. Dev. Suppl. 1, 83–93.

Sieburth, L.E., 1999. Auxin is required for leaf vein pattern in Arabidopsis. Plant Physiol. 121, 1179–1190.

Steynen, Q.J., Schultz, E.A., 2003. The FORKED genes are essential for distal vein meeting in Arabidopsis. Development 130, 4695–4708.

Tohya, S., Mochizuki, A. A new model for leaf venation pattern. J. Theor. Biol., in press.

Uggla, C., Moritz, T., Sandberg, G., Sundberg, B., 1996. Auxin as a positional signal in pattern formation in plants. Proc. Natl Acad. Sci. USA 93, 9282–9286.

- Non-published material -

Appendices

Appendix A

The peak observed can be understood by analyzing a simpler version of the model as follows. Let us consider the model

$$\begin{aligned} \frac{dP}{dt} &= (AP)^2 + q - \delta P \\ \frac{dA}{dt} &= r - AP \end{aligned}, \tag{1}$$

where A is the level of auxin, P is the concentration of carrier protein on one side of the cell, r is the quantity of auxin received by the cell by another one, q is the basic carrier production, δ is the decay rate.

In the simulations, a greater A makes higher peaks of P. Therefore we are interested in the behavior of P according to A as follows

$$\frac{dP}{dA} = \frac{dP}{dt}\frac{dt}{dA} = \frac{(AP)^2 + q - \delta P}{r - AP}. \tag{2}$$

As it is, Eq. (2) is very difficult to analyze, so we are going to make some simplifications. At the beginning of the simulation $P = q$. We consider a case where the initial auxin concentration A_0 is quite larger than q so we neglect $q(1-\delta)$. We can consider the least extreme case by studying the effect of the initial auxin concentration without production, so $r = 0$. Therefore Eq. (2) becomes

$$\frac{dP}{dA} = -AP. \tag{3}$$

Integrating leads to

$$P(A) = qe^{\frac{1}{2}\left(A_0^2 - A^2\right)}. \tag{4}$$

At the end of the simulation $A = 0$ and P is at its maximum value since there is no decay. Therefore we can write that the peak of P in Eqs. (1) is of same order as

$$P_{\max} \approx q e^{\frac{1}{2}A_0^2}, \tag{5}$$

which shows a very strong sensitivity to the initial auxin concentration.

Appendix B

To understand the critical behavior of the model let us consider a simplified version:

$$\begin{aligned} \frac{dP_1}{dt} &= \left(AP_1\right)^2 + q - \delta P_1 \\ \frac{dP_2}{dt} &= \left(AP_2\right)^2 + q - \delta P_2 , \\ \frac{dA}{dt} &= r - A\left(P_1 + P_2\right) \end{aligned} \tag{1}$$

where A is the level of auxin, P_1 and P_2 are the concentrations of carrier proteins on two different sides of the cell, r is the quantity of auxin received by the cell by another one, q is the basic carrier production, δ is the decay rate.

At the steady state this system has three sets of solutions:

$$\begin{array}{lll} \hat{P}_1 = \dfrac{4q + r^2}{4\delta} & \hat{P}_1 = \dfrac{r^2\delta - \sqrt{r^2\delta^2\left(r^2 - 4q\right)}}{2\delta^2} & \hat{P}_1 = \dfrac{r^2\delta + \sqrt{r^2\delta^2\left(r^2 - 4q\right)}}{2\delta^2} \\ \text{Set 1: } \hat{P}_2 = \dfrac{4q + r^2}{4\delta}, & \text{set 2: } \hat{P}_2 = \dfrac{r^2\delta + \sqrt{r^2\delta^2\left(r^2 - 4q\right)}}{2\delta^2}, & \text{set 3: } \hat{P}_2 = \dfrac{r^2\delta - \sqrt{r^2\delta^2\left(r^2 - 4q\right)}}{2\delta^2} \\ \hat{A} = \dfrac{2r\delta}{4q + r^2} & \hat{A} = \dfrac{\delta}{r} & \hat{A} = \dfrac{\delta}{r} \end{array}$$

Solutions for the P_1 and P_2 are symmetric in sets 2 and 3.

If we plot this three set values against r we observe a catastrophe in Figure 7.

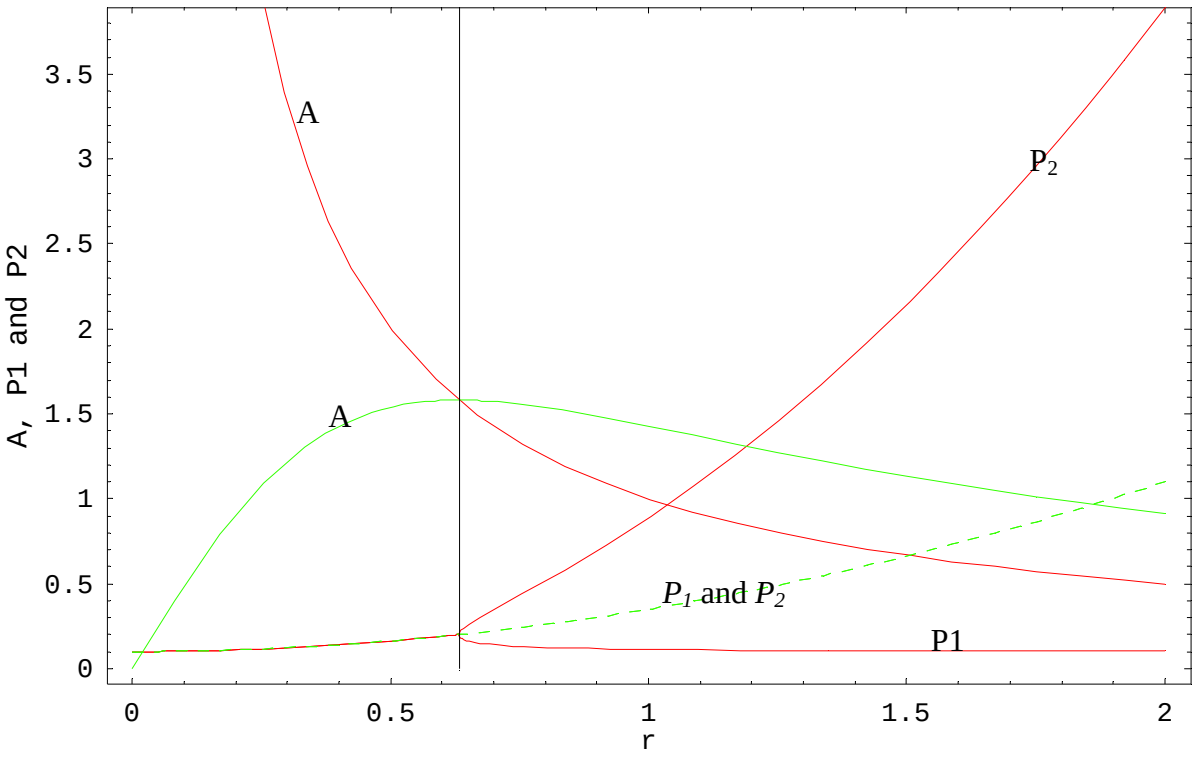

Figure 7: Catastrophe occurring in the steady states of the system. Green shows the set 1 and red shows the set 2. On the left of the vertical line set 1 is stable and set 2 is unstable; on the right of the vertical line it is the reverse situation. Since set 2 and set 3 are symmetrical P_1 and P_2 would be reversed in a plot of set 3.

We did a stability analysis of Eqs. (1). To do so we calculated the Jacobian:

$$J = \begin{pmatrix} -P_1 - P_2 & -A & -A \\ 2\,A\,P_1^2 & 2\,A^2\,P_1 - \delta & 0 \\ 2\,A\,P_2^2 & 0 & 2\,A^2\,P_2 - \delta \end{pmatrix} \tag{2}$$

We first deal with set 1 of solutions. Replacing set 1 in J gives

$$J_1 = \begin{pmatrix} -\frac{r^2+4q}{2\delta} & -\frac{2r\delta}{r^2+4q} & -\frac{2r\delta}{r^2+4q} \\ \frac{r\left(r^2+4q\right)}{4\delta} & \frac{2r^2\delta}{r^2+4q} - \delta & 0 \\ \frac{r\left(r^2+4q\right)}{4\delta} & 0 & \frac{2r^2\delta}{r^2+4q} - \delta \end{pmatrix} \tag{3}$$

We calculate the characteristic polynomial $\lambda I - J_1 = 0$ giving

$$\lambda^3 + \left(-\frac{4\delta r^2}{r^2+4q} + 2\delta + \frac{r^2+4q}{2\delta}\right)\lambda^2 + \left(\frac{4\delta^2 r^4}{(r^2+4q)^2} - \frac{4\delta^2 r^2}{r^2+4q} + \delta^2 + 4q\right)\lambda - r^2\delta + \frac{1}{2}(r^2+4q)\delta = 0, \quad (4)$$

The solutions of the polynomial for lambda give the eigenvalues of the system (1) at the set of solutions 1. Since it is difficult to find solutions for a third degree polynomial we use the Routh-Hurwtiz stability criterion. The algorithm leads to the following matrix:

$$\mathrm{RH}_1 = \begin{pmatrix} 1 & \frac{(r^2-4q)^2\delta^2}{(r^2+4q)^2} + 4q \\ -\frac{4\delta r^2}{r^2+4q} + 2\delta + \frac{r^2+4q}{2\delta} & 2q\delta - \frac{r^2\delta}{2} \\ \frac{\delta r^2 - \frac{1}{2}(r^2+4q)\delta + \left(-\frac{4\delta r^2}{r^2+4q} + 2\delta + \frac{r^2+4q}{2\delta}\right)\left(\frac{(r^2-4q)^2\delta^2}{(r^2+4q)^2} + 4q\right)}{-\frac{4\delta r^2}{r^2+4q} + 2\delta + \frac{r^2+4q}{2\delta}} & 0 \\ 2q\delta - \frac{r^2\delta}{2} & 0 \end{pmatrix} \quad (3)$$

In the resulting matrix of the Routh-Hurwitz method the number of sign changes in the first column equals the number of polynomial roots with positive real part. Therefore we looked for the values of the parameter *r*, *q* and δ in column 1 satisfying this criterion and we obtained the following conditions:

$$4q > r^2 \wedge r > 0 \wedge \delta > 0, \quad (6)$$

Condition (6) means that for set 1 of solutions to be stable δ can take any positive value since $r < 2\sqrt{q}$ with $q>0$. Figure 8 illustrates the relation between δ and *r* for a fixed *q*.

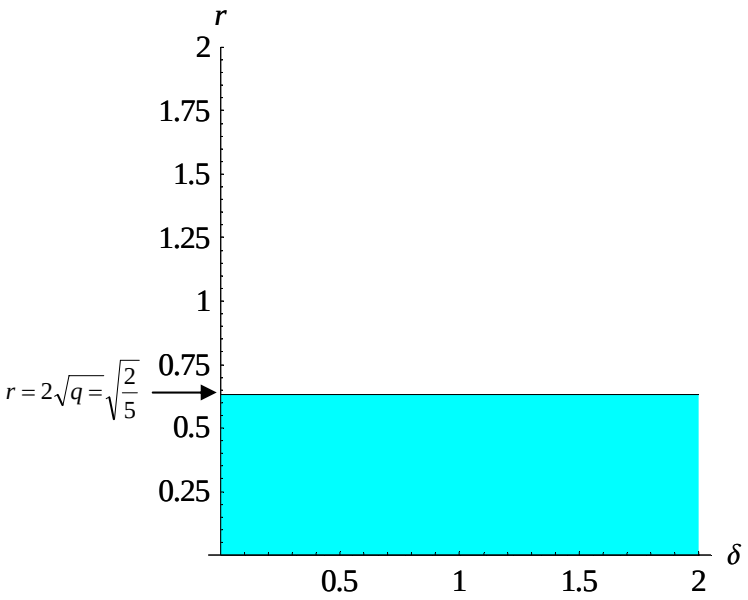

Figure 8: Domain of stability of the system for set 1 of solutions with *q*=1/10. For the set 1 to be stable r can take any value below $2\sqrt{q}$, whatever the value of δ .

Now, using matrix (2) we check stability for set 2 (sets 2 and 3 are symmetrical). Plugging set 2 into matrix (2) leads to

$$J_2 = \begin{pmatrix} -\frac{r^2\,\delta - \sqrt{r^2\,(r^2-4\,q)\,\delta^2}}{2\,\delta^2} & -\frac{\delta\,r^2 + \sqrt{r^2\,(r^2-4\,q)\,\delta^2}}{2\,\delta^2} & -\frac{\delta}{r} & -\frac{\delta}{r} \\ \frac{\left(r^2\,\delta - \sqrt{r^2\,(r^2-4\,q)\,\delta^2}\right)^2}{2\,r\,\delta^3} & & \frac{r^2\,\delta - \sqrt{r^2\,(r^2-4\,q)\,\delta^2}}{r^2} - \delta & 0 \\ \frac{\left(\delta\,r^2 + \sqrt{r^2\,(r^2-4\,q)\,\delta^2}\right)^2}{2\,r\,\delta^3} & & 0 & \frac{\delta\,r^2 + \sqrt{r^2\,(r^2-4\,q)\,\delta^2}}{r^2} - \delta \end{pmatrix} \quad (7)$$

The characteristic polynomial of matrix (7) comes as

$$\lambda^3 + \frac{r^2\,\lambda^2}{\delta} + \left(2\,r^2 - \delta^2 - 4\,q + \frac{4\,q\,\delta^2}{r^2}\right)\lambda + r^2\,\delta - 4\,q\,\delta = 0 \quad (8)$$

Yet again, we apply the Routh-Hurwitz method to Eq. (8) and obtain the following matrix

$$RH_2 = \begin{pmatrix} 1 & 2r^2 - \delta^2 + q\left(\frac{4\delta^2}{r^2} - 4\right) \\ \frac{r^2}{\delta} & (r^2 - 4q)\,\delta \\ 2r^2 - 2\delta^2 - 4q + \frac{8q\delta^2}{r^2} & 0 \\ (r^2 - 4q)\,\delta & 0 \end{pmatrix} \tag{9}$$

For stability of solution sets 2 and 3 the first column of matrix (9) must not have any sign change. Therefore the conditions are

$$r > 0 \bigwedge q > 0 \bigwedge \delta > 0 \bigwedge 4q < r^2 \bigwedge \sqrt{\frac{2qr^2 - r^4}{4q - r^2}} > \delta \tag{10}$$

Condition (10) means that for any value of $\delta < \sqrt{\frac{2qr^2 - r^4}{4q - r^2}}$ and q positive, r as to be larger than $2\sqrt{q}$. Figure 9 shows the domain for which set 2 and 3 are stable.

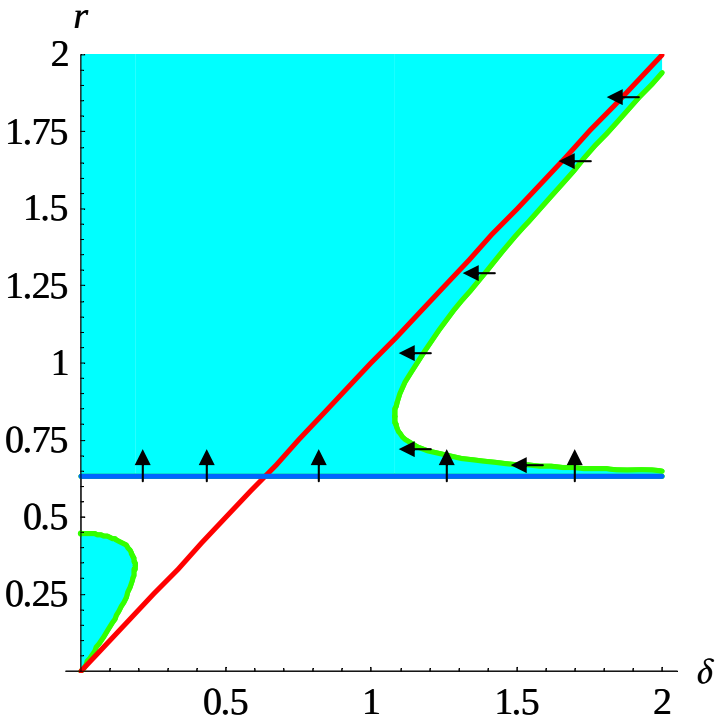

Figure 9: *r* and δ domain stability of the system for sets 2 and 3 with *q* = 1/10. Green lines show $\delta = \sqrt{\frac{2qr^2 - r^4}{4q - r^2}}$ and light blue area shows $\delta < \sqrt{\frac{2qr^2 - r^4}{4q - r^2}}$; dark blue line represents $r = 2\sqrt{q}$ which is also the asymptote of the green line when $r \to 2\sqrt{q}$; red line shows $\delta = r$ which is the asymptote of the green line when $r \to +\infty$. To fill all the conditions *r* and δ must be in the area pointed by the arrows.

We can summarize these results by saying that when a cell receives an amount of auxin *r* lower than $2\sqrt{q}$ (set 1 of solutions is stable), it will send out this auxin through every side with the same strength. This results in cells receiving from numerous cells and distributing to more than one cell. On the other hand, if the cell receives an amount of auxin *r* larger than $2\sqrt{q}$ and that $\delta < \sqrt{\frac{2qr^2 - r^4}{4q - r^2}}$ (set 2 or 3 of solutions are stable), it will send out this auxin through the side having already the highest carrier concentration. This results in cells receiving from numerous cells but sending auxin only toward one second cell. We call them polarized cells. Given the outgoing flow is roughly equal to the sum of the incoming flows, this second cell receiving the flow will have the same behavior, i.e. sending auxin toward a third cell, and so on. If this phenomenon continues to numerous neighboring cells, we obtain a preferential auxin path. The branching of the path is due to the fact that two cells start to be polarized toward one similar cell belonging already to a path.

Alternative models

1. Phyllotaxis model

When I first started to work on that topic, at the end of 2003, I tried models where cells can sense the level of auxin in the neighboring cells rather than the flux of auxin through their sides. I tried the following model assuming that if a cell would have a difference of auxin concentration with a neighboring cell larger than ε, it would increase this difference by sending auxin toward this cell. Equations are

$$\frac{dP_{i,j}}{dt} = \left(T - \sum_{k=1}^{n} P_{i,k} \right) \left[A_j - A_i - \varepsilon \right]_+ - \delta P_{i,j}, \tag{1}$$

$$\frac{dA_i}{dt} = r - A_i - \sum_{j=1}^{n} J_{i,j} + D \sum_{j=1}^{n} \left(A_j - A_i \right), \tag{2}$$

where D is the coefficient of auxin diffusion.

Although it has nothing to do with Turing systems, this model can generate stripes (or rings) that rapidly turn into stable spots of high auxin concentration as seen in Figure 10. The diffusion term is here mainly to avoid too abrupt peaks of auxin concentration.

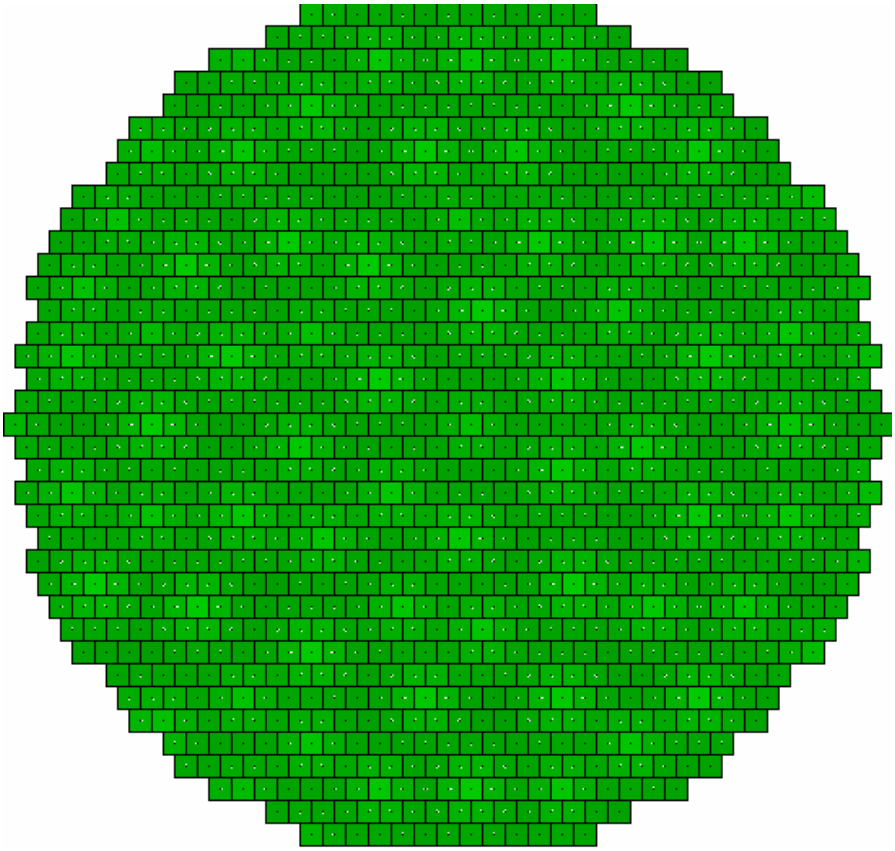

Figure 10. Phyllotaxis model. One cell at the center had a slightly higher initial auxin concentration. The pattern spreads from the center to outside. δ = 1, A_{eq} = 2.1, r = 1, T = 4, ε = 0.001, D = 1.

This behavior reminds phyllotaxis, and it is likely that this phenomenon is close to what actually happens. Models with a similar property have already been applied to phyllotaxis with nice results (Jönsson et al., 2005; Smith et al., 2005).

2. Model of global allocation enhancement

The following is another model based on the canalization of the auxin I tried at the beginning of my research. The model is similar to the model in part 2 except for $P_{i,j}$ and B_i:

$$\frac{dP_{i,j}}{dt} = \left(T - \sum_{k=1}^{n} P_{i,k} \right) \left(B_i \left[J_{i,j} \right]_+ + q \right) - \delta P_{i,j} , \tag{3}$$

$$\frac{dB_i}{dt} = \sum_{j=1}^{n} \left[J_{i,j} \right]_+ - B_i . \tag{4}$$

B_i is the concentration of an enhancer of the carrier allocation in cell i. It is produced proportionally to the activity of the cell which is the sum of all the positive net fluxes. This model gives smooth branching patterns (veins are less biased by the lattice shape). Large auxin paths slowly narrow down as observed in Scarpella et al. (2006), and cells often have more than one side with high carrier concentration. This allows creating loops of veins for a very long, but transient, time. The Figure 11 shows the pattern at equilibrium.

Making some analysis of a version of this model with one cell between two sinks, as in the Section 1.5 or Appendix B, gives only one set of solutions for the steady state, with carrier concentrations equal on every side. This feature allows the formation of bipolar cells easily. Although this model presents no catastrophe it is able to produce preferential paths of auxin.

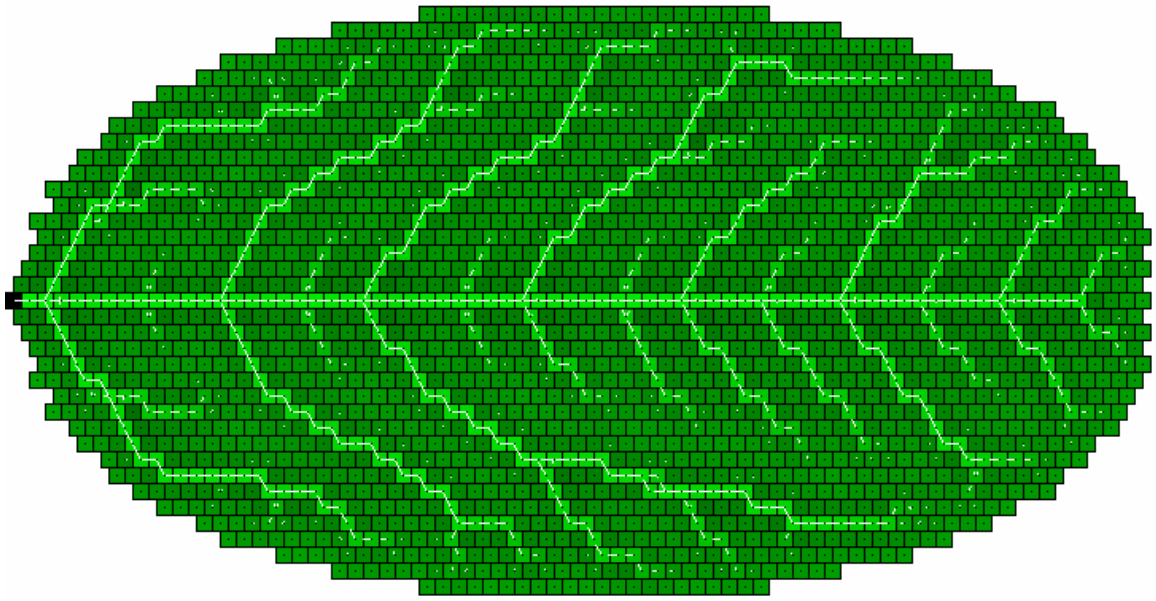

Figure 11. Model of global allocation enhancement after paths had narrowed down. δ **= 1,** q **= 01.,** A_{eq} **= 2.1,** r **= 1.2,** T **= 4.**

I think this canalization model is very promising and can be easily and parsimoniously improved to create connections without having to face the complex behavior due to catastrophes such as the one studied in Appendix B.

General Discussion

So far, we made various models of auxin canalization showing a wide range of patterns. In the first article, to make a robust model, we used a fixed total amount of carrier protein instead of free carrier production, and we used an accelerating response function to create the branching pattern. Only this type of function can create the monopoly in carrier allocation necessary for the pattern to emerge (Appendix B). But, in counter part, allowing only one side to monopolize carriers may have an impact on vein connection, preventing the formation of a closed network. In fact it depends on how one assumes veins connect each other. In theory two types of connections are possible: one tip on one vein side or two tips together.

A recent paper from Scarpella et al. (2006) shows the existence of cells with more than one side rich in carrier proteins. These “bipolar” cells are found in the main vein loops of the leaf and are thought to form the junction of two veins by their tips. It is also interesting to note that other results of their paper are consistent with the canalization hypothesis. In the present work (first and second articles) we found that tips cannot move toward each other because the auxin concentration between two approaching tips becomes low, and thus tips have no more reason to grow by canalization toward a depleted area. Since we could not obtain from veins to connect by their tips, or even tips to come close to each other, we envisaged the connection of a tip on a vein side. For this to occur, we need the cell on which connection occurs to share its flux so that the auxin concentration is uniform in the two branches of the loop. Therefore, in the second article, we introduced the flux-bifurcator. We obtained connections of tips on veins sides, showing bipolar cells at the resulting cross point but not in the middle of the resulting loop, as could give a tip-tip connection.

1. Vascular formation and cell differentiation.

When looking at the vascular pattern of a leaf, we observe the final, static pattern. We can ask whether differentiation takes place before vascular formation is finished, to stop any further vein growth and connection; or differentiation takes place after veins reach a stable state in which they have no need to grow further or connect. By differentiation one means creation of the

cambium, xylem and phloem from the procambial cells. In the former case, the pattern observed is the result of the interfering dynamics of differentiation on the vein growth. In the latter case, the pattern observed is the only result of the steady state of the vein formation dynamics. For robustness and simplicity one can think that the latter case is better. A result that could definitely make the latter case more likely would be that, the cambium cells are always maintaining an auxin flux, and are responding, at any time, to a changing auxin concentration landscape.

Evidence is brought by wound experiments made on the vascular system. A wound cuts a vascular strand (phloem, cambium, and xylem) and the cambium releases the transported auxin among parenchyma cells. The wounded area is soon healed by vascular bridges that connect to nearby vascular system. This shows that cells still react to auxin landscape changes at any time. Thus the observed final pattern may be the result of the steady state of the vein dynamics.

Furthermore, if the observed pattern is the result of the steady state of the vein formation dynamics it means that all the vein configurations are ready to change but remain still because some condition is not filled. Thus, veins which are ready to connect but lack the required condition do not connect, and all the others are already connected. Although they do not connect, they should be in a spatial configuration which requires a rather small displacement to connect. It does not seem sensible that, from the steady state configuration, veins tip have to travel a lot to connect. Therefore the observed configuration should offer opportunities to connect by mean of a short elongation of the vein.

What is surprising is that, on a real leaf, one never observes (statistically speaking) two vein tips facing and away by a short distance. This observation leads to three suppositions illustrated in the Figure 12:

- Pure tip-tip connection, Figure 12a)-c): Two tips come in a critical range. Inside this range tips connect, whereas outside this range they do not. The problem is that one never observes two facing tips in real leaves, even apart by a rather long distance. Therefore, if tip-tip connection is the real type of connection for veins, dynamics should never leave two tips facing each other without connecting them, since one never observes this configuration. This also implies that two tips are necessary, so that one isolated tip remains free.

- Pure tip-vein connection, Figure 12d), g) and h): A vein tip comes in the vicinity of a vein side. Inside some critical range, it connects to the vein, otherwise if the tip is outside the critical

range, it stays in place and connection does not occur since one observes this configuration in real leaves.

- Pseudo tip-vein connection, mixed strategy, Figure 12d), e) and f): A vein tip comes in the vicinity of a vein side. Inside some critical range the tip has an influence on the vein side and triggers the emergence of another minute vein tip onto which it connects; if the tip is outside the critical range it has no influence on the vein side so connection does not occur.

The two last cases are consistent with the absence of vein tips within a critical range around a vein side observed in real leaf patterns. The critical range could be the limit of the auxin drainage basin, as explained later. The tip-tip connection and the pseudo tip-vein connection, which are somehow related, would require an additional mechanism to create the connection.

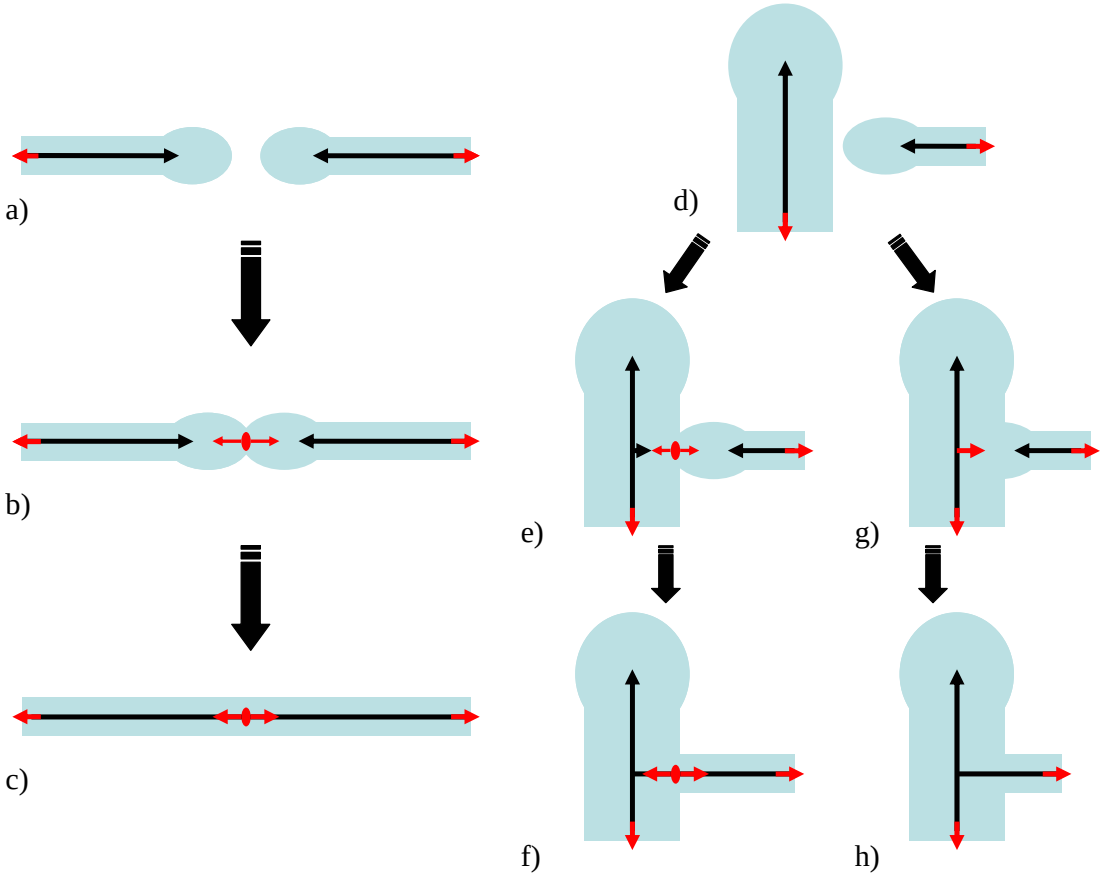

Figure 12 : The three hypothetical types of connections. a)-c) Pure tip-tip connection. d), e) and f) Mixed connection strategy. d), g) and h) Pure tip-vein connection. a) and d) Drainage basins intersect. b) and e) Saddle cell appears. g) Flux bifurcation appear. c), f) and h) Vein connection occurs. Blue color represents the auxin drainage basin; big black arrows show the sequence; thin black lines represent auxin preferential path and small arrow heads indicates the direction of growth of the paths; red ellipse illustrates the saddle cell producing a large amount of auxin and red arrows shows the direction of auxin movement.

2. Tip-tip and pseudo tip-vein connections: the saddle cell hypothesis.

In canalization two tips are naturally repelled because auxin concentration between them is very low. To attract two tips using canalization, an undifferentiated cell at the future probable connection point of the tips should start increasing dramatically its auxin production to become an auxin source with a larger auxin concentration than the surrounding normal cells, and send out auxin through two different sides toward the two tips. This would attract the tips so they come in contact with the connection/source cell and stick to it. The cell at the connection point needs a mechanism to know that its position is between two approaching tips. One can think the auxin concentration landscape is a good candidate. Indeed, at the head of a vein tip one finds a drainage basin (Figure 12 and Figure 13): an area where cells send auxin toward the vein.

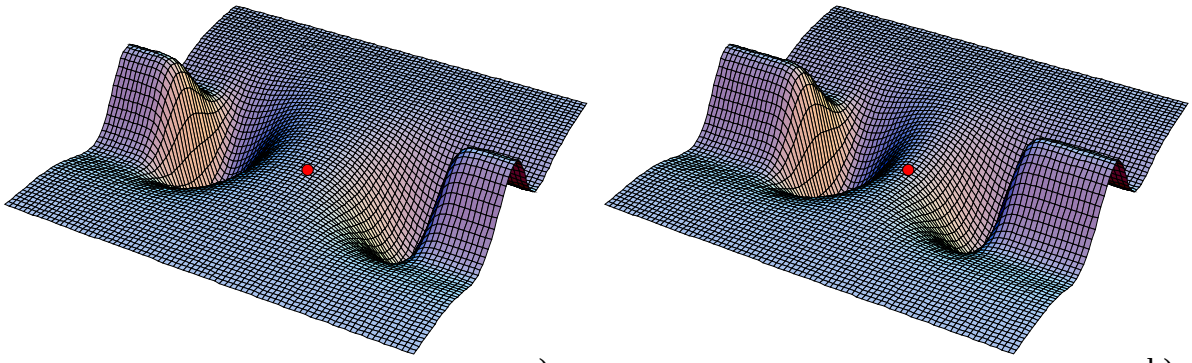

a) b)

Figure 13 : Tip-tip connection: auxin concentration landscape and the saddle cell hypothesis. Highest auxin concentrations are the veins. The drainage basins are surrounding the veins. Vein lateral basin is shallow, tip basin is deep. Other areas are at the auxin equilibrium value. a) Two vein tips approach and their drainage basins are not yet intersecting. The cells around the red circle are not yet under influence of any drainage basin. b) The two drainage basins intersect and create a saddle node in the auxin concentration landscape on which only one cell among all the others receives no auxin from any of its neighbors but sends auxin toward the tips. The red circle shows the position of the saddle cell.

Outside this area, cells are no more influenced by the draining effect of the veins. One observes in the simulation proposed in the previous articles that the drainage basin is larger and

deeper for the vein tip. When two remote tips approach at some critical distance, their drainage basins intersect. At this moment, in the auxin concentration landscape, one cell (or a couple) becomes the saddle node of the drainage basins - and consequently of the auxin concentration landscape. If this cell suddenly increases its auxin production level it can feed the drainage basins, and therefore the tips. As a result both tips are attracted toward the saddle cell. This implies that the saddle cell produces two times more auxin (in order to feed two veins) and allocates carriers on two different sides, exhibiting bipolarity. Thus, canalization models must allow cells to make a kind of bifurcation of the auxin flux even for a tip-tip connection.

Bipolar cells have been observed (Scarpella et al., 2006) but we do not know whether they appear on the saddle node of the auxin concentration landscape of two tips or tip-vein, and whether they produce more auxin than the other cells. Observed bipolar cells are not necessarily saddle cells, but saddle cells are bipolar.

Another possibility for tip-tip connection would be a change in the behavior of the tips to make them approach each other, rather than a change in the cell(s) between them. This alternative is not envisaged here.

3. Pattern of veins emergence.

If veins connection remains unclear, veins emergence seems understood and different modeling converge to the same results. According to Dimitrov et al. (2006) veins emerge from places with the largest auxin gradient. This is actually what happens in canalization models, although cells react to the auxin flux.

Let us start from the same areole used in Dimitrov et al. as explained in the General Introduction, and apply canalization models to it. Cells at rest have all the same carrier proteins ground concentration *q*. Therefore the flux from cell *i* to cell *j* before carriers dynamics start can be written as $J_{i,j} = P_{i,j}A_i - P_{j,i}A_j = qA_i - qA_j = q\left(A_i - A_j\right)$, which is negatively proportional to the gradient, and where *q* plays the role of a diffusion coefficient. Thus, if the intrinsic threshold of the canalization dynamics is exceeded (see appendix B), it will be exceeded at the same places as in the model proposed by Dimitrov et al.. Therefore the places where veins would emerge and where they converge in canalization would be the same as in the model from Dimitrov et al. But at the moment when two or more drainage basins intersect then the story becomes more complicated.

4. Wounds and vascular bundle structures

Given that the cambial cells always transport auxin, when a wound is performed auxin is released among parenchyma cells from the cambial cells upstream to the wound. The area becomes as a result a source of auxin. This area will attract new auxin inward paths emerged from nearby vascular strands, or will emit paths with auxin outward flux that will connect to nearby vascular strand. A combination of both cases also occurs: paths with an outward flux emerge from the wound and connect to paths with inward flux emerged from a nearby sane cambium. This is an asymmetric tip-tip connection. For regeneration to occur the cambium of nearby sane vascular strands has to be accessible. In amphicribral - where the phloem is surrounded by xylem - and amphivasal - where the xylem is surrounded by the phloem - cambium is not accessible since it is surrounded by either xylem or phloem, respectively. It could be interesting to check whether plants with these vascular bundle structures have a particular way to heal wounds, if they do.

5. Cell division criterion

One must keep in mind that all the vascular formation process occurs during leaf growth so that the geometry of the network and the vein hierarchy depends on cell division. Canalization creates auxin preferential paths while cells of the paths divide. One can ask what triggers cell division and what turns out of the paths after their cell number increased?

During vascular formation it is not yet clear what triggers cell division. Observations show that cell's internal auxin concentration (Petrasek et al., 2002) and maybe auxin flux through the membrane play an important role. Indeed, a very downstream cell receives auxin from a large network, such as the estuary of a river. On the other hand, cells upstream near to the tip of a vein receive a low amount of auxin, such as brooks. The auxin decay in a cell cannot be large enough to keep a arbitrary fixed auxin concentration whatever the quantity of auxin entering the cell. As a result, the a downstream cell ends up with a larger auxin concentration (proportional to the upstream length and the number of upstream vein tips) than a cell next to a vein tip. Quantity of auxin, or auxin flux strength, can be a cue for the cell to sense its position in the forming vascular system and the necessity to divide.

Let us suppose that a cell divides to keep a low outward flux. As one moves downstream, the vein cells receive a large amount of auxin and have to pump it toward the next downstream cell. At some extent, the quantity of auxin a cell has to pump can be very large. Therefore if the cell divides into two daughter cells, each one would receive half the auxin flux from the upstream cell and in turn pump less auxin downstream. But this implies that cells must bifurcate the flux.

6. Veins thickness: the roles of flux bifurcations and bipolar/saddle cells.

6. 1 The flux bifurcation.

If one assumes that cell division depends on auxin concentration or auxin flux, then it is worth discussing about the impact of flux bifurcations. Auxin concentration pattern in the network depends on auxin production in each network cell, but especially on the places auxin enters the network from the surrounding cells. One can address two cases:

1. Auxin enters a vein only by the tips.
2. Auxin enters a vein both by vein sides and tips.

The case where auxin enters only by the side is not envisaged since it seems contradictory with the process of canalization.

In the case 1), concentration in cells will increase downstream a vein bifurcation proportionally to the number of tips upstream. Therefore cells will start dividing just at the bifurcation point of the vein and the next downstream cells will continue to divide from near to near (Figure 14, a-c). In this configuration no flux bifurcation will appear and the thickening of the auxin path will move downstream. At the base of the branching pattern each cell is directly linked to one vein tip. But the problem is that, if auxin enters only the vein tips, no vein would never emerge from a vein side, only bifurcating tips create more tips. In the case of an areole, no vein would ever emerge from the surrounding vein loop to fill the areole as it grows. Therefore auxin is not likely to enter only the tips, except if vein emergence depends on other more complicated molecular mechanisms.

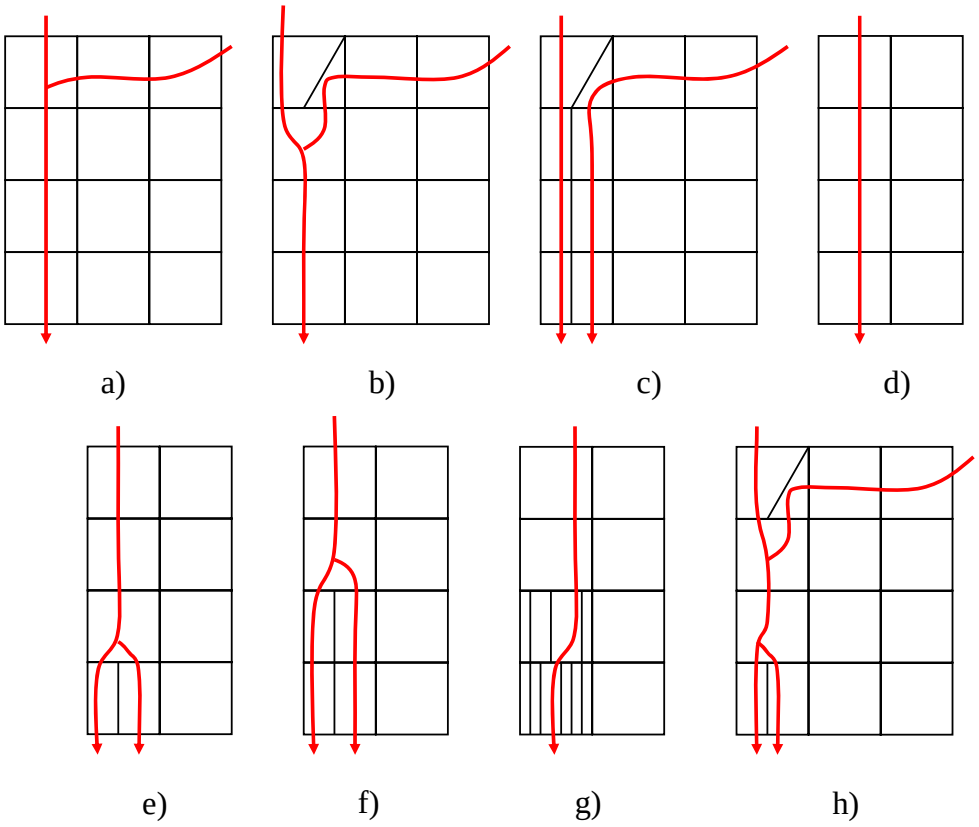

Figure 14 : Preferential paths and cell division. Red arrows are the auxin fluxes through procambium cells, in black lines. a)-c) If auxin enters only by the tips the pattern of division move downstream. e)-f) If auxin enters from the tips and the vein sides, and flux bifurcation is possible, the pattern of division moves upstream. g) If flux bifurcation is not possible, downstream cells divide indefinitely. h) If auxin enters by the tips an the vein sides, and flux bifurcation is possible, the pattern of division is bidirectional.

In the case 2), the auxin concentration and flux increase linearly as we move from the tip to the sink (Figure 14d). Therefore the cell that will divide first is the one next to the sink (Figure 14e). After the division, the second cell from the sink will be in contact with the two daughter cells resulting from the division of the first cell. What happens if there is no flux bifurcation? The second cell chooses to send auxin in one of the daughter cells. As a result this daughter cell receives the whole auxin flux, as its mother cell did. Thus it will divide, and the same problem will start again (Figure 14g). In a sense, absence of bifurcation tends to keep a very thin cambium, but auxin concentration will increase dramatically inside it.

If a flux bifurcation is possible, the second cell shares its auxin flux between the two daughter cells (Figure 14e). As a result, they receive half the flux their mother cell received. So with time and as their PIN pool is reconstituted, their outward flux will decrease as well as their

auxin concentration. While the vein grows, the second cell reaches the required auxin flux/concentration to divide, and so on (Figure 14f). In this case 2) the pattern of division goes upstream. But when a vein bifurcation occurs (at the tip or at the vein side) the pattern of division is such as the case a)-c), giving mixed patterns such as in h) which ends up as in c). In case 2), a growing areole can be filled with newly emerging veins.

To summarize: auxin enters by the tips but should also enter by the sides of a preferential path to allow areoles to be filled by new veins; cells should share their flux otherwise the network will become extremely rich in auxin; without flux bifurcation the paths' thickness cannot exceed one cell in any transversal direction to the path, making impossible to create a ribbon-shaped cambium. Detailed observations of real time growth and cell division would bring information on the thickening pattern, and therefore on the movements of auxin.

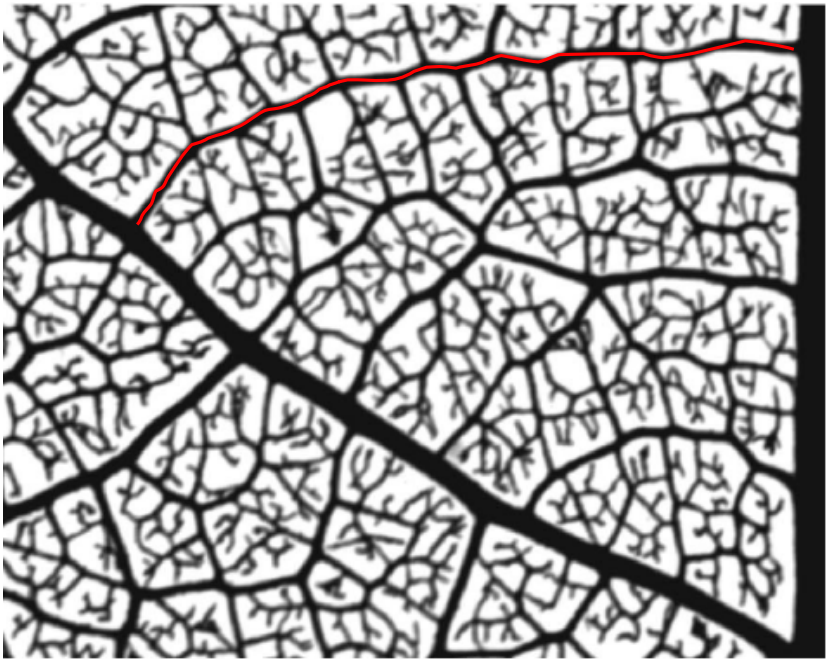

Figure 15: Constant thickness of a vein (in red). Original picture from Bohn et al. 2002.

However, auxin entering by the sides of the preferential paths does not seem to have a strong effect on the thickness increasing when looking at Figure 15. Indeed, between intersections, veins have fairly the same thickness. Even when looking at longer veins, thickness looks rather constant (Figure 15, red line). If auxin concentration in the cambium regulates cell division, and therefore vein thickness, this obzerved vein cannot be consistent with the hypothesis supporting

tip-tip connections which creates only flux junctions, and consequently gradual thickening of veins. Indeed, the vein in red on Figure 15 should become thicker because it meets only flux junctions on its way. But when looking at its thickness, one cannot tell whether auxin would move in the vein on left or on the right of the figure. This constant thickness may be due to an alternating presence of flux junctions and flux bifurcations on the auxin travel, regulating the auxin quantity carried, and thus the vein thickness.

6. 2 The bipolar/saddle cell.

Now let us consider the impact of the bipolar/saddle cell and flux bifurcation hypotheses on the efficiency of the vascular system, given the previous criteria for cell division.

Let us consider a small loop where one unit of auxin flows downward per unit of time. In the case of a flux bifurcation (Figure 16a), the small loop has same vein width at the entrance and at the exit. On the other hand, in case of a bipolar/saddle cell (Figure 16b), the loop is wider at the exit than at the entrance. In the first the network is symmetrical whilst in the second case it is asymmetrical. If the width of the cambium decides the width of the xylem and the phloem, efficiency of the network will depend on the direction of the water flow in the case of an asymmetric network. On the other hand, in a symmetric network water would flow similarly in any direction. Therefore networks made from bipolar/saddle cells would create congestions (Figure 16d), whereas networks made from flux bifurcations are already well balanced in any direction (Figure 16c).

The benefit of flux bifurcation in that situation is that, if there is no traffic jams for auxin in the cambium, there won’t be any traffic jam for fluids in the future xylem and phloem. No last-minute adjustments will be necessary during leaf growth and life.

On must keep in mind that these hypotheses depend on the assumption that cells divide according to auxin flow or concentration.

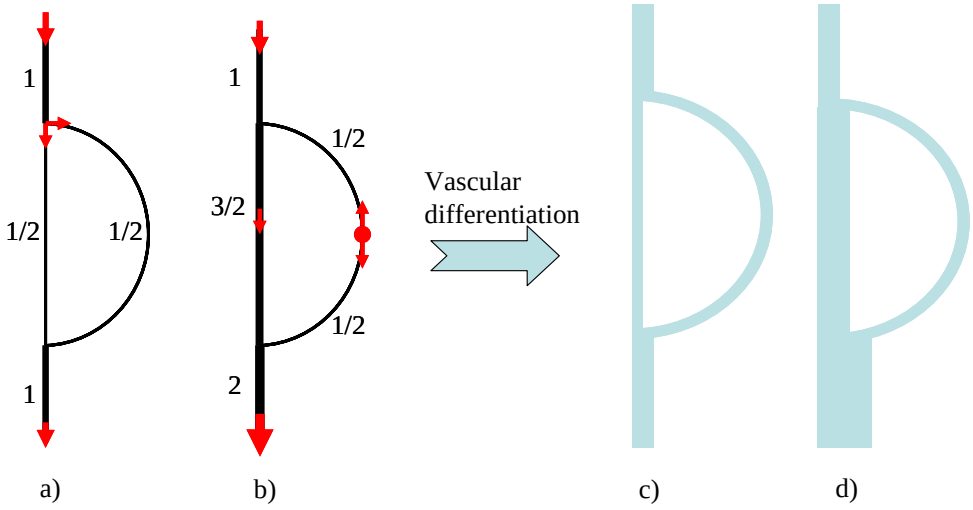

Figure 16: Impact of bipolar saddle cell and flux bifurcation on the future vascular network. Auxin flows (red arrows) in the cambium. a) Flow meets a bifurcation and is separated equally (although proportions are of no importance). b) A bipolar saddle cell produces auxin in the loop. Flow meets only junctions. c) Result after differentiation of the network with a bifurcation. One sees that whatever the directions of water in the network there are no traffic jams. d) Result after differentiation of the network with a bipolar saddle cell. The network is asymmetrical; therefore traffic jams will occur if water goes upward, but not downward.

7. Proposal of an experiment to check the existence of flux bifurcations.

Here I propose an experiment to check existence of flux bifurcations. I have no precise idea about feasibility of this experiment, therefore I whish experimentalists who are familiar with protocols try to improve my proposition. The idea would be to use a direct method to mark auxin molecules (with C^{14} for instance), or indirect methods (gene marker sensitive to an auxin analogous molecule transported the same way auxin is transported) to reveal the path normally took by auxin molecules through the transporting cells. By applying such molecules on a branch of the vascular network, one could confirm, or invalidate, the existence of flux bifurcations.

If there is no way to visualize auxin paths, one can do a more indirect method. By doing exogenous application of an auxin analogous at one point of the forming vascular network, the molecules will start to be transported through the procambial cells (Figure 17). Now, one measures the concentration of the molecule in the branches. Taking a complete branch with many cells gives a better precision for the measure if the concentration is very low. Weighting the value measured by the number of cells, or the length of the branch, gives a better approximation of the

concentration in one cell. In the best case one can measure each branch of the network and, by using conservation law, find the orientation of the flow in each branch of the network. Even by taking a couple of random branch samples of the network one can infer on the presence of bifurcations, but not the orientation of the flux. If flux bifurcations do not exist, molecules should follow only one linear path toward the petiole (Figure 17a). Therefore very few samples should contain the molecule, especially samples remote from the application point and hierarchically similar should not contain it. Samples of the path should have roughly the same concentration per cell if the transport reached a steady state. On the other hand, if flux bifurcations do exist, the molecules should be found in many different branches of the network with very different concentrations (Figure 17b).

The most enlightening may be to measure the complete network of several neighboring areoles.

One must keep in mind that auxin is also able to move in a non polar fashion in the phloem. Therefore it is necessary to find a way to make the distinction between auxin movement in the phloem and in the cambium.

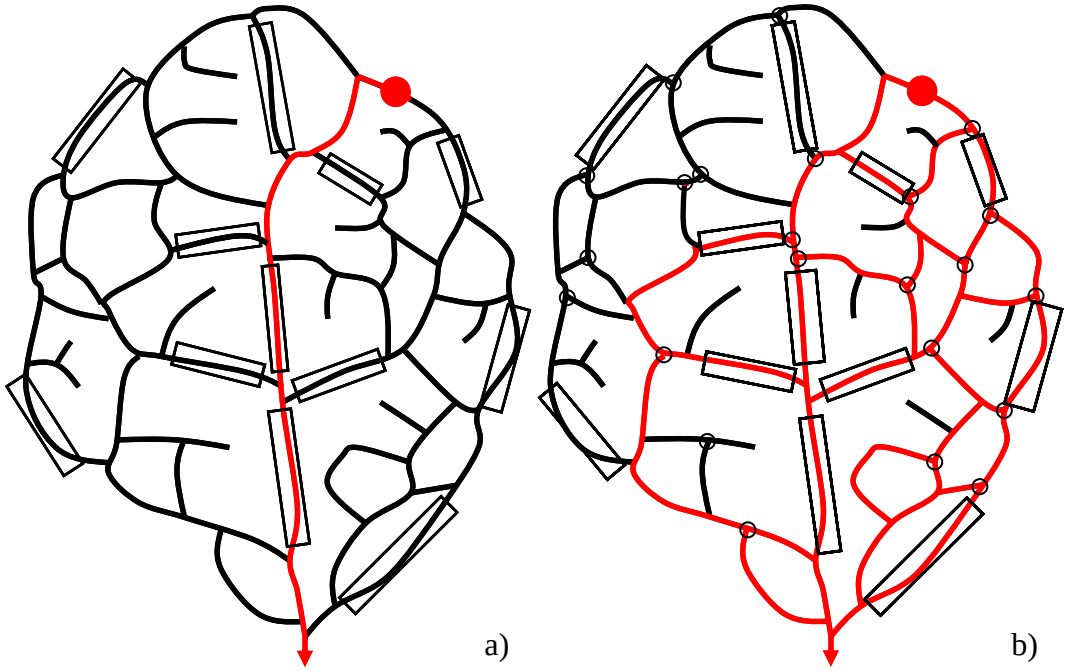

Figure 17 : An experiment to check the existence of flux bifurcations in the vascular system of a leaf. The red circle indicated the place of application of the auxin analogous. Red line is the path took by the molecule in case of a) absence and b) presence of flux bifurcations. Rectangles represent sampling areas. Black circles indicate

flux bifurcations. Many other dispositions of bifurcations exist, but only one flux configuration corresponds to one disposition of bifurcation points. There are 23 empty vein loops, therefore there are 23 bifurcations.

8. Auxin hot spots

As to increase complexity, it seems that PIN1 behavior changes according to the tissue it is expressed in. In the epidermis of the shoot apical meristem (SAM), PIN1 tends to accumulate so that cells send auxin toward neighboring cells with higher auxin level than themselves, resulting in an instability which increases auxin level differences between cells, giving patterns with spots of high auxin concentration. On the other hand, in deeper tissues cells behaves more in a way to evacuate auxin with canalization. These two behaviors are therefore in contradiction. Auxin convergence points driven by PIN1 were observed by Reinhardt et al., (2003), making believe that auxin concentration is high in these areas (Reinhardt, 2005). Indeed, cell proliferation taking place in these areas may indicate a high auxin concentration. This high concentration of auxin has been verified indirectly by computer simulation (de Reuille et al., 2006). Furthermore, as the SAM increases in size, new auxin peaks emerge. It is due to the balance between auxin production and auxin out flux in each cell. During growth, when an auxin minimum (divergent flux point) becomes far enough from surrounding auxin maxima (convergent flux points), its auxin gradient decreases and becomes close to zero. As a result there is no information on where are located auxin peaks to send more auxin. Thus cells in these areas stop sending auxin to their neighbors, and their internal auxin concentration starts to increase due to ground production. This small increase creates as a result a new emerging peak which will reorient surrounding cells and attract auxin. Reversion, where the internal auxin production starts to balance auxin out flux, can occur only at the furthest place from all surrounding auxin maxima, the place where all meeting gradients are the closest to zero i.e. the active auxin transport is almost null. Without growth, peak number and position would be static. It is interesting to notice that this type of behavior has the same properties as what is observed in the experience of Douady and Couder (1996): it can create pattern with spots placed the furthest distance from each others.

9. Probable impact of phyllotaxis dynamics on main vein loops pattern.

It is likely that, for the sake of economy, plants manage phyllotaxis and vascular formation with different behaviors of the same actors. Indeed, since a young leaf primordium is a local sprout of the SAM, the nature of the epidermis of the primordium would be the same as the one on the SAM. Well, the epidermis of the SAM is responsible for the formation of hot spots of auxin on the 2D epidermis surface of the SAM, giving birth to the phyllotactic pattern. Therefore one may think that the same hot spots occur at the margin of the leaf primordium in 1D. Somehow, it seems to be the case. Convergence points were observed on the margin of the leaf lamina (Scarpella et al., 2006). Thus, one can see that the dynamics taking place in the formation of phyllotaxis may also play a role in the pattern formation of leaf main vein loops. Furthermore, main loops of the leaf seem to be influenced by the convergence points on the margin of the leaf lamina (Scarpella et al., 2006). Although these convergence points are observed on the margin of the primordium, they are absent from its surface, meaning that no convergence point will affect the formation of the netlike structure present within the main loops. If that is so, this could explain, in part, why the main veins have a precise and regular positioning regarding the leaf shape, and why all the other higher order veins inside the main loops have no particular positioning regarding the leaf shape. Higher order veins are only affected by the shape of the loop or areole wherein they emerge from, explaining in this way their diversity. But it does not exclude that canalization without convergence points in the leaf margin can give a vein pattern similar to the one with those convergence points. These two hypothesis need to be checked.

If the patterns of phyllotaxis and main veins depend, in part, on the same process (auxin convergence points), different phyllotactic patterns (spiral, decussate…) may have associated or correlated leaf main veins patterns. This point would deserve to be investigated with statistical methods to verify the existence of a relation.

However, the apparent dual behavior of PIN proteins is to clarify. In leaf vascular formation experiments, the ground meristem cells of a young leaf would react by sending auxin toward only one preferred neighboring cell, creating eventually a preferential path of auxin. In the canalization models, this preferred neighboring cell is the one toward which the net flux is the largest - the cell sending back auxin the least. Cells sending to more than one cell do not create any preferential path.

On the other hand, Experiments and models of phyllotaxis assume quite the reverse thing. The question is, are these two principles exclusive, or do they act together at variable degrees in phyllotaxis and vein formation?

10. Conclusion

Canalization seems strongly involved in vascular formation in plants, but at the same time brings many questions. For example, it creates auxin preferential paths with polar cells, but polar cells prevent the creation of a reticulate network with connection. To create a vein connection (whatever the type of connection) it is necessary that one cell at the connection point allocates auxin carriers on two different sides to feed both connected veins with auxin. Practically, a bipolar cell allocate PIN1 on two different sides to connect two tips without although I do not know whether auxin flux is really bifurcated, whereas a cell with the Bifurcator connects a tip on a vein side by bifurcating the flux. The impact of each hypothesis on the network is very different. With bipolar cells the network contains only auxin flux junction, and therefore veins should always gradually thicken from the bipolar cell to the sink, giving at the end very thick veins. With flux bifurcations, auxin concentration in the network is quite regular and prevents long veins to become too rich in auxin and too thick. The way cells would bifurcate the flux is still a theory but the Bifurcator brings some light on its likelihood and the impact on the network. On the other hand, whereas bipolar cells have already been observed, we do not know whether they produce more auxin and if they are saddle cells. Nevertheless, these cells would satisfy tip-tip connections and pseudo tip-vein connections with the same principle, which is an economic strategy. But the becoming of these cells in the adult leaf is uncertain and the resulting network shape does not seem consistent with real leaf networks.

For future modeling we must take into account other key behaviors such as auxin production pattern, or carriers (PIN and AUX) production and allocation. The cell population dynamics is crucial too. Auxin is a good candidate for the regulation of cell division, and carrier allocation seems to decide the orientation of the division axis.

By looking at the way plant manipulates auxin one can imagine a more anthropomorphic behavior of the plant, which is obviously artificial but gives a more intuitive meaning of auxin. For example, during a wound, as soon as auxin is released among surrounding cells, it attracts newborn

vessels that drain the free auxin toward the auxin transport network (the cambium of a nearby vascular bundle). Thanks to the auxin signal these new vessel connect to wounded vein. As if free auxin were a signal of distress. When a hydathodes or a primordium is forming, cells grow and need resources and water. They produce and release auxin which attracts new vessels that will remove the free auxin and create vascular system bringing resources for their growth. As if auxin were a “feed me” message. As if free auxin had to be contained in the vascular system. If not, it would mean that there is a problem, or a need. Therefore one can imagine that plant “tries” to contain its auxin within its vascular system for everything to work fine. By doing so, each cell and organ would be “satisfied”.

Nevertheless, vascular formation includes many more actors than just PIN1 and auxin. More data on the localization of these other actors would be helpful to validate the major role of PIN1. More than ever, nice experimental studies are welcome and simple models are needed to capture complex behaviors for a better understanding.

Acknowledgment

I would like to thank Jacob Koella for his patience and his kind support; Yoh Iwasa for the great experience I had with him; Stéphane Douady for his interest and his availability; Christophe Godin for his advices; Steffen Bohn for nice discussions; Hiroo Fukuda for inviting me to his lab in the Tokyo University for a talk and for the nice discussions; Munetaka Sugiyama for the discussion and the visit of the botanical garden in Tokyo; Przemyslaw Prusinkiewicz for the interesting discussions in French; Enrico Scarpella and Thomas Berleth for enlightening discussions about their work; Akira Sasaki for his kind discussions and invitations; my family for their unconditional support; Mieko Ishibashi for her kindness and the good time we had for one year; friends in Japan for discussions and support: Ben Adams, Yoshihiro Morishita, Jun Nakabayashi, Hisashi Ohtsuki, Akiko Ohtsuki, Shôko Sakurai, Suzuki Sayaki, Robert Schlicht, Ryô Taku, Takashi Uehara, Hiroyuki Yokomizo… and all the others I am sorry to forget…

References for General introduction and General discussion

Barbier de Reuille, P., Bohn-Courseau, I., Ljung, K., Morin, H., Carraro, N., Godin, C., 2006. Computer simulations reveal properties of the cell-cell signaling network at te shoot apex in *Arabidopsis*. PNAS, 103, 1627-1632.

Bohn, S., Andreotti, B., Douady, S., Munzinger, J., Couder, Y., 2002. Constitutive property of the local organization of leaf vein networks. Physical Review E, 65, 1-12.

Douady, S., Couder, Y., 1996. Phyllotaxis as a Dynamical Self Organizing Process. Part I : The Spiral Modes Resulting from Time Periodic Iterations. J. theor. Biol., 178, 255-274.

Honda, H., Yoshizato, K., 1997. Formation of the branching pattern of blood vessels in the wall of the avian yolk sac studied by a computer simulation. Develop. Growth Differ., 39, 581-589.

Jönsson, H., Heisler, M.G., Shapiro, B.E., Meyerowitz, E.M., Mjolsness, E., 2005. An auxin-driven polarized transport model for phyllotaxis. PNAS, 103, 1633-1638.

Markus, M., Böhm, D., Schmick, M., 1999. Simulation of vessel morphogenesis using cellular automata. Mathematical Bioscience, 156, 191-206.

Meinhardt, H.,1976. Morphogenesis of lines and nets. Differentiation 6, 117-123.

Meinhardt, H., 1998. Reprint of a chapter that appeared in: Symmetry in Plants (D. Barabe and R. V. Jean, Eds), World Scientific Publishing, Singapore; pp. 723-758.

Mitchison, G.J.,1980. The Dynamics of Auxin Transport. Proceedings of the Royal Society of London. Series B, Biological Sciences, Vol. 209, 489-511.

Mitchison, G.J. (1981) The polar transport of auxin and vein patterns in plants. Philos. Trans. R. Soc. Lond. B, 295, 461-471.

Petrasek, J., Elckner, M., Morris, D.A., Zazimalova, E., 2002. Auxin efflux carrier activity and auxin accumulation regulate cell division and polarity in tabacco cells. Planta 216, 302–308.

Reinhardt[a], D., Frenz, M., Mandel, T. & Kuhlemeier, C., 2003. Microsurgical and laser ablation analysis of interactions between the zones and layers of the tomato shoot apical meristem. Development, 130, 4073–4083.

Reinhardt[b], D., Pesce1, E.R., Stieger1, P., Mandel, T., Baltensperger, K., Bennett, M., Traas, J., Friml, J., Kuhlemeier, C., 2003. Regulation of phyllotaxis by polar auxin transport. Nature, 426, 255-260.

Reinhardt, D., 2005. Phyllotaxis - a new chapter in an old tale about beauty and magic numbers. Current Opinion in Plant Biology, 8, 487-493.

Rolland-Lagan, A.-G., Prusinkiewicz, P., 2005. Reviewing models of auxin canalization in the context of leaf vein pattern formation in Arabidopsis. The Plant Journal, 44, 854-865.

Runions, A., Fuhrer, M., Lane, B., Federl, P., Rolland-Lagan, A.-G. and Prusinkiewicz, P., 2005. Modeling and visualization of leaf venation patterns. ACM Trans. Graphics, 24(3), 702-711.

Sachs, T., 1969. Polarity and the Induction of Organized Vascular Tissues. Annals of Botany, 33, 263-275.

Scarpella, E., Marcos, D., Friml, J., Berleth, T., 2006. Control of leaf vascular patterning by polar auxin transport. Genes & Dev. 2006 20: 1015-1027.

Shipman, PD, Newell, AC., 2005. Polygonal planforms and phyllotaxis on plants. J Theor Biol., 236(2), 154-97.

Smith, R.S., Guyomarc'h, S., Mandel, T., Reinhardt, D., Kuhlemeier, C., Prusinkiewicz, P., 2005. A plausible model of phyllotaxis. PNAS, 103, 1301-1306.

Turing, A.M., 1952. The basis of morphogenesis. Phil. Trans. Roy. Soc. Lond. B 237, 37-72.

Résumé en français

J’étudie la formation du système vasculaire des feuilles des plantes à l’aide de modèles mathématiques. L’hypothèse de canalisation d’une phytohormone, l’auxin, stipule que l’auto activation de son transport entre les cellules crée des chemins préférentiels qui se différencieront plus tard en système vasculaire. J’entreprends une analyse numérique de modèles de canalisation sur une grande matrice et parviens à créer des motifs branchés dans lesquels circule l’auxin. Une analyse de stabilité d’un modèle simplifié nous éclaire sur les raisons de la formation de ces motifs et l’impossibilité de créer un réseau réticulé. La majorité des plantes ayant un système vasculaire réticulé, je modifie le modèle de façon à obtenir ce type de réseau. En ajoutant une variable biologiquement plausible je parviens à créer un réseau réticulé dans lequel l’auxin circule uniformément. Enfin, je discute des relations entre la formation du système vasculaire et de la spirale de phyllotaxie.